UCSF

UC San Francisco Electronic Theses and Dissertations

Title

Scanning electron microscopic observations of labyrinthine sense organs and fiber degeneration studies of secondary vestibular and auditory pathways in caiman crocodilus

Permalink

https://escholarship.org/uc/item/0fb931t9

Author

Leake, Patricia Ann

Publication Date

1976

Peer reviewed|Thesis/dissertation

SCANNING ELECTRON MICROSCOPIC OBSERVATIONS OF LABYRINTHINE
SENSE ORGANS AND FIBER DEGENERATION STUDIES OF SECONDARY
VESTIBULAR AND AUDITORY PATHWAYS IN <u>CAIMAN</u> <u>CROCODILUS</u>

by

Patricia Ann Leake
B.S., Baldwin-Wallace College, 1970
M.A., University of California, San Francisco, 1974

DISSERTATION

Submitted in partial satisfaction of the requirements for the degree of

DOCTOR OF PHILOSOPHY

in

ANATOMY

in the

GRADUATE DIVISION
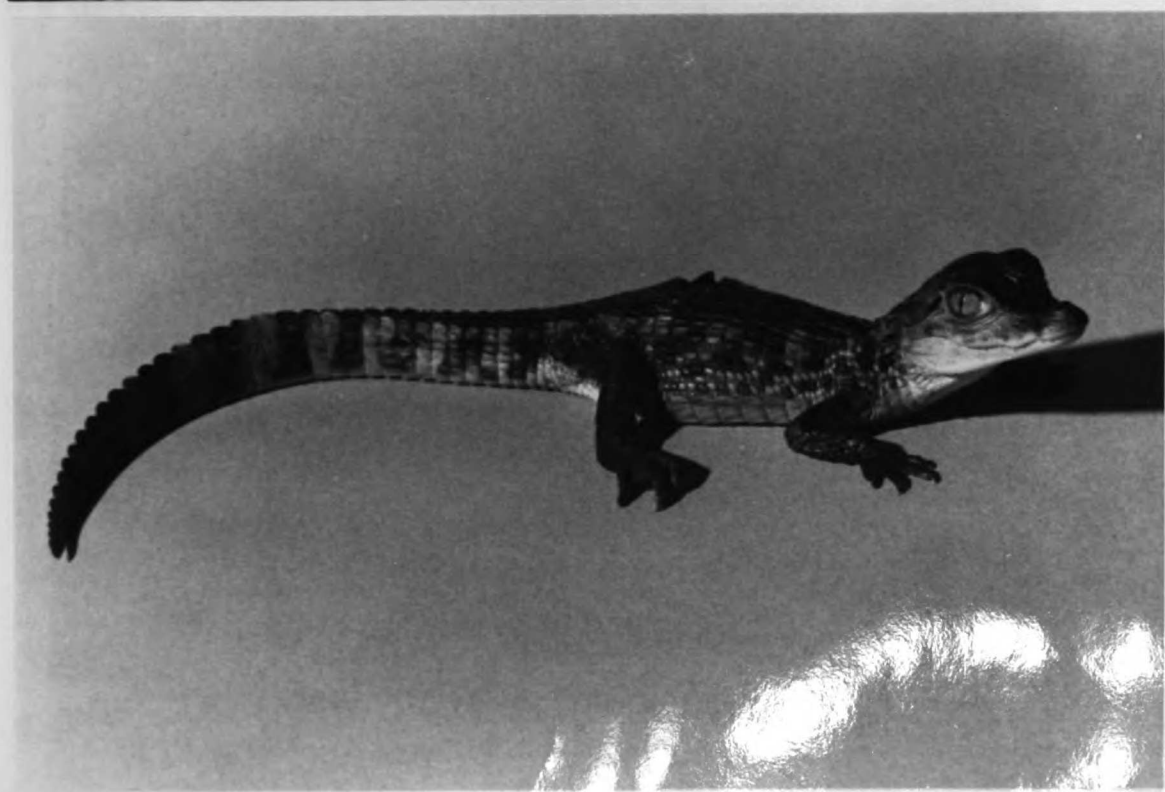
(San Francisco)

of the

UNIVERSITY OF CALIFORNIA

TABLE OF CONTENTS

ACKNOWLEDGEMENTS

ABSTRACT

Auditory and vestibular receptors and the connections of the brainstem nuclei to which their nerves project were studied in the South American alligator, Caiman crocodilus. Labyrinthine sensory structures were examined with the scanning electron microscope. Secondary fiber connections of the auditory and vestibular nuclei were determined in studies of patterns of anterograde axonal degeneration resulting from discrete experimental brainstem lesions.

A distinct cochlear duct (analogous to the mammalian cochlea) is present in the reptilian labyrinth. In Caiman, it is a curved structure housing an elongated sensory neuroepithelian strip, the basilar papilla. Ultrastructural features of the sensory hair cells include a polarization of ciliary bundles at the lateral cell border and an organ-pipe arrangement of the stereocilia. A kinocilium was also identified. It is longer than the tallest stereocilia in the young animals used in this study, supporting the hypothesis that the kinocilium retrogresses during maturation.

The reptilian vestibular labyrinth is comprised of three semicircular canals and three otolithic organs, the utricle, saccule and lagena. The ampullary structure of the horizontal semicircular canal differs from that of the vertical canals. By SEM, two morphologically distinct hair cell types were seen in the planar region of the crista ampullaris. Further studies are needed to determine whether these correspond to the type I and II hair cells described in mammals. There are also at least two different types of hair cells in the utricular macula of Caiman. One type is similar to ampullary hair cells of the

cristal ridge; other utricular hair cells resemble saccular sensory cells.

The saccular neuroepithelium is a C-shaped strip oriented sagittally with the opening of the C directed anteriorly. An otolithic membrane is attached to the microvilli of supporting cells and is continuous with a large statolith laterally. The orientation of the saccular hair cells reverses along a line approximately halfway across the width of the macula, dividing it into two strips of hair cells with opposite orientation.

In previous experimental studies, the primary afferent projections of the VIIIth cranial nerve to auditory and vestibular nuclei were defined. The examination of secondary fiber connections in the present study was an extension of this earlier work.

Vestibulospinal fibers arising from the ventrolateral vestibular nucleus (VL) form a well-defined tract comparable to that of other vertebrates and similar in its course to that described in amphibians. These fibers descend in the medial longitudinal fasciculus (MLF) to the ventral funiculi. Projections from various specific VL sectors reach different spinal cord levels. Vestibular commissural fibers, though never great in number, arise from all portions of the vestibular nuclear complex (VNC). Secondary vestibular fibers ascending in the MLF project bilaterally to extraocular motor nuclei. Similarities between these vestibular oculomotor connections in the advanced reptile and in mammals were noted.

An extensive degenerated projection to the cerebellar granular layer resulted from lesions in certain VNC regions. Although these fibers appeared to originate in the vestibular nuclei, it was impossible

to be certain that no fibers of the spinocerebellar tract had been interrupted by these lesions.

Secondary auditory fibers in the Caiman project bilaterally to the superior olivary complex, contribute fibers to the lateral lemniscus and its nucleus and ascend to terminate in a lateral portion of the torus semicircularis. Ascending auditory projections were primarily crossed in the material examined. The superior olive appears to receive an ipsilateral input to its lateral border and a projection from the contralateral auditory nuclei to its medial side. A projection to the contralateral nucleus laminaris, similar to that described in birds, was also found.

INTRODUCTION

All vertebrates from cyclostomes to mammals posses a specialized equilibrium organ for orientation with respect to the earth's gravitational field and for coordination of the animal's movements in three-dimensional space. Consisting of utricular, saccular and lagenar maculae and semicircular canals, the vestibular labyrinth has a structural plan which is essentially constant throughout the vertebrates. The brainstem cell groups receiving centripetal axon terminals of primary neurons from the vestibular receptor cells have been recognized in most vertebrates. A relative lack of central change across phylogeny, suggested by similarities in the basic mode of distribution of the primary vestibular fibers in different species (Mehler, 1972), may reflect the evolutionary stability of the receptors. Unfortunately, there are, however, many gaps in our knowledge concerning the vestibular nuclear complex (VNC) and its connections in non-mammalian vertebrates.

In the context of phylogenetic development, the reptilian nervous system is interesting and provocative since the reptiles are generally believed to occupy a strategic intermediate position in the mainstream of tetrapod evolution. Certainly there are no living reptilian forms which are considered to be directly descended from the amphibians or directly ancestral to the primitive mammals. Yet, the brains of living reptiles show considerable advancement in differentiation beyond the amphibians and toward the complexity of the warm-blooded vertebrates.

The caiman and other advanced reptilian forms in the order of
Crocodilia are of particular interest to comparative morphologists
since their brains greatly resemble the brains of avian forms. An
understanding of the various components of the brains of these
animals may contribute substantially to our understanding of the
evolution of the brain as well as to our understanding of the structure
and function of the homologous components.

It is thus disappointing that in view of the volume of descriptive
information concerning the vestibular nuclei (see Discussion),
experimental studies of the vestibular system in Reptilia are almost
non-existent. In fact, at the time the present experiments were
initiated only a single relevant experimental study of a reptile,
Lacerta viridis, (Robinson, 1969) was available. Robinson traced out
the projections of bulbospinal fibers and defined their nuclei of
origin using axonal degeneration and retrograde chromatolysis
techniques. However, only one vestibular nucleus, the reptilian
equivalent of Deiter's nucleus, and the position of its descending
fibers in the spinal cord were considered in this investigation. As
Mehler (1972) pointed out, other vestibular connections which have been
described in the literature based on normal fiber studies of reptiles
need to be verified experimentally.

In view of the lack of experimental work on these systems in
reptiles, an experimental degeneration study of the central projections
of the statoacoustic nerve of an advanced reptile, Caiman crocodilus,

was initiated in 1971 (Leake, 1973, Master's Thesis). The <u>Caiman</u> was chosen because of the general phylogenetic significance of the crocodilian brain mentioned previously, and because the crocodilian ear and acousticovestibular region are among the most highly specialized within the Reptilia; further, a number of electrophysiological investigations of the auditory system in this animal have been published (Wever and Vernon, 1957; Manley, 1970; Manley, 1971; Wever, 1971a). The present study, a continuation of the previous work (Leake, 1974), was designed to provide a detailed experimental analysis of secondary vestibular pathways in <u>Caiman</u>.

MATERIALS AND METHODS

The thirty-four animals utilized in this investigation were juvenile specimens of the common South American alligator Caiman crocodilus (previously Caiman sclerops). The "spectacled caiman," as this species is commonly known, was readily available as an experimental animal until recently. However, during the past two years procurement has become exceedingly difficult. In this study specimens were imported from Columbia by the Western Zoological Supply Company (Monrovia, CA) and by Gators of Miami. Animals ranged in snout-vent length from 10 to 19 cm although the majority were smaller specimens of approximately 10 to 13 cm. The younger Caiman were preferred since they respond more readily to hypothermic anesthesia and their skulls are still largely cartilagenous, facilitating dissections and surgical procedures.

A. **Studies of Normal Structure**

   1. **Light Microscopy.** Previous investigation (Leake, 1974) provided a thorough knowledge of labyrinthine, statoacoustic nerve and brain morphology of the caiman. A three-dimensional scale model (Fig. 1) of the otic capsule, adjacent medulla and middle ear structures produced from serial horizontal sections of a whole caiman head was invaluable in surgical planning of the experimental lesions. These materials were later supplemented with a second whole head series in the transverse plane. Several isolated

membranous labyrinths with intact seventh and eighth cranial nerves,stained in bulk with Sudan Black B (Rasmussen, 1961), were also employed as references for orientation in dissections for subsequent ultrastructural studies.

2. **Ultrastructural Studies.** Five _Caiman_ were prepared for ultrastructural studies of labyrinthine sensory epithelia. These animals were anesthetized by intraperitoneal injection of sodium pentobarbital and perfused by arterial injection of normal saline, followed by 3.0% glutaraldehyde (Polysciences, Inc.) in 0.1 M cacodylate buffer. After decapitation, the ear flaps, tympanic membranes, stapes and part of the cartilagenous labyrinths were removed bilaterally. The heads were then immersed in a large volume of glutaraldehyde to permit fixation of the labyrinths _in situ_. A minimum of 7 days at 4°C with frequent addition of fresh fixative was desirable for adequate hardening of the tissue. The membranous labyrinths were dissected from the skull and the vestibular receptors were excised and trimmed for study under the scanning electron microscope (SEM). The ampullae of the semi-circular canals were carefully trimmed with iridectomy scissors close to the crest and the planum semilunarum. Several attempts at mechanical removal of the cupula at various stages in the preparation of ampullary specimens were uniformly unsuccessful, resulting in tearing of the underlying sensory epithelium and distortion of the normal three-dimensional contours of the ampullary crest. In contrast, the saccular and utricular otoliths

were easily dislodged with a microcurette, exposing the hair cells for direct visualization with the SEM. After initial disappointing experiences of adjacent membranous labyrinth tissue folding onto and obscuring the sensory epithelium, this excess membrane was trimmed from subsequent specimens.

The trimmed specimens were dehydrated through a graded series of alcohols to absolute alcohol (20%, 30%, 50%, 70%, 80%, 2 x 95%, 2 x 100%) and dried by the CO_2 critical point method of Anderson (1951). In this process absolute alcohol in the tissue is replaced by liquid CO_2 which, in turn, is replaced directly by its gas phase upon heating in a sealed bomb. Surface tension artifacts which would result from air drying are greatly reduced with this technique. Dehydrated specimens were mounted in a drop of silver paint on SEM specimen holders and coated in a vacuum evaporator with a thin (approximately 150 Å) coat of (0.9999) pure gold or gold palladium at 2.0 - 3.0 x 10^{-5} torr. Three-dimensional observations of the vestibular end organs were made with a Kent Cambridge S_4 SEM at 10 or 20 kV.

One posterior ampulla from a right labryinth preserved for SEM was prepared for evaluation in the transmission electron microscope (TEM). This specimen was post-fixed in ice-cold 2% buffered OsO_4 for 2 hours, dehydrated in acetone and embedded in Epon 812 (Luft, 1961). The block was sectioned with a Porter--Blum MT II ultramicrotome with glass or diamond knives in a plane transverse to the ampullary crest. Sections were stained with

uranyl acetate and lead citrate, and examined in a Philips EM 201. Evaluation of transmission electron micrographs indicated that the previously described SEM preparation procedures provided adequate preservation of surface membranes and immediate subsurface structure.

B. Experimental Procedures

Experimental lesions were produced in the brainstem vestibular nuclear complex (VNC) or cerebellum of 28 juvenile caimen. Analysis of the resulting patterns of neuronal degeneration were undertaken utilizing modern reduced silver impregnation techniques.

1. Surgical Preparation. A surgical level of anesthesia was achieved by cooling the reptiles for approximately 20 minutes at 4°C. The anesthesia was maintained throughout surgery with an ice bath or ice bag. All surgery was done under a Zeiss operating microscope. The external ear flap was separated from the head near the skull and the underlying tympanic membrane excised. Utilizing this approach, exposure of the lateral aspect of the brainstem and cerebullum was possible through the middle and inner ear with very little bleeding or trauma. The braincase was opened by enlarging the VIIIth nerve foraminae medialwards, through the floor of the saccule.

Platinum-plated glass-coated platinum-iridium microelectrodes with tips 2 - 5 μm in diameter were mounted in a micrometer drive apparatus on a Baltimore Instruments H-bar. Electrode placement

on the brain surface was largely reliant on visual landmarks.
The angle and depth of electrode penetration for specific target
cell groups within the brain were estimated from measurements
made in the previously described scale reconstruction (Fig. 2).
With a specially designed D.C. lesion maker, lesioning currents
ranged from 15 to 50 µamps applied 15 to 30 seconds. The
resulting electrolytic lesions were 50 to 200 µm in diameter.

Attempts were made in various experiments to localize
lesions in the dorsolateral, dorsomedial, ventromedial and
descending vestibular nuclei. Restricted regions of the ventro-
lateral vestibular (Deiter's) nucleus and cerebellum were targets
in other experiments. Lesions were unilateral in all cases. In
a few cases (74-V3, 74V4, 74-V6, 75-V21 and 75-V25) two penetra-
tions were made. After the electrode was withdrawn, the ear
cavity was loosely packed with Gelfoam and the amputated ear flap
sutured back into position.

2. Sacrifice and Tissue Preservation. In most cases
experimental animals were sacrificed 12 or 13 days after surgery,
as this survival period had proven optimal for the simultaneous
demonstration of anonal and preterminal patterns of degeneration
in a previous study conducted in the Caiman (Leake, 1974).
Animals were anesthetized by intraperitoneal injection of sodium
pentobarbital and perfused with normal saline, followed by 10%
neutral formalin. After decapitation, the dorsal surface of the
brain was usually exposed as far rostral as the cerebullum.

Specimens were stored in 10% formalin at 4°C for several days to allow further hardening of the brain tissue before removal from the skull.

3. Histology. The isolated and fixed brains were washed overnight in running tap water and soaked in a 30% aqueous sucrose solution for approximately 48 hours. The tissue was then step infiltrated at 37°C and embedded in a final concentration of 20% gelatin in 1% phenol. Gelatin blocks were marked for later orientation of individual sections and hardened in 10% formalin for 24 hours. Serial sections were cut at 26 µm on the freezing microtome in a transverse plane. Sections were stored in 2% formalin at 4°C in plastic trays divided into 36 compartments. Several histological techniques for the selective silver impregnation of degenerating neurons were employed to study sections which could be selected in precise order from the storage trays.

A Nauta silver impregnation technique, using an hour pretreatment in 5% aqueous uranyl nitrate (Method 5: Ebesson and Nauta, 1970) was used routinely to demonstrate neuronal degeneration within the normal fibrillar architecture of the brain. A modification (Mehler, unpublished) of the more suppresive Fink-Heimer II silver method (1967) gave excellent results with the gelatin embedded material and was especially valuable in determining patterns of degenerating preterminal fibers and terminal fields. Supplemental sections processed according to the

Fink-Heimer I silver technique (1967) provided additional data.

In each case cytoarchitectural details were studied in adjacent sections stained with cresylecht violet or in silver sections which were bleached in 1 to 5% aqueous potassium ferricyanide and counterstained with cresylecht violet. After histological processing sections were mounted on glass slides, using the alcoholic gelatin technique of Albrecht (1954).

After initial examination of all cases, 13 were selected for detailed study. Patterns of degeneration were analyzed under the light microscope and charted on microprojector tracings of individual sections.

RESULTS

PART I: ULTRASTRUCTURE OF THE INNER EAR

A. <u>Introduction</u>

The reptilian labyrinth represents an important phylogenetic advance in inner ear structure in that: 1) there is a distinct cochlear duct analogous to the mammalian cochlea and 2) the organization of labyrinthine parts is comparable to that in birds and some lower mammals. This general evolutionary significance and the hope of providing a less complex model for understanding basic mammalian auditory mechanisms have stimulated studies of the reptilian auditory organ. During the past ten years, many additions have been made to our knowledge of otic gross morphology and histology in these species (Hamilton, 1964; Wever, 1965, 1967a, b, 1970; Miller, 1966a, b, 1968; Baird, 1967, 1969, 1970a; Smith and Takasaka, 1971).

It is of interest to comparative morphologists that the structure of the cochlear duct and particularly the papilla basilaris (analogous to the mammalian organ of Corti) show considerable variation among the Reptilia. These structural modifications may represent states in several different lines of "evolutionary experiments" with the primary auditory receptor. Ultrastructural descriptions of reptilian basilar papillar structure have been correlated with the light microscopic findings in studies conducted by Baird (1969, 1970a, b, 1974), Mulroy (1968) and by Baird and Marovitz (1971). Recently, rather spectacular variations in surface details of cochlear duct fine structure have been

demonstrated in different reptilian species with the scanning electron microscope (SEM) (Miller, 1973a, b, 1974a, b; Bagger-Sjöbäck and Wersäll, 1973; von Düring, Karduck and Richter, 1974).

The crocodilian ear represents the highest degree of specialization occurring within the Reptilia (Baird, 1970a). It is not surprising, then, that the cochlear duct of Caiman crocodilus has been the subject of several light (Baird, 1970b; Wever, 1971b; Leake, 1974) and electron microscopic (Mulroy, 1968; Baird, 1970b, 1974; Von Düring, et al, 1974) observations. Consequently, discussion of cochlear duct morphology in this report will be relatively limited.

Most investigations of the reptilian labyrinth have been conducted on auditory structures (Baird, 1974). In contrast, very little additional information on the vestibular structures has been gathered since the pioneering work of Retzius (1884) and the classical observations of de Burlet (1934). Recent SEM studies have, however, been reported in other non-mammalian species (Barber and Boyde, 1968: mollusc; Hama, 1969: goldfish; Lim and Lane, 1969: pigeon; Landolt, Correia and Young, 1972: pigeon; Lewis and Nemanic, 1972: mudpuppy; Lewis and Li, 1973, 1975: frog; Lim, 1973b, 1974: pigeon, frog, goldfish, ray; Correia, Landolt and Young, 1974: pigeon; Hillman, 1974: frog) as well as in certain mammals (Lim, 1969, 1971, 1973a, b; Lim and Lane, 1969; Engeström, 1970; Lindeman and Ades, 1972). These investigations have demonstrated that the SEM, because of its excellent resolution ($\sim$150 Å), depth of field ($\sim$1 mm) and variable magnification, is ideal for examination of the highly irregular surface topography of

the vestibular labyrinth. The present report represents the initial SEM application to the vestibular apparatus of reptiles.

B. Cochlear Duct

The primary auditory receptor of Caiman crocodilus consists of a 3.6 mm strip of sensory epithelium, the basilar papilla, housed in an elongated, obtusely curved portion of the membranous labyrinth, termed the cochlear duct (Figs. 3, 4). The foot-plate of the stapes is suspended in an oval aperture in the lateral wall of the proximal, enlarged end of the structure. The narrower distal extremity of the duct contains the lagenar macula. The hollow, fluid-filled organ is appended to the posterior region of the saccule (part of the vestibular labyrinth) by the small sacculo-cochlear or reunient duct.

A scanning electron micrograph taken at low magnification of a left cochlear duct is shown in Figure 7. In this specimen a portion of the more distal (lagenar) part of the basilar membrane is exposed (arrows) so that the sensory epithelial surface may be studied to better advantage. The basilar membrane is composed of sensory hair cells surrounded by supporting cells which have microvillar luminal surfaces. The crocodylids are unique among the reptiles in that two types of hair cells, analogous in position to the mammalian inner and outer hair cells, are present in the inner ear (Retzius, 1884; Mulroy, 1968; Baird, 1970b, 1974; von Düring et al, 1974). A cross-section through the cochlear duct of Caiman crocodilus (Figs. 5, 6) illustrates certain differences in morphology as well as the respective

positions of these two hair cell types on the basilar membrane,

Outer hair cells from the lagenar portion of the basilar membrane are shown in Figure 8. Their appearance is strikingly different from that of the outer hair cells in the more proximal portion of the basilar membrane (Fig. 9), as revealed in a right cochlear duct SEM specimen (see Fig. 10 for a low power view of this specimen). The longitudinal diameter of outer hair cells gradually increases from the proximal to the distal end of the papilla. The cilia also increase in length along this dimension, being longest in the lagenar portion of the basilar membrane. In addition, the shape of the sensory cells changes considerably, being hexagonal or pentagonal proximally and more elongate distally.

Certain ultrastructural features, on the other hand, are common to all hair cells. The ciliary bundles are always polarized at the lateral margin of the cell surface, leaving the majority of the luminal surface free. The cilia of each sensory cell are arranged in organ-pipe fashion with the tallest stereocilia comprising the most lateral rows of the ciliary bundles. The kinocilium can frequently be identified in the tallest row of stereocilia by its greater diameter at the point of attachment to the hair cell (Figs. 9, 11, arrows). The stereocilia are, however, enlarged at their apical ends and their largest diameter may actually exceed that of the kinocilium which remains constant or diminishes toward its apex,

The apparent length of the kinocilium in scanning micrographs (Figs. 9, 11) is of great interest in that it appears to be

substantially longer than the tallest stereocilia. Von Düring et al. (1974) have reported that the kinocilium in their 50 to 80 cm animals is always shorter than the tallest stereocilia, having a length "similar to the medium-sized stereocilia." The reduced kinocilium seen in this previous study suggests a morphological parallel between the Caiman papilla basilaris and the organ of Corti in mammals where the kinocilium of sensory cells is rudimentary. Von Düring speculated further that the kinocilium in Caiman may retrogress to the basal body during maturation as is the case in cats (Spöndlin, 1966; Hamilton, 1969). Since the animals examined in the present study were smaller (none exceeded 40 cm in length) that those used by von Düring et al, the lengthened kinocilium found in these younger animals supports the possibility of kinocilial retrogression. This interesting question might be resolved by examining the sensory cells in the papilla basilaris of a mature Caiman specimen.

Each sensory cell of the basilar papilla is surrounded by several supporting cells. The microvilli protruding from the luminal surface of these cells are especially prominent in a high magnification SEM micrograph (Fig. 11). The microvilli are about 1 μm in length, and the exposed surface of the supporting cells is approximately 2 μm in width. The recent discovery by von Düring et al (1974) that these supporting cells and another non-sensory element, the hyaline cells, are apparently innervated by efferent eight nerve axons is very interesting. It has been suggested that these specialized cells may exert an indirect effect on the generation of receptor potentials in

the afferent auditory fibers by altering the ionic milieu of the endolymphatic fluid around the hair cells. This question certainly merits additional investigation.

C.   Vestibular Ampullary Structures

The superior division of the reptilian vestibular labyrinth consists of three semicircular canals and an otolithic organ, the utricle. The semicircular canals are oriented in planes roughly perpendicular to each other and are directly related to the utricular chamber medially. Each canal is enlarged at its opposite end to form a bulbous chamber, the ampulla. Contained within the ampulla is the crista ampullaris, a sensory organ which detects the vector component of angular motion in the plane of its respective canal. The crista forms a ridge or crest in the wall of the ampulla and its long axis is oriented perpendicular to the plane of the related semicircular duct. This transverse ridge is comprised of connective tissue containing a vascular and nerve supply and is covered by neuroepithelial hair cells.

A gelatinous mass, the cupula, covers the ampullary receptor cells and is firmly adherent to the crista ampullaris. In scanning microscopy, remnants of this structure in Caiman ampullae often obscure the underlying sensory epithelium (Figs. 14, 15, 16).

The ampullary structure of the two vertical (anterior and posterior) semicircular canals is very similar in Caiman. In low magnification scanning micrographs (Figs. 12, 14, 15) the gross

contours of the ampulla are easily appreciated. The crista is slightly enlarged at the midpoint of its long axis. This region is called the torus (de Burlet, 1935). From its maximum height at the torus, the crista slopes downward toward the floor of the ampulla and then upward again, forming an expanded area of attachment to the ampullary wall. Surrounding this region is a crescent-shaped elevation in the wall of the ampulla called the planum semilunatum (Figs. 12, 14) by Steifensand (1835).

The characteristic protruberances, the cruciate eminences (Dohlman, 1961) are evident in the vertical canal ampullae (Figs. 12, 15, 19). These structures are projections from the ampullary floor at the base of the crista and, hence, are completely devoid of hair cells. They intersect the cristal ridge in the region of the toral enlargement, giving an overall cruciform shape to the ampullary structures. The cruciate eminences are not equal in size. The eminence on the side of the crest related to the semicircular canal is much less prominent than its counterpart on the side of the ampulla which opens into the utricle.

Figure 19 shows the distribution of sensory hair cells on the crista of a posterior ampulla in which the cupula is absent. The hair cells are restricted to the lateral slopes of the crest, with a midline areas of the torus free of sensory cells (Fig. 20). More laterally, each of the two hair cell strips astride the crest expands into a crescentic area of neuroepithelium on the lateral wall of the vertical ampulla. this planar expansion of the hair cell region is especially evident in Figure 16.

The structure of the ampulla of the horizontal or lateral semicicular canal is quite different from that previously described for the vertical canals. In Figure 21 it is evident that the torus and eminentia cruciatae are absent in the lateral ampulla. Only one planar expansion of the crista and a single planum semilunatum exist; these are located on the dorsal ampullary wall. The crest is oriented in a sagittal plane and, thus, is perpendicular to the horizontal canal. The ventral end of the crest blends directly with the floor of the ampulla.

The sensory hair cells of the Caiman crista ampullaris exhibit the usual organ pipe arrangement of stereocilia. They are surrounded by supporting cells which have numerous microvilli and often a rudimentary kinocilium protruding from their apical surfaces (see Figs. 22, 23). The sensory cells on the cristal ridge are shown at various magnifications in Figures 20 (1650x), 22 (2400x), 23 (6100x) and 24 (1800). In Figure 24 several extremely long cilia are seen in relationship to remnants of the cupula. The tortuous appearance of the kinocilium in certain micrographs (Figs. 22, 24) may be due to stretching secondary to shrinkage of the cupula during the critical point drying process.

Hair cells from the planar expansion of the crista ampullaris are shown in Figures 17 and 18. In addition to the type of hair cell seen previously on the cristal ridge, a second and morphologically distinct hair cell population is present in the planar region. This type of hair cell (a in Fig. 18) appears to have only a single long cilium,

presumed to be the kinocilium. The stereocilia are arranged in organ pipe fashion, but the several extremely long stereocilia associated with the kinocilium and cupula in the other hair cell type (a in Fig. 18) are absent. This finding of two hair cell types in the Caiman ampullary crest is noteworthy, as only one type of sensory cell, the type II cell (Wersäll, 1956) has been reported in previous studies of the reptilian ampulla (Baird, 1974), Ultrastructural studies of bird and mammalian ampullary neuroepithelia have, in contrast, demonstrated the presence of both type I and type II cells. It seems likely that transmission electron microscopy of the Caiman ampulla will confirm that both type I and type II hair cells, corresponding to the two hair cell types distinguished in the SEM, are also present in this advanced reptilian form.

The orientation of hair cells on the Caiman ampullary crests is unidirectional except for occasional aberrant hair cells near the planum semilunatum. In the vertical canals hair cells are oriented with their kinocilium toward the semicircular canal and the shortest stereocilia toward the more prominent cruciate eminence and the utricle.

In the horizontal crista, the hair cells are oriented with their kinocilia pointed toward the utricle and with the shortest stereocilia toward the horizontal canal. This opposite polarization of hair cells in vertical and horizontal canals, described here for the first time in a reptile, very closely parallels the situation in mammals as described by Lim (1971: guinea pig, mouse and dog).

D.   Saccule

The superior and inferior divisions of the labyrinth are joined by a short tube between the utricle and the saccule, the utriculo--saccular duct. The otic or endolymphatic duct also arises from the saccule just anterior to the utriculo-saccular duct. In Figure 3 this endolymphatic duct is seen curving under the utricle. From here it passes through the vestibular aqueduct and into the cranial cavity where it empties into the endolymphatic sac.

The saccule is a large, bulbous chamber, housing an otolithic organ, which is responsible for detection of gravitational forces. The saccular macula consists of a U-shaped, curved strip of sensory neuroepithelium which is oriented in a roughly sagittal plane with the bottom of the U directed anteriorly. The neuroepithelium is comprised of sensory hair cells surrounded by supporting cells with many microvilli. An otolithic membrane attaches to the microvilli of the macular-supporting cells and is continuous with a large statolith laterally. The macula is widest anteriorly, where it is approximately 25 hair cells across. The superior and inferior limbs of the U-shaped macular hair cell strip gradually taper posteriorly.

In Figure 25, a saccular SEM specimen is shown at low magnification (40x). This specimen demonstrates the curling and folding of the saccule which occurred during SEM preparation procedures and made impossible the examination of the entire hair cell population in any one saccule. The whole inferior limb of the saccular macula could, however, be studied in a saccule which was bissected longitudinally

after dehydration (Fig. 26).

Details of macular ultrastructure in the saccule are shown in higher magnification scanning micrographs in Figures 30, 31 and 32. The stereocilia of the sensory hair cells have an organ pipe arrangement similar to that of the ampullary hair cells, but they are not as long as the ampullary stereocilia. The kinocilium is significantly longer than the longest stereocilia and is attached to the statolithic membrane. Supporting cells which surround the macular sensory cells are obscured by the statolithic membrane since, as noted previously, this membrane attaches to the microvilli of the supporting cells. Although the membrane lies above the hair cells, it is attached to them only by their kinocilia. In certain areas the membrane appears to be fenestrated, with stereocilia protruding through the fenestrae (Figs. 30, 31). Figure 32 shows the tapered end of the inferior limb of the saccular hair cell strip where the statolithic membrane is intact and covers the hair cells.

Careful examination of high magnification scanning micrographs (Figs. 30, 31) reveals that hair cell orientation is not unidirectional in the Caiman saccule. Rather, the polarization of hair cells abruptly reverses approximately halfway across the width of the macula, dividing the neuroepithelium into strips of hair cells with opposite orientation. The position of this line of polarization reversal in the inferior portion of the Caiman saccular macula, as determined in higher magnification scanning micrographs, is illustrated by dashed lines in Figures 27, 28 and 29. The hair cells

are oriented with their kinocilia away from the reversal line. Thus, in hair cells central to the line (i.e. on the left side of the dashed lines) the kinocilia are on the central sides of the cells and the shortest stereocilia face peripherally and toward the midline. In the peripheral portion of the macula the kinocilia are on the peripheral sides of the hair cells and the shortest stereocilia face centrally and, hence, toward the midline. Hair cell counts indicate that the hair cell strip on the peripheral side of the reversal line is 2 to 5 hair cells narrower than the region central to it. The line of polarization reversal has been observed to coincide with the striola in other animals, but its functional significance is unknown.

The large saccular statolith is roughly pyramidal with the base of the pyramid facing laterally and oriented in an approximately sagittal plane. The statolith consists of statoconia embedded in a gelatinous matrix. It is continuous with the statolithic membrane medially. Details of surface ultrastructure of the statoconia seen in the SEM (Figs. 33, 34) are very similar to those described in the frog.

E. Utricle

The Caiman utricle is an enlarged tubular chamber positioned medially in the superior division of the labryinth. Its relationship to the semicircular canals and the common crus are illustrated in Figure 3. The utricle, like the saccule, houses an otolithic organ which is a gravity receptor.

The gross contours of the sensory neuroepithelium or macula are

shown in Figure 35. The structure is somewhat cup-shaped with a slight indentation posteriorly. The nerves to the anterior and horizontal semicircular canals are seen cut in cross-section at the anterior and lateral margins of the utricle respectively.

At higher magnification many of the hair cells and the otolithic membrane appear to be very similar to those in the saccule (Fig. 38). However, hair cells which have several extremely long stereocilia and closely resemble the ampullary sensory cells are also present (Figs 36, 37). Since the statolithic membrane obscured hair cells in several areas (Fig. 9) and the ciliary bundles were twisted and distorted in many of the exposed hair cells, no statement can be made concerning the orientation or polarization of the hair cells within the utricle.

PART II: EXPERIMENTAL RESULTS

A. Central Projections of the VIIIth Cranial Nerve

The Caiman primary auditory and vestibular receptors described in the preceding section are innervated by the statoacoustic or eighth cranial nerve. Primary afferent fibers from the anterior and horizontal cristae, the utricle, and the saccule comprise the anterior or ventral root of the eighth nerve. The cell bodies of these neurons are restricted to the anterior ganglion (Fig. 40). Since the anterior ganglion is purely vestibular, it may be considered at least functionally homologous to the mammlaian Scarpa's ganglion. However, it should be noted that in mammals the ganglion cells of neurons from all the vestibular receptors are restricted to Scarpa's ganglion. In Caiman, on the other hand, nerves from the posterior crista, the lagenar macula and a small fiber component from the posterior saccule coalesce with fibers from the basilar papilla to form the posterior or dorsal division of the statoacoustic nerve (Fig. 40). The associated posterior ganglion is thus comprised of a mixed population of vestibular and auditory neuronal cell bodies, in contrast to the purely auditory mammalian spiral ganglion.

The central distribution of the primary afferent fibers of the Caiman eighth nerve has been analyzed in a previous investigation utilizing contemporary experimental and reduced sliver impregnation techniques (Leake, 1974). The primary auditory and vestibular nuclei

defined by preterminal degeneration patterns in the earlier study
are labelled in an abbreviated photographic atlas of the Caiman
brainstem presented in Figure 41.

Eighth nerve fibers bifurcate immediately after penetrating the
medulla oblongata to form ascending and descending branches. The
terminal region of these two branches within the brainstem is
commonly called the acousticolateral area. Comparison of patterns of
anterograde fiber degeneration resulting from differential experimental
lesions of the nerve indicates that first order neurons from the
papilla basilaris project only to ipsilateral nuclei angularis,
magnocellularis medialis and lateralis, and to the neuropil above
laminaris. These cell groups comprise the cochlear nuclear complex
(CNC) which occupies the so-called acoustic tubercle. Differential
degeneration patterns resulting from small electrolytic lesions
suggest a spatial ordering of the auditory projection within these
brainstem nuclei.

Primary afferents from vestibular sensory organs distribute to six
nuclei ipsilaterally: ventrolateralis (Deiter's), ventromedialis,
descendens, tangentialis, dorsolateralis and dorsomedialis. These
cell groups comprise the Caiman vestibular nuclear complex (VNC) which
is situated for the most part ventral to the CNC, extending fairly
equal distances above and below the entering nerve. First order
vestibular neurons also project bilaterally to the granular layer of
the cerebellum at more rostral levels.

B. Vestibulospinal Projection

Figure 2 presents a schematic illustration of the specific
locations and sizes of experimental lesions in the thirteen Caiman
cases selected for analysis in this report.   Lesions produced in
five of these specimens (cases V10, V14, V15, V17, V24) resulted in
degenerated fibers which descend to the spinal cord.   In case V10 the
lesion is restricted to the lateral and ventral parts of the left
Deiter's or ventrolateral vestibular nucleus (VL). In its rostro--
caudal dimension this lesion is coextensive with the abducens or sixth
cranial nerve nucleus.   The pattern of degeneration which occurred
following this lesion is illustrated in Figure 43. Degenerated fibers
emerge from the ventral and medial borders of the lesion and arch
toward the midline.   In this region two prominent fiber bundles, the
medial longitudinal fasciculi, lie on either side of the midline
ventricular sulcus and the sulci limitans.   In several adjacent silver
impregnated sections through and just caudal to the lesion in case V10,
a small fascicle of degenerated fibers is observed to collect in the
ipsilateral medial longitudinal fasciculus (MLF). The contralateral
MLF receives a more substantial contribution of degenerated neurons
from this VL lesion.

The descending MLF projection may be traced caudally to the
cervical spinal cord where degenerating vestibulospinal fibers occupy
a medial and ventral position in the anterior funiculi. A few of these
fibers descending in the ventral white columns cross the midline in the

white matter ventral to the central canal to reach the corresponding region of the opposite side. Fine degenerated neuronal fragments are observed bilaterally close to motoneurons in the ventromedial part of the anterior horn in cervical spinal cord sections. These were interpreted as preterminal patterns since degenerating fibers could not be demonstrated at more caudal spinal levels.

Another group of degenerating fibers in case V10 is followed through the ipsilateral descending vestibular nucleus into the lateral funiculus of the cervical spinal cord. These lateral degenerated fibers turn medially and are associated with fine preterminal neuronal degeneration fragments close to the dorsolateral motoneurons in the ventral horn of the spinal cord at cervical levels. No degenerating fibers appear to reach more caudal spinal levels.

The degeneration pattern in V10 is essentially repeated in cases V15 and V24. In V15 the lesion is situated in the ventral part of VL, more medial than the V10 lesion. The lesion in case V24 is positioned even more medially, interrupting vestibulospinal fibers just ventral to the point of their emergence from the ventrolateral vestibular nucleus.

A large lesion produced in case V17 destroyed a greater portion of VL, including for the first time much of the dorsal subdivision of this nucleus. Following this lesion the pattern of degeneration in the cervical spinal cord is similar to that previously described for case V10. However, in V17 degenerating fibers are observed in the

ventral funiculi throughout the entire length of the spinal cord, descending at least as far as 1 cm caudal to the lower extremeity.

In contrast to the consistent degeneration pattern seen in the cervical spinal cord of all previous cases, only the lateral fiber system degenerated in Caiman case V14. The lesion involved parts of the descending and medial vestibular nuclei and encroached also upon the white matter of the medulla oblongata just ventral to the VNC (Fig. 42). No degenerating fibers occur in the anterior funiculi as a result of this lesion.

Degeneration patterns resulting from all other lesions illustrated in Figure 5 do not extend caudally to the spinal cord.

C. Vestibular Commissural Projections

Commissural connections have been demonstrated in Caiman between each vestibular nucleus and the homonymous nucleus of the contralateral side, with the single exception of nucleus tangentialis. The latter cell group was not damaged in any lesion of the present experimental series.

In the available material the most prominent degenerated commissural projection occurs in animals with lesions affecting the ventrolateral vestibular nucleus (cases V7, V10, V16, V17 and V18). The trajectory followed by the bulk of these degenerating fibers is illustrated in Figures 43c and d). Commissural fibers emerge from the dorsomedial margin of VL lesions and run medially through the

periventricular gray matter, coursing dorsal to or passing through
the nuclei of the VIIth and VIth cranial nerves. Medially, many
fibers disappear from the transverse plane of section, arching
orally to cross the midline. On the opposite side of the brainstem
commissural fibers course dorsolaterally to reach the contralateral
acousticolateral region. Here preterminal degenerating fibers are
seen in a region of VL which approximately corresponds to the
location of the lesion. In case V10, for example, the lesion
damaged ventral and lateral subdivisions of VL, and the resulting
preterminal degeneration depicted in Figure 41d is restricted
chiefly to these same areas contralaterally.

Cases V16, V17 and V18 demonstrate commissural fibers between the
dorsal and rostral parts of the ventrolateral nucleus. Since the
lesion in case V17 is substantially larger than other VL lesions,
it is not surprising that the greatest number of degenerating commissu-
ral fibers occurs in this animals. The lesions in cases V7, V16 and
V18 also damaged more oral parts of the VNC. The V7 lesion is
restricted chiefly to the dorsolateral nucleus, while in V16 and V18
a small lateral portion of dorsomedialis is affected as well.
Degenerated decussating fibers at these rostral levels course
ventromedially above the motor nucleus of the trigeminal (fifth
cranial) nerve nucleus, cross the midline close to the midline
ventricular sulcus and ascend through the contralateral rostral VNC to
enter the cerebellar peduncle of the opposite side. Patterns highly

suggestive of preterminal degeneration are seen in the oral vestibular region; however, many degenerating fibers in these cases pass through the rostral vestibular nuclei and ascend into the cerebellum.

At caudal levels through the Caiman VNC, a small commissural fiber component is observed to connect the ventromedial vestibular nucleus to its contralateral counterpart. Lesions of the medial vestibular nucleus demonstrating this sparse projection are found in cases V6 and V14. The diffuse cell population comprising the descending vestibular nucleus was damaged sufficiently to produce a small number of degenerating commissural fibers only in case V6.

It should be noted that the dense neuropil in which the Caiman vestibular neurons are intercalated may contain fibers whose origin has not yet been determined. Experimental lesions of the VNC might, therefore, interrupt non-vestibular fibers which project to or contribute decussating collaterals to the contralateral vestibular nuclei (see Discussion).

D.   Vestibular Projections to Extraocular Motor Nuclei

1.   Morphology of the Nuclei. The abducens or sixth cranial nerve nucleus in Caiman (Fig. 46) is a lossely packed column of cells which is situated just lateral to the MLF. The posterior two-thirds of this column occupies a position dorsomedial to the motor nucleus of the facial or seventh cranial nerve, although the latter cell group reaches a slightly more caudal level than does the abducens nucleus. Approximately one-third of

the abducens cell column extends rostral to the oral border of the seventh nucleus. In sections stained with cresylecht violet, the multipolar abducens cells appear pale and measure approximately 20 to 25 μ. Root fibers of the sixth nerve take a ventral and slightly lateral course to emerge from the brain-stem at all levels of the brainstem containing abducens cells.

The trochlear nuclei (Fig. 47) are comprised of polygonal cells similar to the abducens cells in size and shape although they stain intensely with cresylecht violet. At caudal levels the nucleus is situated dorsal to the MLF in the floor of the fourth ventricle. The posterior border of this cell group is found at roughly the same level as the oral tip of the motor nucleus of the trigeminal nerve. At its maximum development in more rostral sections the trochlear nucleus expands downward along the lateral border of the MLF. Trochlear root fibers pass dorsally through the periaqueductal gray to decussate in the anterior medullary velum and emerge from the dorsum to the brainstem just behind the optic tecta.

The oculomotor nuclei (Fig. 45) are confined to the dorsal tegmental region of the mesencephalon, dorsal to the raphé. Each oculomotor nucleus surrounds the ipsilateral MLF on all but its lateral side. The nuclei are thus arranged in the shape of the letter "C" with the opening of the C directed laterally. Caudally the deep midline ventricular sulcus

separates the oculomotor nuclei of opposite sides, but through-
out the greater part of their rostro-caudal dimension the third
nerve nuclei are apposed along their medial borders. The
ventral part of the oculomotor nucleus does not extend as far
rostrally as does the dorsal wing-like expansion. The dorsal
cells reach the level of the posterior hypothalamus; this level
is also characterized by the maximum development of the torus
semicircularis (i.e. approximately halfway through the optic
tectum). Many of the pale-staining oculomotor cells are
observed in cresylecht violet sections to be larger than cells
of the other eye muscle nuclei, measuring up to 35 μ.

2. <u>Vestibular Connections with Eye Muscle Nuclei</u>. Most of the
experimental lesions resulted in fiber degeneration which
project to the abducens, trochlear and oculomotor nuclei described
in the previous section.

Lesions restricted to caudal levels of the VNC produced
degenerated fibers which ascend in the medial longitudinal
fasciculi to the trochlear and oculomotor nuclei. Since lesions
in this region unfortunately extended into both the descending
and ventromedial vestibular nuclei, specific conclusions concern-
ing ascending MLF projections from the individual cell groups
cannot be made from the available material. Nevertheless, certain
observations of the ascending MLF projections from this caudal VNC
region including both nuclei, are possible. Neither side of this

projection system is large, but the contralateral degenerated
fibers are more numerous than those on the ipsilateral side.
The preterminal degeneration pattern in the trochlear nuclei is
more prominent than that seen in the oculomotor nuclei. The
initial trajectory of these degenerated fibers from the VNC
lesion area is identical to that of commissural fibers. It is
not possible, therefore, to distinguish between degenerated fibers
of the two systems as they course ventromedially through the
medial vestibular region toward the midline. Since many of
these fibers pass through the nuclei of the VIth and VIIth
cranial nerves, possible vestibulo-abducens projections are
obscured by numerous degenerated fibers en passant. Elucidation
of these projections must await subsequent investigations
utilizing the appropriate experimental techniques (see
Discussion).

Degenerated projections to eye muscle nuclei are noted in
four cases with lesions involving the ventrolateral vestibular
nucleus (V10, V15, V17, V24). In V10 and V15 lesions of the
ventral portion of VL produced degenerated fibers which ascend
bilaterally in the medial longitudinal fasciculi. The
ipsilateral MLF receives a slightly stronger projection than
the contralateral MLF. Fragments of neuronal degeneration are
observed in relation to abducens, trochlear and oculomotor cells.
Fine degeneration fragments suggestive of preterminal fibers are

seen in the VIth nuclei of case V10. As previously noted, however, there are many degenerated fibers en passant in this region and this point should be confirmed with electron microscopy or other techniques. Cases V17 and V24 also exhibit degenerated fibers ascending bilaterally in the medial longitudinal fasciculi, but in these cases the contralateral degenerated fiber contingent is greater than that of the ipsilateral side. The lesion in V24 involved a more medial part of the ventrolateral nucleus than the previous lesions, and in V17 VL damage was situated more dorsally and caudally. The variation in the pattern of degenerated ascending projections seen in these cases may thus be a result of differential projections of the VL subdivisions upon the various ipsi- and contralateral eye muscle nuclei (see Discussion). However, it should be noted that the medial border of the V24 lesion and a small medial secondary lesion in V17 might have directly damaged a few of the fibers of the ipsilateral MLF immediately rostral to the abducens nucleus in each of these cases, thus changing the rostral degeneration patterns through the addition of a possible non-vestibular fiber component.

A lesion confined to the cerebellar peduncle and affecting parts of both the dorsolateral and dorsomedial nuclei (case V16) gave rise to a substantial degenerated fiber projection to ipsilateral trochlear and oculomotor nuclei. A somewhat weaker

projection to the contralateral homonymous cell groups is seen. Following a lesion of the dorsolateral nucleus (V7) which is restricted to caudal levels of this cell group posterior to its maximum development, the ascending degeneration pattern is similar but less prominent than that observed in case V16.

E. Vestibulo-cerebellar Connections

A small fascicle of primary vestibular afferent fibers degenerates following evulsion of the VIIIth nerve ganglia (Leake, 1974). This diffuse bundle passes through the medial aspect of the dorsolateral vestibular nucleus toward rostral cerebellar levels. Orally, these fibers proceed medially and are found close to the midline where they turn dorsally to terminate in the granular layer of the cerebellum bilaterally.

Lesions produced in this study give rise to a voluminous pattern of cerebellar afferent degeneration which appears to be superimposed upon the relatively restricted degeneration pattern of primary vestibulo-cerebellar fibers previously described. Compact fascicles of degenerated fibers ascending from VNC lesions occupy a lateral position in the cerebellar peduncle. Other, more diffusely organized degenerated fibers, course medially through the rostral VNC, filtering through or slightly above the cerebellar nuclei. Such fibers cross the midline at all levels in the base of the cerebellum near the roof of the fourth ventricle or in the anterior medullary velum.

Decusssting fibers destined for the cerebellum also occur at more caudal levels, as described in the discussion of vestibular commissural projections.

Unless direct damage is inflicted upon the auricles as in case V8 (Fig. 45d), these lateral wing-like protrusions of the cerebellum remain free of degeneration. Degenerated cerebellar afferents interrupted in VNC lesions appear to terminate chiefly in the medial two-thirds of the cerebellar granular layer. The degeneration does not extend to caudal levels of the cerebellum, and the oral pole of the cerebellar lobe frequently is clear of degenerated neuronal fragments. It is of considerable interest that this region of termination for vestibulo-cerebellar fibers roughly corresponds to the region of the cerebellum eliciting the "medial--area" behavioral pattern of Goodman and Simpson (1960).

In general, lesions of the oral VNC produced greater numbers of degenerated cerebellar afferents than are observed following lesions at more caudal levels. In one case, V6, in which the VIIIth nerve ganglia remained intact and a lesion was localized in the medial and descending vestibular nuclei, the cerebellum is completely free of degeneration.

Following damage to the auricle in case V8, degeneration can be observed throughout the cerebellar granular layer at the level of the lesion and in more caudal sections. In the ipsilateral oral VNC, degenerated preterminal-like neuronal fragments are especially

prominent in the dorsomedial vestibular nucleus. Some degenerated fibers also extend caudally into the ventrolateral vestibular nucleus. An ascending degenerated projection is noted bilaterally in the medial longitudinal fasciculi in this case. This projection is not voluminous, but fibers appear to reach both trochlear and oculomotor nuclei.

F. Auditory Pathways

Concomitant damage to cochlear nuclei and/or interruption of secondary auditory fibers in several cases yielded data elucidating certain basic aspects of the Caiman secondary auditory pathways.

1. Normal Anatomy. Two auditory relay nuclei are delineated by terminal degeneration in the experimental material: the superior olivary complex and a nucleus of the lateral lemniscus. The morphology of these cell groups was studied in silver and Nissl stained sections.

A detailed description of the superior olivary complex in a related species, Alligator mississippiensis, has been presented by Ariëns Kappers, Huber and Crosby (1936) and since the major features of its structure are similar in Caiman crocodilus we have followed the nomenclature of these authors. This small-celled nucleus consists of two parts which are continuous with each other for a short distance at a level which roughly coincides with the caudal pole of nucleus laminaris. The caudal and more dorsal portion is situated ventrolateral to

the large cells of the dorsal division of the motor facial
nucleus. This caudal portion of the superior olive is
wedge-shaped (Figs. 44b, 48);its contours are very similar to
the ventral division of the motor nucleus of the VIIth nerve
which abuts against and assumes the position of this olivary
subdivision at more oral levels (Figs. 44b, c).

The second part of the superior olive is recognized more
ventrally, embedded in the dense fiber meshworks comprising the
trapezoid body and lateral lemniscus. In sections at caudal
levels it appears as a ventromedial extension of the previously
described olivary subdivision (Fig. 44b). This triangular
nucleus extends far rostrally in the portine tegmentum, and
at oral levels assumes a progressively more ventral and lateral
position in the caudal mesencephalon (Fig. 44d).

The large-celled nucleus of the lateral lemniscus is in the
dorsolateral tegmentum at a level through the caudal pole of the
optic tectum. It is roughly coextensive with the anterior
one-third of the trochlear nucleus and the posterior half of
the oculomotor mucleus. Rostrally there appears to be two
separate cell groups, one situated dorsal to the other with a
small cell-poor region intervening. However, the cells of the
two regions are identical and at caudal levels these cell
groups become contiguous.

Auditory responses have been recorded from single units in

the midbrain of Caiman crocodilus (Manley, 1971) in the

region described by Ariëns Kappers et al (1936) as the

torus semicircularis, the presumptive reptilian homologue of

the mammalian inferior colliculus. Recently a more detailed

account of the normal anatomy of this midbrain auditory area

has been presented by Pritz (1974a). The torus protrudes into

each tectal ventricle over the caudal two-thirds of the

midbrain. It is subdivisible into two large nuclei. A

peripheral external nucleus consists of a periventricular

layer of cells which is continuous with the deep layers of the

tectum. The large homogeneous mass of gray matter constituting

the bulk of the torus is designated the central nucleus.

2. Auditory Projections Defined by Neuronal Degeneration

The trajectory of degenerated auditory fibers apparently

originating in nucleus angularis, is illustrated in Figure 44

(a schematic diagram of the degeneration pattern in case V18).

The lesion is slightly ventrolateral to nucleus angularis and

interrupts a large compact fiber bundle which issues from the

ventral border of this primary auditory nucleus (Fig. 50).

This fascicle runs from nucleus angularis along the marginal

aspect of the brainstem, coursing for the most part lateral to

the large spinal nucleus and tract of the trigeminal nerve

(see Figure 44c). Ventromedial to this latter cell group

degenerated fibers 1) turn caudalward to terminate in the

dorsocaudal part of the ipsilateral superior olive (Fig. 44b),
2) terminate in the ventral and cephalic part of the ipsilateral
superior olive (Fig. 44d), or 3) enter the trapezoid body to
reach the contralateral superior olivary complex and/or
lateral lemniscus (44d, e, f). The trapezoid body is
comprised of large caliber decussating fibers which extend
across the ventralmost part of the medulla. Degenerationg
secondary auditory fibers reach the cephalic part of the contra-
lateral superior olivary complex via the trapezoid body, and
fine preterminal degeneration is observed in this cell group.
Degenerated fibers which pass ventral to the olive turn sharply
rostralward near its lateral border and ascend in the lateral
lemniscus. Orally, these lemniscal fibers turn dorsally and
run along the lateral margin of the mesencephalon. At this
level the nucleus of the lateral lemniscud is situated medial
to the bulk of the degenerated lemniscal fibers. It receives
fine caliber collateral-like degenerated fibers which course
perpendicular to the grain of the lemniscus and enter the
nucleus from its lateral margin. The remainder of degenerating
lemniscal fibers proceed dorsally in the lateral tegmentum
to a point on a level with the sulcus limitans, where they
turn abruptly toward the midline and distribute to cells in the
dorsolateral portion of the torus semicircularis. Degenerated
fibers in the torus are diffusely organized and can be observed,

in small numbers, at most levels rostral to the nucleus of the lateral lemniscus.

Degenerated auditory fibers which follow trajectories similar to those described in case V18 also can be observed in cases V7, V16, V25. However, certain variations in degeneration patterns are noted. Figure 44b depicts a cuadal level of the brainstem in case V18 showing that degeneration in the caudal portion of the ipsilateral superior olive in this case is confined to the lateral aspect of the nucleus. Following the lesion in case V16 which is situated ventromedial to nucleus angularis at a rostral level, a more medial group of degenerating fibers can be observed. Some of these degenerated fibers arch ventrally and run parallel and immediately adjacent to the medial aspect of the ipsilateral olive. In V16 the caudal portion of the olive does not present the fine terminal degeneration seen in case V18; rather, degeneration is observed in the ventral part of the olive and is most prominent at more rostral levels. This case also differs from the previously described animal in that the ipsilateral degenerating fiber contingent, ascending in the lateral lemniscus, is greater then its contralateral counterpart.

Lesions in two cases, V17 and V25, damaged both the medial and lateral fiber systems described in V18 and V16 respectively. Degenerated fibers in these cases are observed in relation to

both medial and lateral aspects of the caudal olivary nucleus.
The fine "peppered" appearance of degeneration in this nucleus
appears restricted to the medial and ventral part of the
caudal superior olive in V17 (a pattern similar to case V16),
whereas degeneration is more evenly distributed throughout
the dorsocaudal superior olive at a level slightly caudal to the
lesion in case V25. The ascending lemniscal projection is
bilateral but considerably more voluminous on the contalateral
side in both animals, V25 and V17.

In addition to the projections described previously,
degenerated fibers issuing from the medial portions of lesions
in cases V16, V17 and V25 also are observed to reach the
midline in the dorsal tegmentum, where they turn sharply
ventralward to enter the trapezoid body and course to the medial
contralateral superior olive. Fibers following this midline
trajectory are especially prominent in V17 and V25 in which
lesions extend relatively far medially into the acoustic tubercle.
Fine preterminal degeneration fragments can be ovserved in the
ventromedial portion of the contralateral superior olive in
these cases.

No consistent pattern of degeneration could be observed in
the contralateral auditory nuclei as a consequence of lesions in
this study. In most cases the contralateral acoustic tubercle
is completely devoid of degenerating neuronal fragments. However,

a convincing degenerated projection to the ventromedial aspect
of the contralateral nucleus laminaris can be found in one
animal (case V25). A thick fascicle of degenerated fibers
coalesces from the ventral border of a lesion undercutting nucleus
laminaris. These fibers presumably originate from one or both of
the two nuclei, magnocellularis lateralis and laminaris, which occupy
the medial portion of the acoustic tubercle in this region. This
degenerating fascicle assumes a periventricular position, curving
rostrally and ventrally toward the midline, and then coursing dorso-
medially toward the contralateral nucleus laminaris. Degeneration is
seen in the neuropil immediately ventral to the bipolar cells consti-
tuting the medial one-third of the opposite nucleus laminaris at
approximately the same level as the lesion, and in several more rostral
sections.

DISCUSSION

The morphology of the vestibular nuclear complex and the connections of the statoacoustic nerve in reptiles was initially described by Holmes in 1903, and additional observations were made early in the twentieth century by Edinger (1908), Beccari (1912) and van Hoevell (1916). The crocodilian vestibular nuclear complex was illustrated and described in some detail by Ariëns Kappers, Huber and Crosby (1936). More thorough analyses of this area and its fiber connections in a variety of reptiles were presented by Weston (1936) and Stefanelli (1944). These and other reports contributed a considerable amount of descriptive information about the vestibular nuclei and eighth nerve connections, which was resynthesized by Larsell in 1967. Mehler's 1972 synopsis provided a critical assessment of the natural history of the VNC and pointed out various areas in which experimental studies are needed to establish or verify assumed homologies and fill gaps in our knowledge concerning the nonmammalian vestibular nuclear complex.

A recent renewal of interest in the vestibular system has resulted in a number of experimental studies of the VNC, especially its afferent connections, in nonmammalian species. The distribution of primary eighth nerve afferents in the frog has been defined in three separate experimental studies (Hillman, 1969a; Gregory, 1972; Mehler, 1972). Similar analyses have been provided in larval

petromyzonts (Rubinson, 1974) and in bony fishes (Maler, 1974). Other investigations have contributed analyses of the central distribution of the statoacoustic nerves in two reptiles, Caiman crocodilus (Leake, 1974), and the tegu lizard, Tupinambis nigropunctatus (DeFina and Webster, 1974). The classical work of Boord and Rasmussen (1963), who utilized the Nauta-Gygax method to define the central projections of the cochleolagenar nerve in pigeon, has been continued to provide a more complete description of the distribution of primary lagenar fibers in the pigeon acousticolateral area (Boord and Karten, 1974).

Some experimental data, although limited in amount, has also been presented on nonmammalian secondary vestibular connections. Commissural projections from the nuclei of termination of the eighth nerve (Grofová and Corvaja, 1972) and vestibulospinal projections (Corvaja and Grofová, 1972; Corvaja, Grofová and Pompeiano, 1973) have been described in the toad (Bufo bufo L.) A more comprehensive study of VNC projections has been carried out recently in the bullfrog by Fuller (1974). The reptilian secondary vestibular connections have not previously been examined with contemporary experimental and silver degeneration techniques; and the analysis of these pathways in Caiman crocodilus presented herein appears to be a logical next step in filling the gaps in our knowledge concerning nonmammalian vestibular systems.

A.   Vestibulospinal Projection

Descending vestibulospinal fibers appear to arise primarily from
the ventrolateral vestibular nucleus in Caiman.   The lack of a spinal
cord projection from more rostral vestibular nuclei, dorsomedialis and
dorsolateralis, suggests an organization parallel to that described in
mammals, in which the vestibulospinal tract originates from the
lateral and medial vestibular nuclei. In this regard, it is somewhat
perplexing that the most caudal vestibular nuclei in Caiman, the
descending vestibular nucleus and ventromedialis, do not appear to
contribute fibers to the vestibulospinal projection. The limited
number and size of lesions in ventromedialis, the apparent reptilian
homologue of the mammalian medial vestibular nucleus, might acount for
the failure to observe such fibers in the present material.

The vestibular spinal projection to the ventral funiculi in Caiman
is a well-defined tract which is comparable to that seen in other
vertebrates and is similar in its course to that described in amphibi-
ans (Corvaja et al, 1973: toad; Fuller, 1974: bullfrog). It seems
probable that the degenerated lateral funicular descending pathway
encountered in the present experiments might have a supraspinal origin
other than the vestibular nuclei, since lesions of the VNC unavoidably
interrupt many fibers of passage. Further, in a case in which no
descending MLF or anterior funicular projection could be demonstrated,
this lateral funicular fiber system degenerated independently, the

segregation of the two systems in this case also suggests that there are different origins for the two projections.

Differential patterns of degeneration within the ventrolateral vestibular nucleus resulting from damage to posterior as opposed to anterior and horizontal ampullary nerves have been reported in Caiman (Leake, 1974). These results suggest that, as in mammals, nerves from specific semicircular canals project to restricted regions of the vestibular nuclei. In mammals, the VL cells which give rise to vestibulospinal fibers also exhibit a somatotopic organization (See review in Brodal, Pompeiano and Walberg, 1962). Dorsocaudal Deiter's cells contribute fibers to lumbar and sacral spinal levels; ventral and rostral VL neurons project to thoracic ventral horn cells; and fibers from the medial vestibular nucleus project to the cervical spinal cord. In contrast, lesions of ventral Deither's nucleus in the reptile result in a degenerated projection that extends only to cervical ventral horn cells. When the dorsal aspect of VL is damaged, the vestibulospinal projection can be traced caudally to lumbar and sacral cord levels. This variation in degeneration patterns indicates that, although differing in the details of their organization, reptili-an and mammalian vestibulospinal projections appear to share certain basic functional features in that different sectors of VL are related to different, specific cord levels.

No differential projection to various spinal cord levels has been

found in amphibians (Corvaja et al, 1973; Fuller, 1974). Lesions in
the VNC of these species result in degenerating vestibulospinal fibers
which descend throughout the length of the spinal cord. Thus the
Caiman vestibulospinal system may represent a significant advance in
the central processing of vestibular information relating to postural
tonus.

B.   Vestibular Commissural Connections

Vestibular commissural projections are observed from lesions
within all portions of the Caiman VNC. These fibers, though never
great in numbers, cross the midline dorsally in the brainstem and
course along the border of the periventricular gray matter to reach
the contralateral vestibular nuclei. Weston (1936) described the
trajectory of these fibers in crocodilians, but he reported that many
of them were "commissural primary vestibular fibers". Recent experi-
mental work has shown, however, that no primary afferents of the
statoacoustic nerve cross to the opposite side of the medulla in Caiman
(Leake, 1974). From the present observations it appears that secondary
commissural projections exist between homonymous vestibular nuclei, and
that the decussating primary vestibular afferents described by Weston
were actually secondary fibers. It is also possible that some of
these decussating fibers are "fibers of passage" which might
originate, for example, from the cerebellar nuclei ipsilateral to the
lesion.

In the toad a weak commissural projection following a trajectory

similar to that described in the Caiman has been demonstrated (Grofová and Corvaja, 1972). In addition, a prominent projection also has been noted by these authors which emerges from the VNC ventrally, follows the margin of the ipsilateral medulla, crosses the midline and ascends dorsally to enter the contralateral vestibular region from its medial aspect. Other vestibular commissural fibers in the toad emerge medially from the VNC and continue medially through the periventricular gray, turn sharply ventalward near the midline and course along the ventral and lateral margin of the contralateral medulla to enter the VNC from its ventral aspect. A similar trajectory is also followed by the secondary vestibular commissural projection in the bullfrog as reported by Fuller (1974). VNC fibers in Caiman were never observed to follow either of these two ventral pathways described for secondary vestibular fibers in the amphibians.

C.   Ascending MLF Projection

There are still some unanswered questions concerning the overall distribution of ascending secondary vestibular fibers in mammals. It is generally agreed, however, that those coursing in the medial longitudinal fasciculus are destined chiefly for the cranial nerve nuclei supplying the extrinsic ocular muscles. Such fibers probably arise only from the superior vestibular nucleus and from the anterior portion of the medial vestibular nucleus in mammals (see Tarlov, 1970 for review). In the Caiman lesions throughout the VNC produce degenerating fibers which ascend in the MLF reach extraocular motor nuclei. A regional

origin of vestibulo-oculomotor connections, based on differential VNC
lesions, is not apparent in the crocodilus, but certain similarities
become evident when details concerning the trajectories of these
connections in Caiman are compared with data from mammalian studies.

In mammals, fibers from the superior vestibular nucleus ascend
only in the ipsilateral MLF. These fibers decussate at rostral levels
so that connections to trochlear and oculomotor nuclei actually are
bilateral, although the ipsilateral projection is much more prominent.
Similarly, in Caiman, lesions of the rostral VNC (especially those
involving the dorsomedial vestibular nucleus) result in degenerated
fibers which ascend in the ipsilateral MLF to trochlear and oculomotor
nuclei, while only a few such fibers occur on the contralateral side.
Lesions of the rostral ventrolateral nucleus result in a similar
pattern of degeneration. The lack of degenerated fibers projecting to
the abducens nucleus following the above-described lesions also
parallels observations in mammals, in which a substantial projection to
this nucleus arises only from lesions in the rostral portion of the
ipsilateral medial vestibular nucleus.

The mammalian medial vestibular nucleus projects rostrally via
the contralateral MLF and sends terminal fibers to the ipsilateral
abducens nucleus, the contralateral trochlear nucleus and the oculomotor
nuclei of both sides. Projections from the Caiman caudal VNC, including
the descending and ventromedial vestibular nuclei and caudal portions
of VL, are quite similar. A slight exception occurs in that some fibers

also course rostrally in the ipsilateral MLF and a weak terminal
projection is noted to the ipsilateral trochlear nucleus of the reptile.

In mammals, the lateral vestibular nucleus probably does not
give rise to projections to any of the extraocular motor nuclei, while
the homologous reptilian ventrolateral vestibular nucleus as described
above apparently has such connections. Thus, despite the resemblance
in organization of the vestibular nuclei and some of their connections
found between Caiman and mammalian forms, the phylogenetic differentia-
tion of these nuclei appears to be still incomplete and a greater
functional overlap probably occurs among these cell groups. Yet there
appears to be a basic pattern within the anatomical connections sub-
serving ocular movements induced by vestibular stimuli which is common
to reptilian and mammalian species.

D. Cerebellar Connections

The secondary vestibulocerebellar projection appears to be more
extensive than the projection of primary vestibulocerebellar fibers.
The observation in the present material that vestibular fibers
ascending to the cerebellum are most prominent in a region corresponding
approxiamtely to that eliciting the "medial-area" behavioral pattern
of Goodman and Simpson (1960) and "vermal zone" of Goodman (1969) is
provocative. Yet the temptation to speculate upon the possible signifi-
cance of this correlation should be avoided. It is impossible in the
present material to distinguish between true vestibulocerebellar
fibers and fibers of the spinocerebellar tract which might have been

interrupted in many or all lesions of the VNC.

The observation that cerebellar corticofugal fibers pass from the auricle to the ipsilateral rostral VNC (including the dorsomedial and dorsolateral nuclei) and in lesser quantities to rostral VL agrees well with data reported by Senn and Goodman (1969). These authors noted that long corticofugal fibers which originate in this regions from Purkinje cells distribute ipsilaterally to "nucleus anterior vestibu-laris" and nucleus Deiters.

In contrast to the vestibulocerebellar projection in Caiman these fibers in frogs have been found to project to the granular layer of both the auricular lobe and the corpus cerebelli by Fuller (1974). This author further reported that secondary vestibulocerebellar fibers also appear to reach the molecular layer of the corpus cerebellum. Degenerated fibers were never observed in the molecular layer in the available Caiman material. It has been suggested (Hillman, 1969) that the cerebella of the frog and the alligator represent unique stages in evolutionary development. Rana is considered an example of a species in which cerebellar development has lagged, as demonstrated by certain primitive characteristics of its cerebellar circuitry. The Caiman, on the other hand, is said to have progressed in a distinct manner, developing features which may be representative of an inter-mediate stage in the development of mammalian-like cerebelli. The contrasting experimental data presented in these species appears to be consistent with this notion.

E.   Auditory Projections

Auditory responses have been recorded from single units in the torus semicircularis of Caiman crocodilus by Manley (1971), and Pritz (1974a) has studied in detail the ascending toral projections as well as the connections of a thalamic auditory area (1974b) delineated by degenerated toral efferents. Characteristic frequencies of auditory neurons in the Caiman "cochlear nuclei" have been determined by Manley (1970) and the projection and distribution of primary eighth nerve afferents upon these cell groups has been demonstrated experimentally (Leake, 1974). In spite of this renewed interest in the reptilian auditory system, the fiber pathways of higher order neurons connecting the brainstem auditory nuclei to the auditory midbrain area have not been experimentally defined. Thus, although the present data is incomplete, it appears worthwhile to make certain observations on these pathways.

Secondary auditory projections in nonmammalian species have been studied in detail only in the pigeon with the Nauta method (Boord, 1968). The course and connections of ascending auditory neurons from nucleus angularis and nucleus laminaris described in this avian form is strikingly similar to that seen in the Caiman case V18 and illustrated in Figure 44. Boord demonstrated that, in the pigeon, a similar lateral fiber contingent is separable into two components: one component consists of a third order axons from nucleus laminaris and the other component arises from the medial part of nucleus angularis.

These fibers, as in the reptile, contribute abundant preterminal degeneration to the ipsilateral superior olive, cross the raphé as part of the trapezoid body and extend rostralward into the lateral lemniscus near the contralateral superior olive. The avian ventral and latero-ventral nuclei of the lateral lemniscus are also reported to receive preterminal degeneration. These cell groups are quite similar in morphology and position to the two parts of the Caiman nucleus of the lateral lemniscus which, in the present experiments, have been demonstrated to receive similar degenerated lemniscal fibers. In addition, a dorsal nucleus of the lateral lemniscus has been identified in pigeons, although preterminal degeneration does not appear to occur within it. A similar cell group is present in Caiman, but no evidence of its possible auditory nature could be obtained. Upon consideration of the implied homology, the designation of this cell group as the "dorsal nucleus of the lateral lemniscus" in Caiman does not appear to be warranted at the present time.

In pigeons, nucleus magnocellularis cells project in an orderly sequence to the dorsal portion of the underlying nucleus laminaris. In addition, selective lesions of the caudal nucleus magnocellularis reveal a fiber projection which crosses the raphé dorsally (in the dorsal acoustic stria) and terminates along the ventral border of the contralateral nucleus laminaris. Similar fibers are evident in Caiman as a result of a medially placed lesion in the acoustic tubercle, although it is not clear whether these fibers originate in the contra-

lateral nucleus magnocellularis, nucleus laminaris or in both. From analysis of the limited available data, it appears that the cell morphology and fiber connections of nucleus laminaris in the Caiman and in avian species is very similar. Confirmation of this supposition must await studies employing selective lesions of the reptilian brainstem auditory nuclei. Nucleus laminaris is of particular interest as it is considered to be homologous to the mammalian medial superior olive (Boord, 1968).

In Caiman an additional "medial" auditory fiber component also can be observed. These fibers course medially in the dorsal tegmentum, turn ventralward at the midline raphe to join the trapezoid fibers and project to the medial portion of the contralateral superior olive. No equivalent fiber system has been demonstrated in the pigeon and only an ipsilateral auditory input to the superior olive has been reported in this species. This point is of consiereable importance in establishing the homology of this nonmammalian cell group. In mammals significant and approximately equal bilateral auditory inputs are considered to be a basic organizational and functional feature of the superior olivary complex. In the present Caiman material an organization which parallels that of the mammalian superior olivary sub-divisions is suggested in that the lateral border of the caudal superior olive receives a lateral fiber projection from ipsilateral auditory nuclei while the medial border receives a contralateral auditory input via a medial trajectory. From the standpoint of

comparative anatomy, details of the origins of these and other fiber
components related to the Caiman superior olive merit additional
investigation,

LITERATURE CITED

1. Albrecht, M. H. 1954 Mounting frozen sections with gelatin. Stain Technol., 29: 89-90.

2. Anderson, T. 1951 Techniques for the preservation of three--dimensional structure in preparing specimens for the electron microscope. Trans. N. Y. Acad. Sci., Ser. II, 13: 130-350.

3. Ariëns Kappers, C. U., G. C. Huber and E. C. Crosby. 1936 The comparative anatomy of the nervous system of the vertebrates, including man. MacMillan, New York.

4. Bagger-Sjöbäck, D. and J. Wersäll. 1973 The sensory hairs and tectorial membrane of the basilar papilla in the lizard, Calotes versicolor. J. Neurocytol., 2: 329-350.

5. Baird, I. L. 1967 Some histological and cytological features of the basilar papilla in the lizard, Anolis carolinensis. Anat. Rec., 157: 208-209.

6. Baird, I. L. 1969 Some findings of comparative fine structural studies of the basilar papilla in certain reptiles. Anat. Rec., 163: 149.

7. Baird, I. L. 1970a The anatomy of the reptilian ear. In: Gans, C. and Parsons, T. (eds), Biology of the reptilia, vol. 2, p. 193-275. Academic Press, New York.

8. Baird, I. L. 1970b A preliminary report on light and electron microscopic studies of a crocodilian basilar papilla. Anat. Rec., 166: 274.

9. Baird, I. L. 1974 Anatomical features of the inner ear in submammalian vertebrates. In: Keidel, W. D. and Neff, W. D. (eds), Handbook of sensory physiology, vol. V, p. 159-212. Springer-Verlag, New York.

10. Baird, I. L. and W. F. Marovitz. 1971 Some findings of scanning and transmission electron microscopy of the basilar papilla of the lizard, Iguana iguana. Anat. Rec., 169:270.

11. Barber, V. C. and A. Boyde. 1968 Scanning electron microscopic studies of cilia. Z. Zellforsch., 84: 269-284.

12. Beccari, N. 1912 La constituzione, i nuclei terminali e le vie di connessione del nervo acustico nella Lacerta Muralis. Arch. Ital. Anat. Embriol. 10: 646-698.

12. Beccari, N,   1912 La constituzione, i nuclei terminali e le vie
     di connessione del nervo acustico nella Lacerta Muralis,
     Arch, Ital, Anat. Embriol. 10: 646-698,

13. Boord, R. L.   1968   Ascending projections of the primary
     cochlear nuclei and nucleus laminaris in the pigeon.
     J. Comp. Neurol, 133: 523-542,

14. Boord, R. L. and H. J. Karsten.   1974   The distribution of
     primary lagenar fibers within the vestibular nuclear complex
     of the pigeon. Brain Behav, Evol., 10: 228-235.

15. Boord, R. L, and G. L. Rasmussen. 1963   Projection of the
     cochlear and lagenar nerves on the cochlear nuclei of the
     pigeon. J. Comp, Neur., 120: 463-475.

16. Brodal, A. O. Pompeiano and F. Walberg, 1962   The Vestibular
     Nuclei and their Connections, Anatomy and Functional
     Correlations. Thomas: Springfield, Illinois,

17. Correia, M. J., J. P. Landolt and E. R. Young. 1974   The
     sensura neglecta in the pigeon: A scanning electron and light
     microscope study. J. Comp. Neurol., 154: 1235-1240,

18. Corvaja, N. and I. Grofová. 1972   Vestibulospinal projection in
     the toad. Prog. Brain Res., 37: 207-307.

19. Corvaja, N., I. Grofová and O. Pompeiano. 1973   The origin,
     course and termination of vestibulospinal fibers in the toad.
     Brain Behav. Evol., 7: 401-423.

20. de Burlet, H. M. 1934   Vergleichende Anatomie des statoakustis-
     chen Organs. a) Die innere Ohrsphäre; b) Die mittlere
     Ohrsphäre. In: Handbuch der vergleichenden Anatomie der
     Wirbelthiere, II, 2 Hälfte, Urban und Schwarzenberg, Berlin
     und Wien,

21. de Burlet, H. M. 1935   Die Ungleichwertigkeit der Bogengänge,
     Z, Anat. Entwickl,-Gesch,, 104: 79-102,

22. DeFina, A. V. and D, B, Webster. 1974   Projections of the
     intraotic ganglion to the medullary nuclei in the tegu
     lizard, Tupinambis nigropunctatus, Brain Behav, Evol., 10:
     197-211,

23. Dohlman, G. 1961   On the case for repeal of Ewald's second law.
     Acta Otolaryng., Suppl., 159: 15-24.

24. Ebbesson, S. O. E. and W. J. H. Nauta. 1970 Contemporary Research Methods in Neuroanatomy. Springer-Verlag, New York.

25. Edinger, L. 1908 Vorlesungen uber den Bau der nervosen Centralorgane des Menschen und der Tiere, Teil. 2. F. C. W. Vogel, Leipzig.

26. Engström, E. 1970 The first-order vestibular neuron. In: Fourth Symposium on the Role of the Vestibular Organs in Space Exploration. NASA SP-197 (Naval Aerospace Medical Institute, Pensacola, Florida), p. 123.

27. Fink. R. P. and L. Heimer. 1967 Two methods for selective silver impregnation of degenerating axons and their synaptic endings in the central nervous system. Brain Res., 4: 369-374.

28. Fuller, P. M. 1974 Projections of the vestibular nuclear complex in the bullfrog (Rana catesbiana). Brain Behav. Evol., 10: 157-169.

29. Goodman, D. C. 1969 Behavioral aspects of cerebellar stimulation and ablation in the frog and alligator and their relationship to cerebellar evolution. In: R. Llinás (ed), Neurobiology of Cerebellar Evolution and Development. Amer. Med. Ass., Chicago, p. 467-473.

30. Goodman, D. C. and T. J. Simpson. 1960 Cerebellar stimulation in the unrestrained and unanesthetized alligator. J. Comp. Neurol., 114: 126-136.

31. Gregory, K. M. 1972 Central projections of the eighth nerve in frogs. Brain Behav. Evol., 5: 70-88.

32. Grofová, I. and N. Corvaja. 1972 Commissural projection from the nuclei of termination of the VIIIth cranial nerve in the toad. Brain Res., 42: 189-195.

33. Hama, K. 1969 A study of the fine structure of the saccular macula of the goldfish. Z. Zellforsch., 94: 155-171.

34. Hamilton, D. W. 1964 The inner ear of lizards. I. Gross structure. J. Morp., 115: 255-271.

35. Hamilton, D. W. 1969 The cilium on mammalian vestibular hair cells. Anat. Rec., 164: 253-258.

36. Hillman, D. E. 1969a   Light and electron microscopical study of the relationships between the cerebellum and vestibular organs of the frog. Exp. Brain Res., 9: 1-15.

37. Hillman, D. E. 1969b   Neuronal organization of the cerebellar cortex in amphibia and reptilia. In: R. Llinás (ed), Neurobiology of Cerebellar Evolution and Development. Amer. Med. Ass., Chicago, p. 279-326.

38. Hillman, D. E. 1974   Cupular structure and its receptor relationship. Brain Behav. Evol., 10: 52-68.

39. Holmes, G. 1903   On the comparative anatomy of the nervus acusticus. Trans. Roy. Irish Acad., 32: 101-144.

40. Landolt, J. P., E. R. Young and M. J. Correia. 1972   Vestibular ampullary structures in the pigeon: A scanning electron microscope overview. Anat. Rec., 174: 311-324.

41. Larsell, O. 1967   The comparative anatomy and histology of the cerebellum from myxinoids through birds. University of Minnesota Press, Minneapolis.

42. Leake, P. A. 1973   Central projections of the statoacoustic nerve in Caiman crocodilus. Masters Thesis: University of California, San Francisco.

43. Leake, P. A. 1974   Central projections of the statoacoustic nerve in Caiman crocodilus. Brain Behav. Evol., 10: 170-196.

44. Lewis, E. R. and C. W. Li. 1973   Evidence concerning the morphogenesis of saccular receptors in the bullfrog (Rana catesbeiana). J. Morph., 139: 351-362.

45. Lewis, E. R. and C. W. Li. 1975   Hair cell types and distributions in the otolithic and auditory organs of the bullfrog. Brain Res., 83: 35-50.

46. Lewis, E. R. and P. Nemanic. 1972   Scanning electron microscope observations of saccular ultrastructure in the mudpuppy (Necturus maculosus). Z. Zellforsch., 123: 441-457.

47. Lim, D. J. 1969   Three-dimensional observation of the inner ear with scanning electron microscope. Acta Oto-Laryngol. Suppl. 255.

48. Lim, D. J. 1971 Vestibular sensory organs. A scanning electron microscopic investigation. Arch Otolaryngol., 94: 69-76.

49. Lim, D. J. 1973a Formation and fate of the otoconia. Scanning and transmission electron microscopy. Ann. Otol. Rhinol. Largyngol., 82: 23-35.

50. Lim, D. J. 1973b Ultrastructure of the otolithic membrane and the cupula. A scanning electron microscopic observation. Adv. Oto-Rhino-Larygn., 19: 35-49.

51. Lim, D. J. 1974 The statoconia of the non-mammalian species. Brain Behav. Evol., 10: 37-51.

52. Lim, D. J. and W. C. Lane. 1969 Vestibular sensory epithelia. A scanning electron microscopic observation. Arch. Otolaryngol., 90: 283-292.

53. Lindeman, H. H. and H. W. Ades. 1972 Scanning electron microscopy of the vestibular end organs. In: Fifth Symposium on the Role of the Vestibular Organs in Space Exploration.

54. Luft, J. H. 1961 Improvements in epoxy resin embedding methods. J. Biophys. Biochem. Cytol., 9: 409-414.

55. Maler, L. 1974 The acousticolateral area of bony fishes and its cerebellar relations. Brain Behav. Evol., 10: 130-145.

56. Manley, G. A. 1970 Frequency sensitivity of auditory neurons in the caiman cochlear nucleus. Z. Vergl. Physiol., 66: 251-256.

57. Manley, J. A. 1971 Single unit studies in the midbrain auditory area of Caiman. Z. Vergl. Physiol., 71: 255-261.

58. Mehler, W. R. 1972 Comparative anatomy of the vestibular nuclear complex in submammalian vertebrates. Prog. Brain Res., 37: 55-67.

59. Miller, M. R. 1966a The cochlear duct of lizards. Proc. Calif. Acad. Sci., 33: 255-359.

60. Miller, M. R. 1966b The cochlear duct of lizards and snakes. Amer. Zool., 6: 421-429.

61. Miller, M. R. 1968 The cochlear duct of snakes. Proc. Calif. Acad. Sci., 35: 425-475.

62. Miller, M. R. 1973a A scanning electron microscope study
        of the papilla basilaris of Gekko gecko. Z. Zellforsch.,
        136: 307-328.

63. Miller, M. R. 1973b Scanning electron microscope studies of
        some lizard basilar papillae. Amer. J. Anat., 138:
        301-330.

64. Miller, M. R. 1974a Scanning electron microscope studies of
        some skink papillae basilares. Cell Tissue Res., 150:
        125-141.

65. Miller, M. R. 1974b Scanning electron microscopy of the lizard
        papilla basilaris. Brain Behav. Evol., 10: 95-112.

66. Mulroy, M. J. 1968 Ultrastructure of the basilar papilla of
        reptiles. Doctoral Dissertation, University of California,
        San Francisco.

67. Pritz, M. B. 1974a Ascending connections of a midbrain
        auditory area in a crocodile, Caiman crocodilus. J. Comp.
        Neurol., 153: 179-197.

68. Pritz, M. B. 1974b Ascending connections of a thalamic
        auditory area in a corcodile, Caiman crocodilus. J. Comp.
        Neurol., 153: 199-213.

69. Rasmussen, G. L. 1961 A method of staining the statoacoustic
        nerve in bulk with Sudan black B. Anat. Rec., 139:
        465-469.

70. Retzius, G. 1884 Das Gehörorgan des Wirbeltiers. II. Das
        Gehororgan de Reptilien, der Vögel und der Säugetiere.
        Samson & Wallin, Stockholm.

71. Robinson, L. R. 1969 Bulbospinal fibers and their muclei of
        origin in Lacerta viridis demonstrated by axonal degeneration
        and chromatolysis respectively. J. Anat. (Lond.), 105:
        59-88.

72. Rubinson, K. 1974 The central distribution of VIII nerve
        afferents in larval Petromyzon marinus. Brain Behav. Evol.,
        10: 121-129.

73. Senn, D. and D. C. Goodman. 1969 Patterns of localization in
        the cerebellar corticofugal projections of the alligator
        (Caiman sclerops). In: R. Llinás (ed), Neurobilogy of

Cerebellar Evolution and Development. Amer, Med. Ass., Chicago, p. 475-480.

74. Smith, C. A. and T. Takasaka. 1971   Auditory receptor organs of reptiles, birds and mammals.   In: Contributions to sensory physiology, vol. 5, Academic Press, New York-London.

75. Spöndlin, H.   1966   The organization of the cochlear receptor. Fortschr. Hals-Nas.-Ohren-Heilk, 13: 26-37.

76. Stefanelli, A.   1944   I centri statici e della coordinazione motoria dei rettili.   Commentat.   Pontif. Acad. Scient. 8: 147-293.

77. Steifensand, K.   1835   Untersuchunger über die Ampullen des Gehörörganes.   Arch. Anat, Physiol. Wiss. Med., 2: 171-189.

78. Tarlov, E.   1970   Organization of vestibulo-oculomotor projections in the cat.   Brain Res., 20: 159-179.

79. van Hoevell, J. L. D.   1916   The phylogenetic development of the cerebellar nuclei.   Kön Akad. v. Wetensch. te Amsterdam, Proc. Sec. Sc., 18: 1431.

80. von Düring, M., A. Karduck and H.-G. Richter   1974 The fine structure of the inner ear in Caiman crocodilus. Z Anat Entwickl. -Gesch., 145: 41-65.

81. Wersäll, J.   1956   Studies on the structure and innervation of the sensory epithelium of the cristae ampullares in the guinea pig.   Acta Oto-Laryngol. (Stockh.), Suppl., 126: 1-85.

82. Weston, J. K.   1936   The reptilian vestibular and cerebellar gray with fiber connections.   J. Comp. Neurol., 65: 93-119.

83. Wever, E. G.   1965   Structure and function of the lizard ear. J. Auditory Res., 5: 331-371.

84. Wever, E. G.   1967a   The tectorial membrane of the lizard ear: Types of structure.   J. Morph., 122: 307-320.

85. Wever, E. G.   1967b   The tectorial membrane of the lizard ear: Species variations.   J. Morph., 123: 355-372.

86. Wever, E. G.   1970   The lizard ear: Cordylus, Platysaurus and Gerrhosaurus.   J. Morph., 130: 37-56.

87. Wever, E. G. 1971a   Hearing in the crocolilia. Proc. Nat.
        Acad. Sci., Wash., 68: 1498-1500.

88. Wever, E. G. 1971b   The mechanics of hair-cell stimulation.
        Trans. Amer. Otol. Soc., 59: 89-107.

89. Wever, E. G. and J. A. Vernon. 1957   Auditory responses in the
        spectacled caiman. J. Cell. Comp. Physiol., 50: 333-339.

65

Figure 1. Acryllic scale reconstruction of the membranous labyrinth

and adjacent medulla, traced from horizontal serial

sections through whole head of Caiman crocodilus.

Figure 2. Transverse section from Caiman whole head series

illustrating approximate trajectory of lesioning

electrodes.

Figure 3.   Drawings of lateral (left side) and medial (right side)

views of the right membranous labyrinth of <u>Caiman</u>

<u>crocodilus</u>.

Abbreviations:

AC   anterior semicircular canal

AG   ganglion cells of the anterior root of the
VIIIth nerve

CC   common crus

ED   endolymphatic

HC   horizontal semicircular canal

ML   macula of the lagena

PB   papilla basilaris

PC   posterior semicircular canal

PG   ganglion cells of the posterior root of the
VIIIth nerve

S   saccule

U   utricle

Figure 4.   Stereophotographic pairs showing the right membranous

labyrinth of <u>Caiman</u> <u>crocodilus</u>, X8:

a. Lateral aspect of the labyrinth, <u>in</u> <u>situ</u>.

b. Medial aspect of the excised labyrinth.

Figure 3. AC, CC, HC, PC, S, PB, ML, ED, U, AG, PG
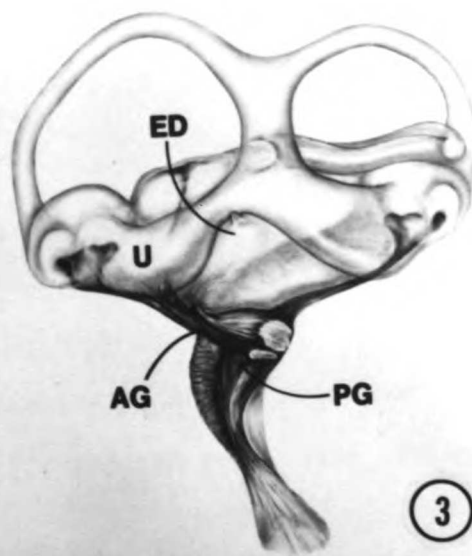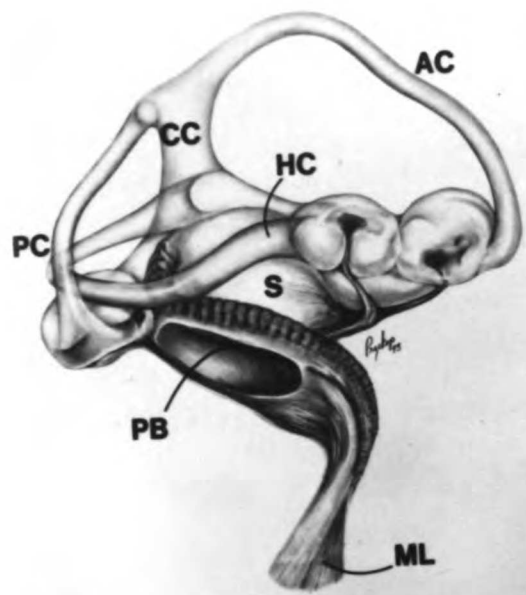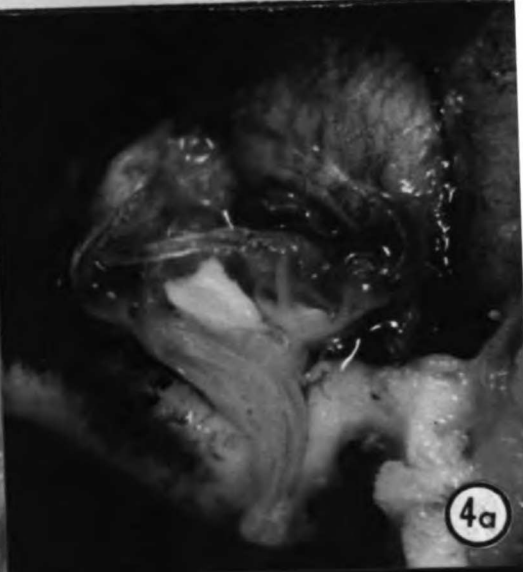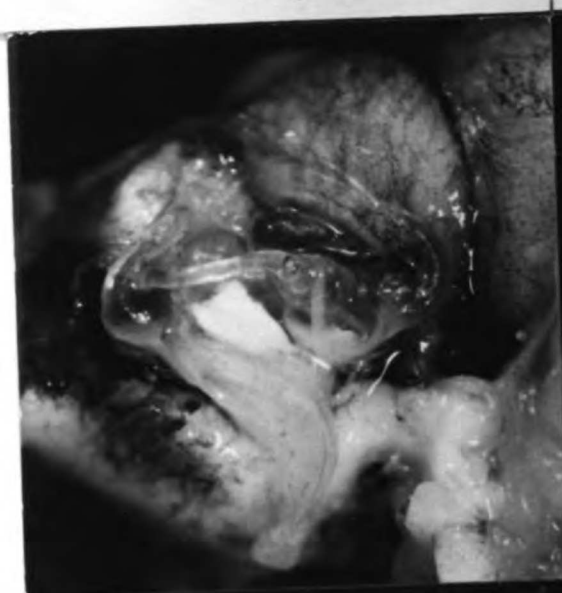
Figure 4a

Figure 4b

Figure 5. Illustration of cross-sectional view of the inner ear of

Caiman crocodilus. X170   (Reproduced from Wever, 1971b)

Figure 6. Appearance of Caiman cochlear duct in histological section

taken from whole head series.

Medial limbus
Scala vestibuli
Reissner's membrane
Limbic epithelium
Stria vascularis
Inner hair cells
Cochlear duct
Outer hair cells
Columnar cells
Tectorial membrane
Tympanic lamella
Supporting cells
Giant cells
Basilar membrane
Inner sulcus cells
Lateral limbus
Medial limbus
Blood vessels
Scala tympani
Nerve fibers
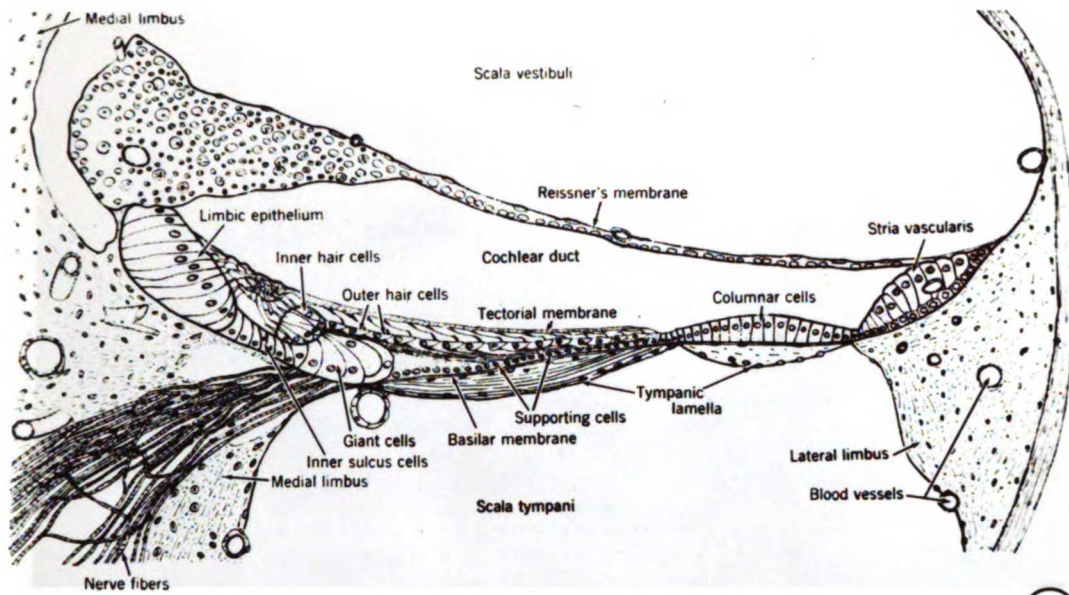
⑤
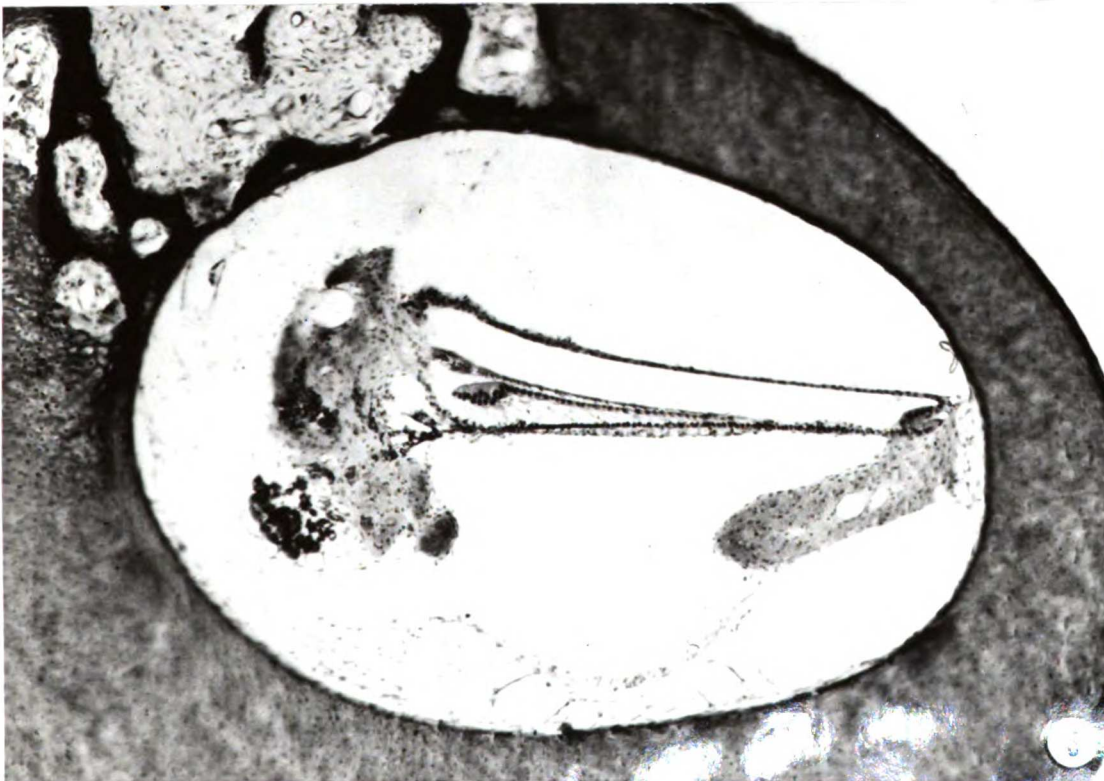
Figure 7. Low magnification scanning electron micrograph of left

cochlear duct. Arrows point out exposed portion of the

papilla basilaris. ML, portion of the cochlear duct

housing the lagenar macula. ~X40

Figure 8. Outher hair cells of the papilla basilaris from the

lagenar portion of the cochlear duct. ~X7,000

Figure 9. Outer hair cell os the proximal (dorsal) portion of the

cochlear duct. ~X10,000

Figure 10. Low magnification view of the exposed hair cells on the

basilar papilla near the proximal end of the cochlear

duct. ~X300
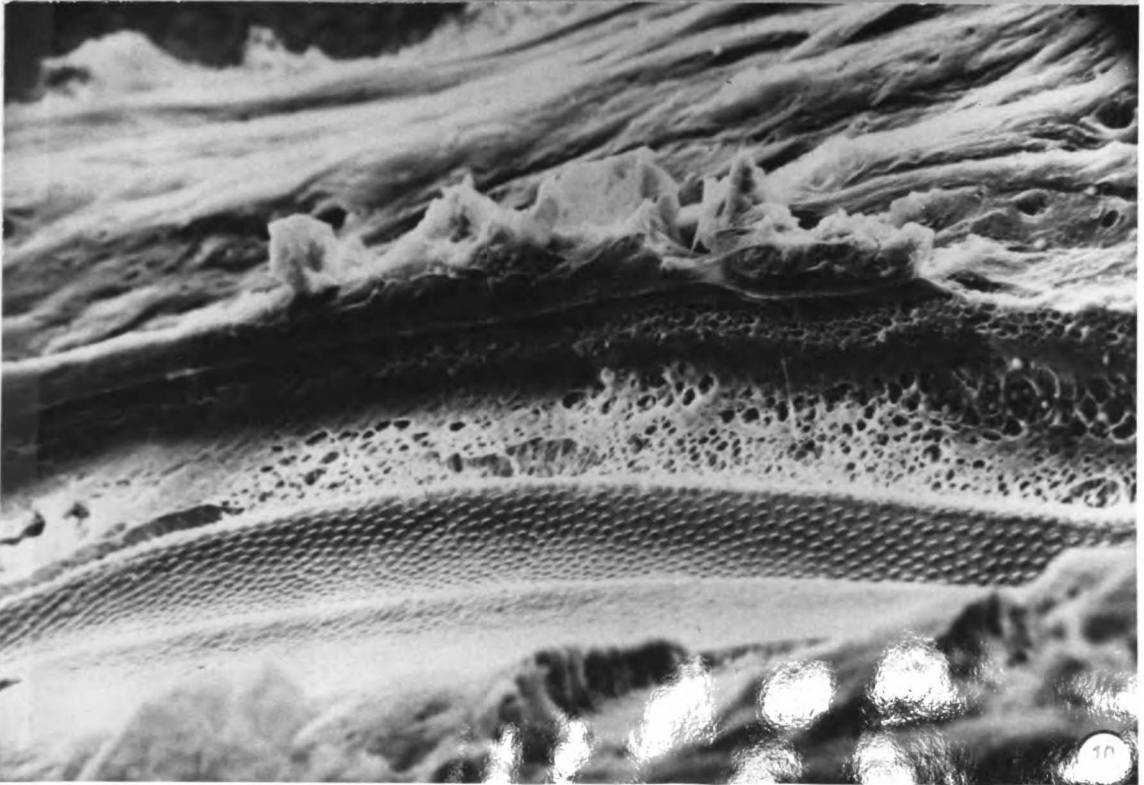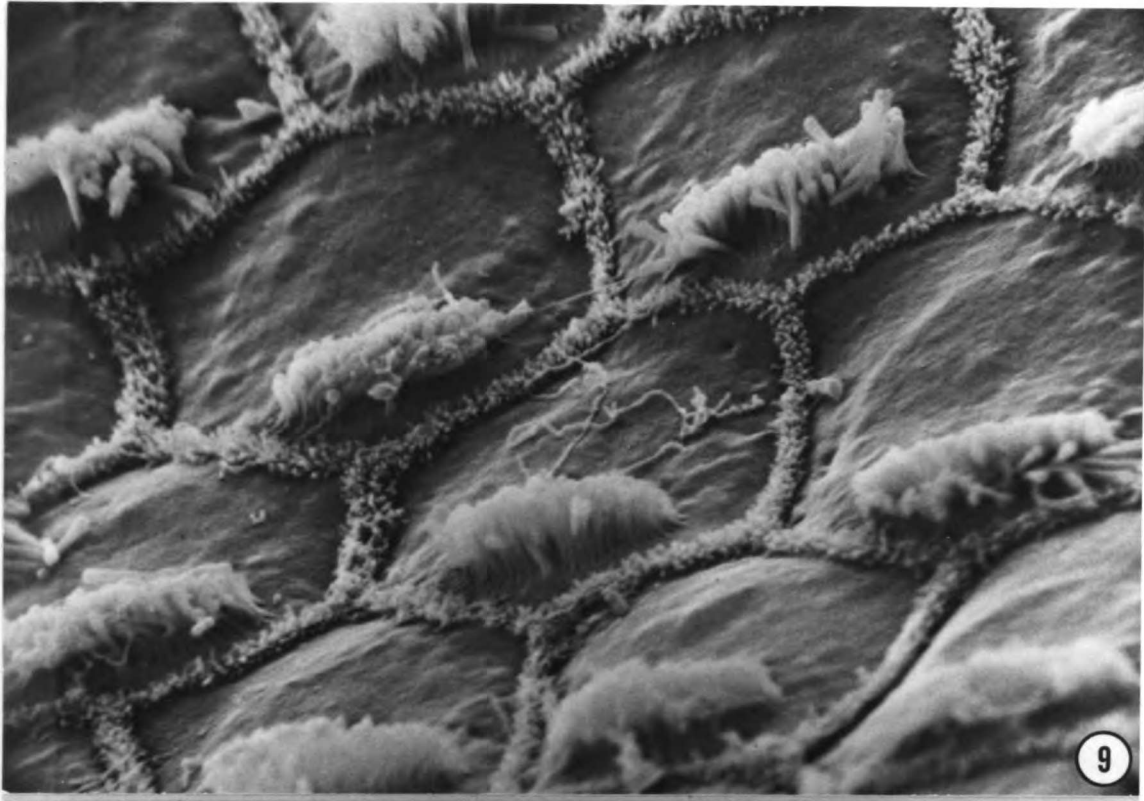
Figure 11. Outer hair cell from the proximal papilla basilaris
showing a kinocilium (arrows) which is longer than the
tallest stereocilia. ~X20,000
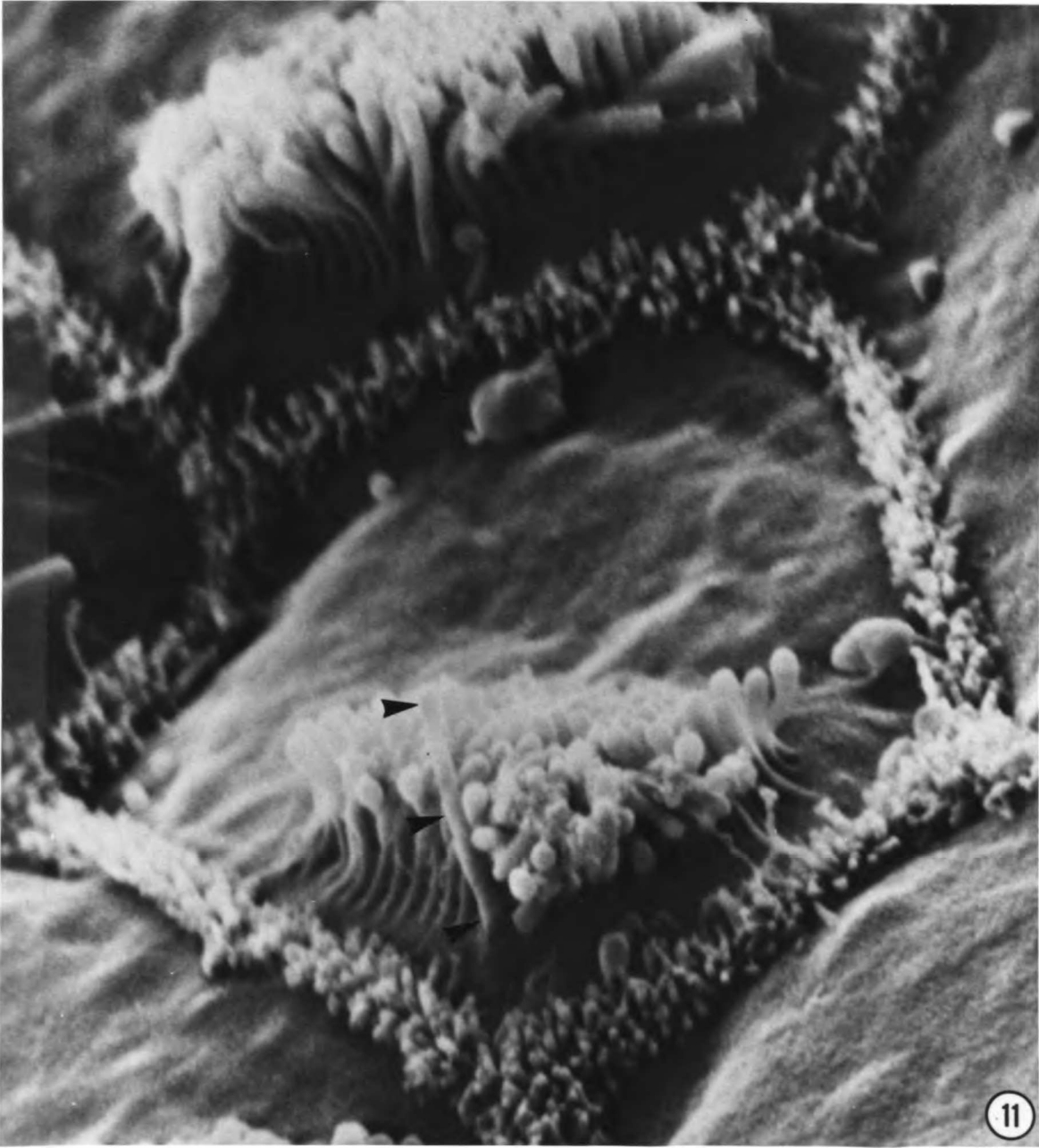
Figure 12.   Low magnification view of a right anterior ampulla.   ~X70

        Ant   portion of ampulla which was divided from the anterior canal

        CE   cruciate eminence on side of crest facing the utricle

        PS   planum semilunatum

        U   a small portion of the utricular neuroepithelium

Figure 13.   Montage of outlined area in Figure 12, taken at higher magnification.   X1,000

PS

Ant

CE   U

Med

12   13

Figure 14. Posterior half of the crista ampullaris and adjacent

ampullary wall in a left posterior ampullary specimen.

~X200

    C   remnants of the cupula

    PS   planum semilunatum

    T   toral enlargement

Figure 15. Low power view of a left posterior ampulla. ~X125

    C   cupula

    CE   cruciate eminence on utricular side of ampullary
           crest

    T   toral enlargement
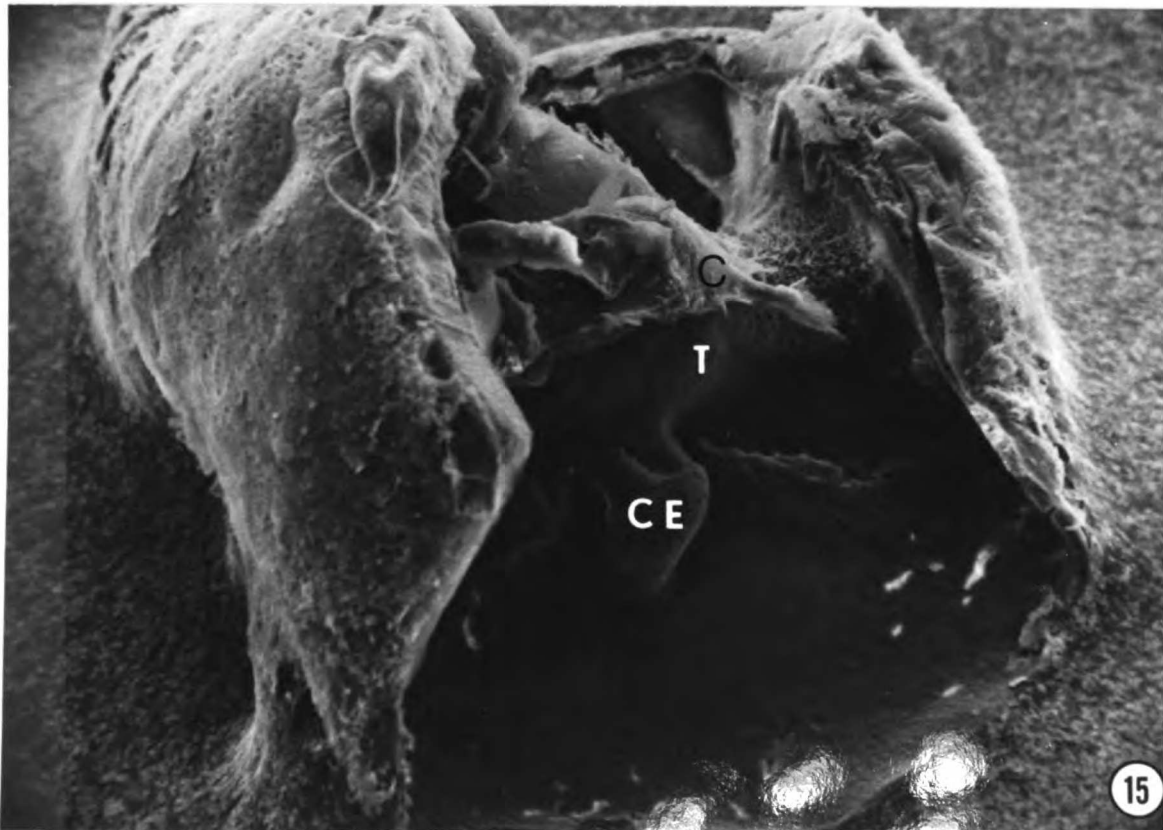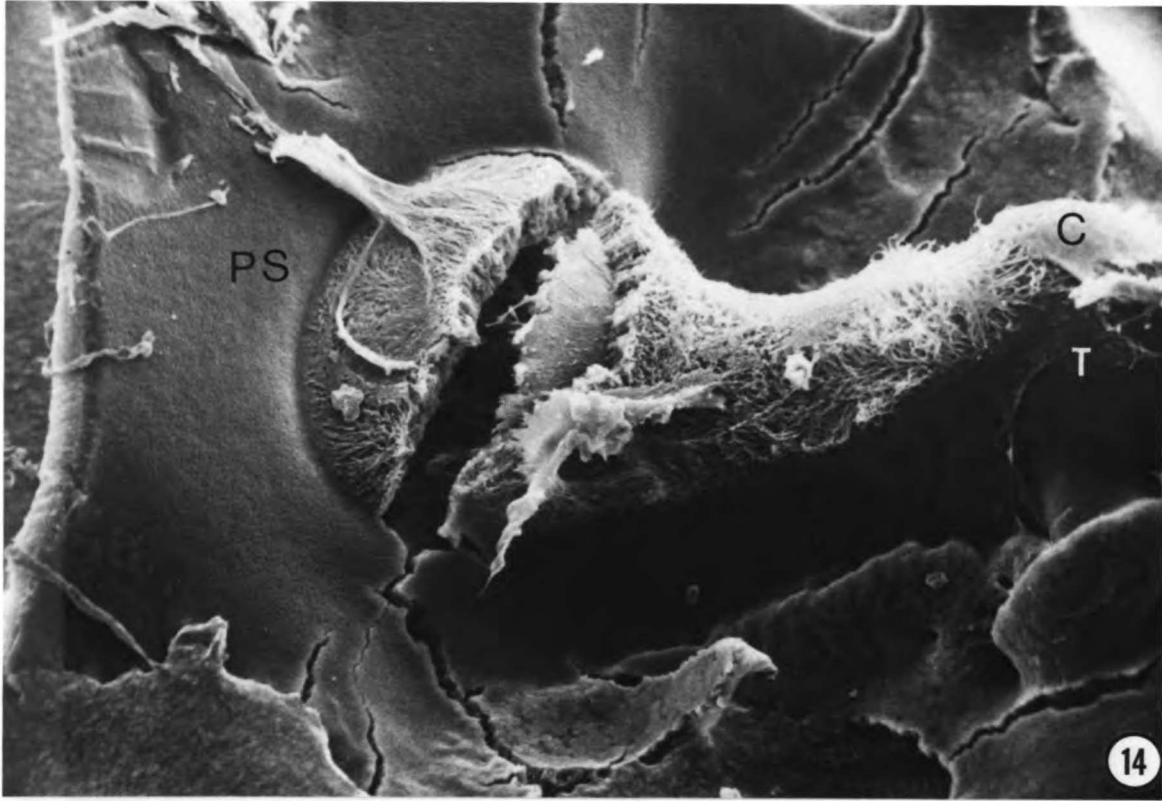
Figure 16. Higher magnification of anterior portion of left

posterior ampulla of Figure 15, showing exposed area of

cristal neuroepithelium on the anterior planar expansion.

~X400

   C   cupula

   HC   sensory hair cells on the cristal planar expansion.

Figure 17. High power view of hair cells in the center of the exposed

area of the anterior cristal planar expansion shown in

Figure 16. ~X3,000
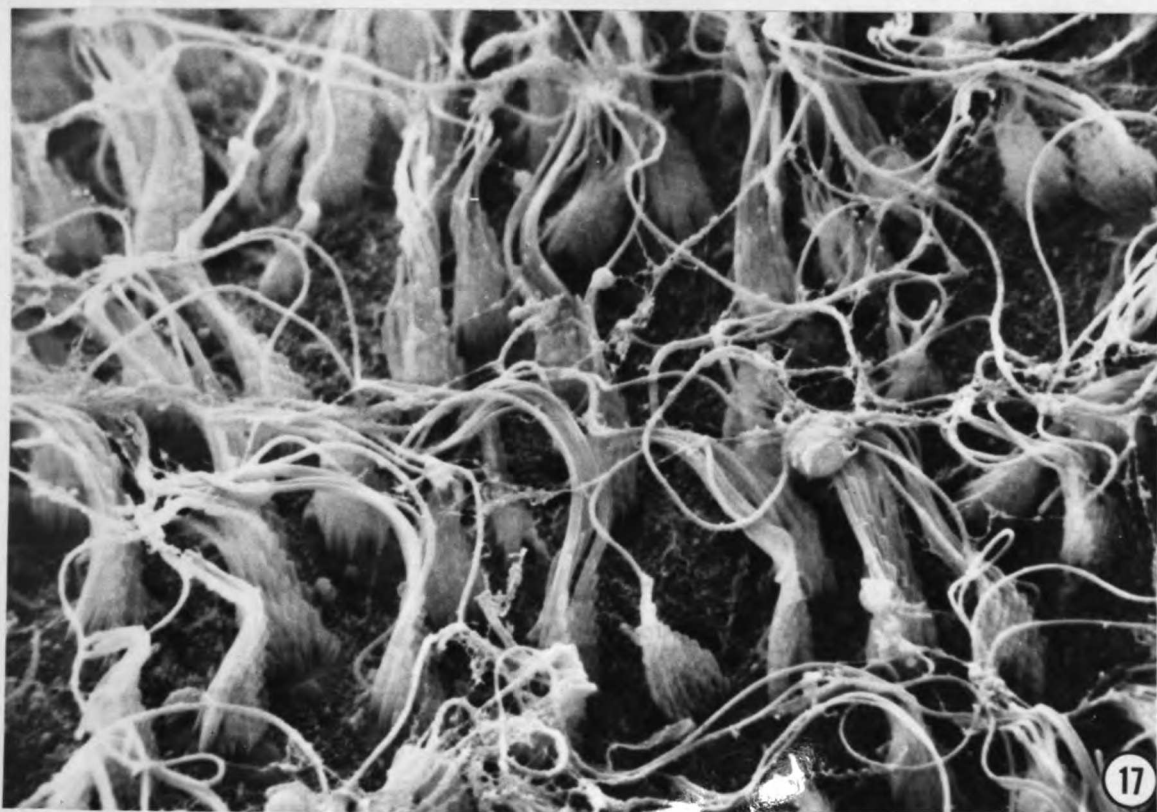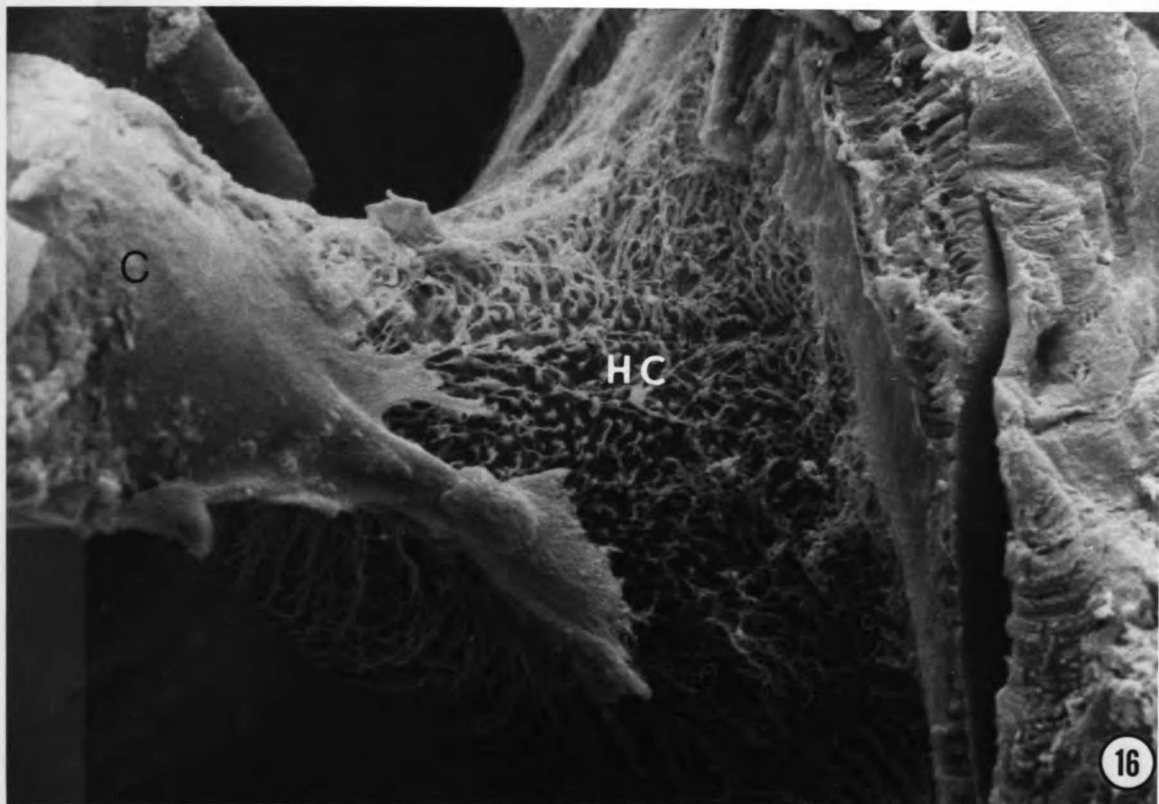
Figure 18. The two hair cell types (a, b) found in the planar region

of the crista ampullaris. (Taken from the specimen shown

in Figures 15-17). X12,000
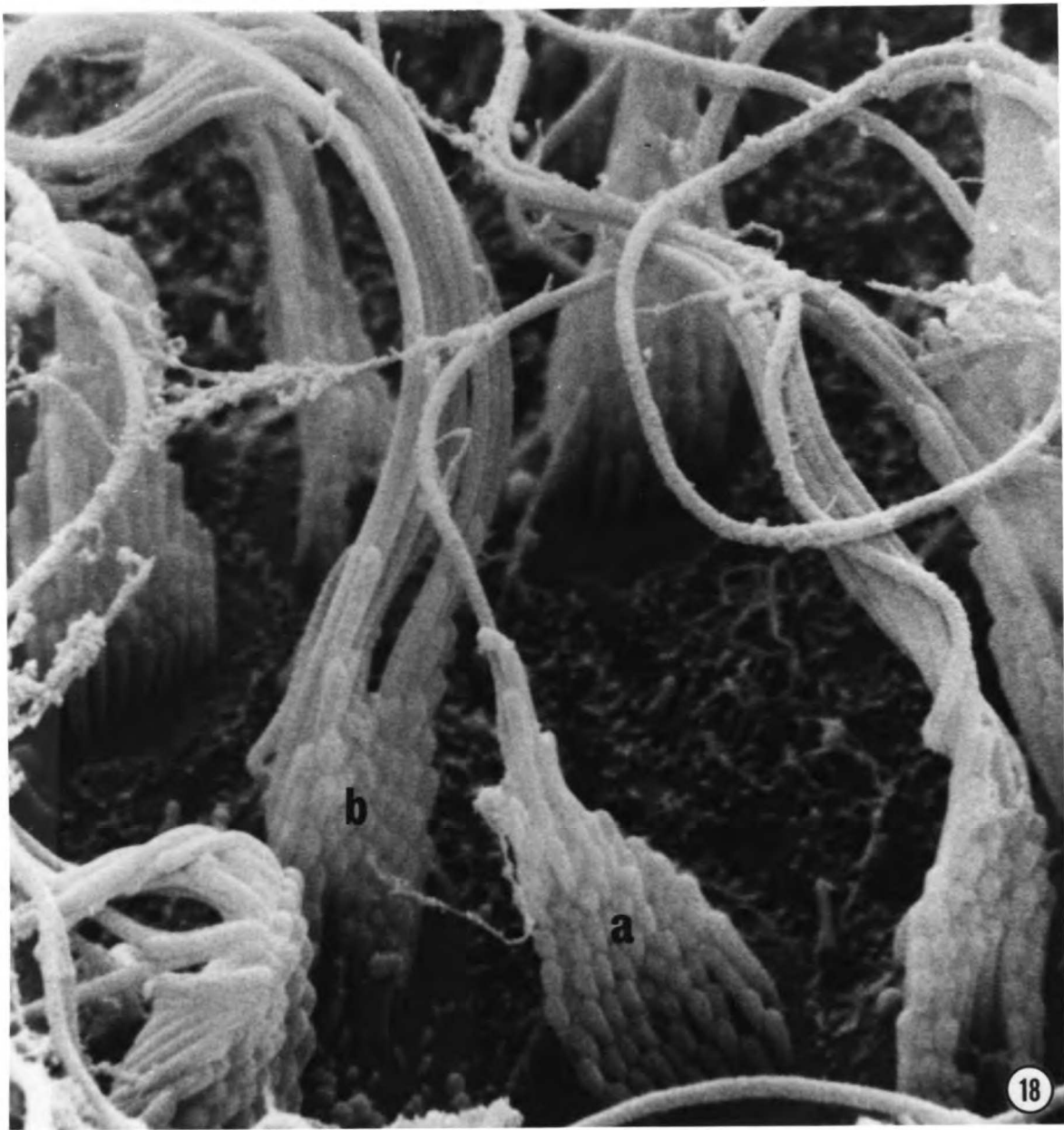
Figure 19. Toral region of a left posterior cirsta illustrating the
            midline area devoid of hair cells (arrows). Utricular
            cruciate eminence (CE) is more prominent than the cruciate
            eminence on the side of the crista facing the posterior
            semicircular canal (ce). ~X400

Figure 20. Close-up view of hair cells near the midline toral region
            of the specimen shown in Figure 19. Note that the
            orientation of hair cells in this vertical canal is with
            the kinocilium toward the semicircular canal and the
            shortest stereocilia toward the utricle. ~X3,000

CE

ce

19

20
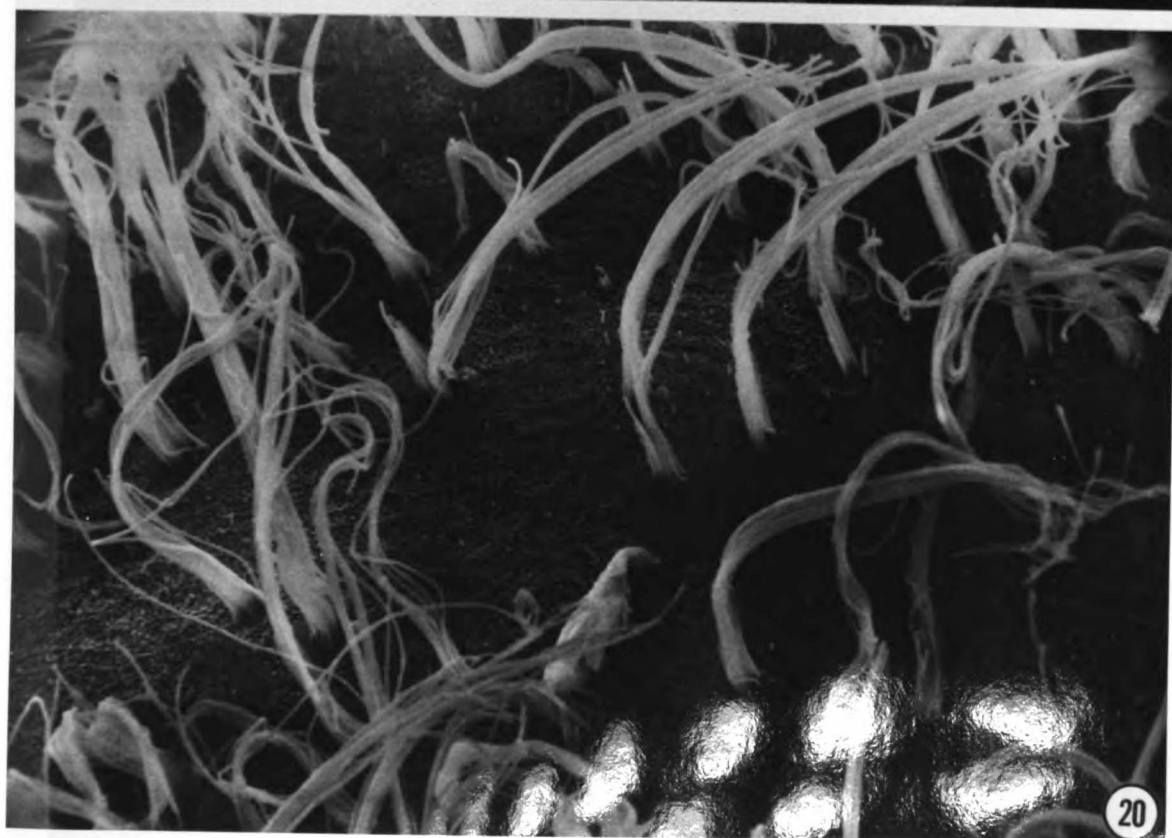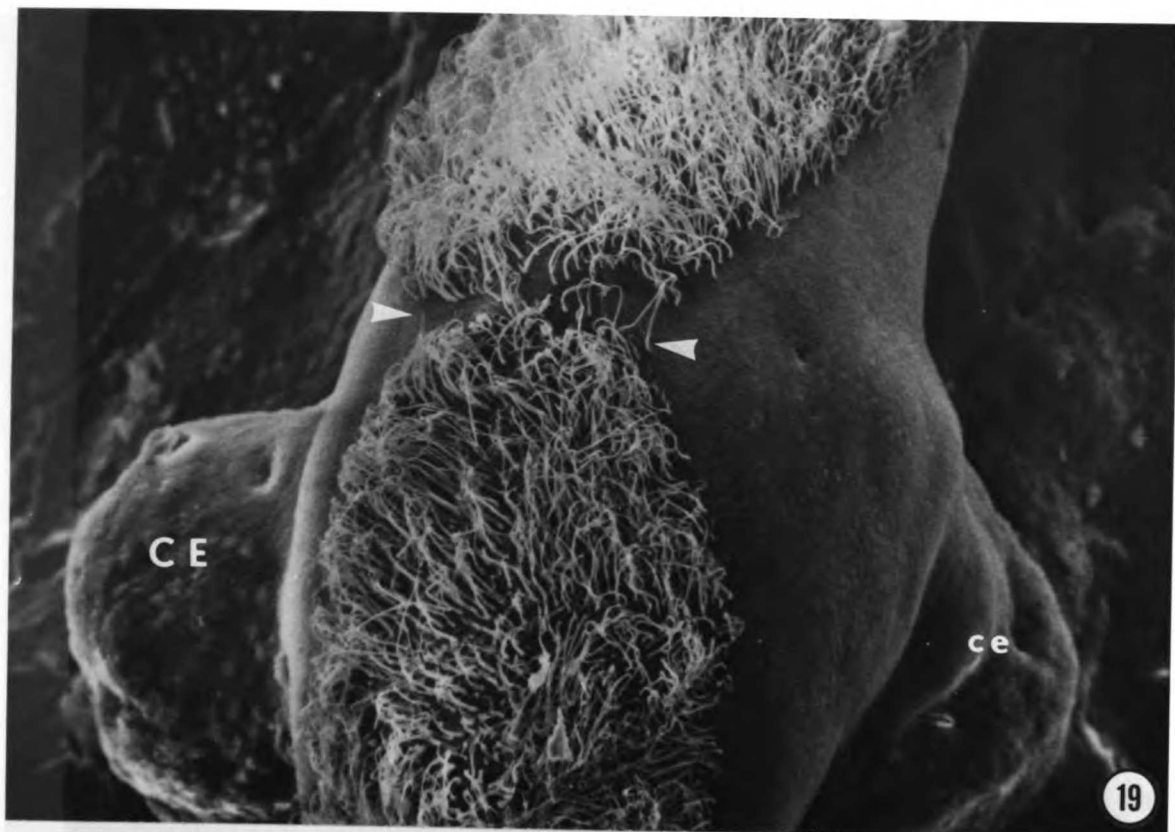
Figure 21.   Right horizontal ampulla. Note that only a single planar

expansion of the crista is present (on the dorsal

ampullary wall). ~X200

Figure 22.   Hair cells from the right hand margin of the ampullary

cristal of the neuroepithelium shown in Figure 21. Black

arrows point out tortuous kninocilium of sensory hair

cells; white arrows show rudimentary kinocilia of

adjacent supporting cells. ~X4,500

Dors

Ant

Post

Vent

21

22
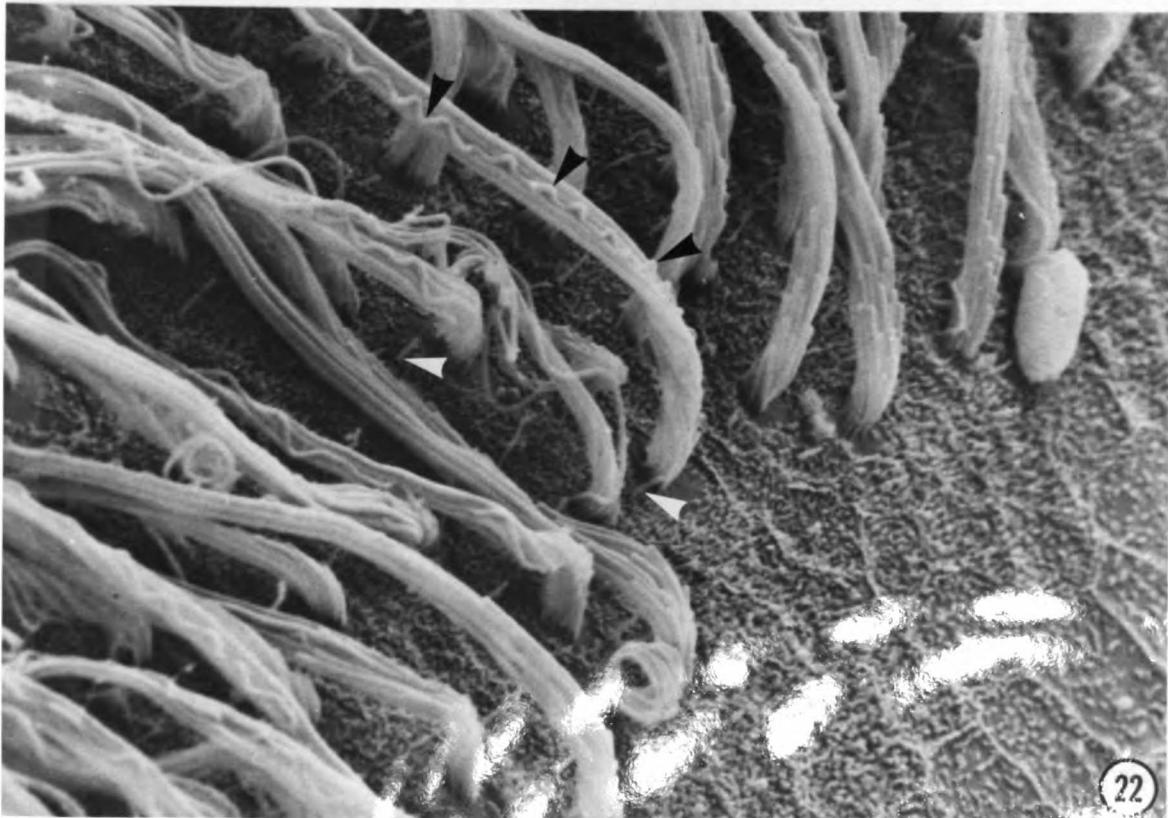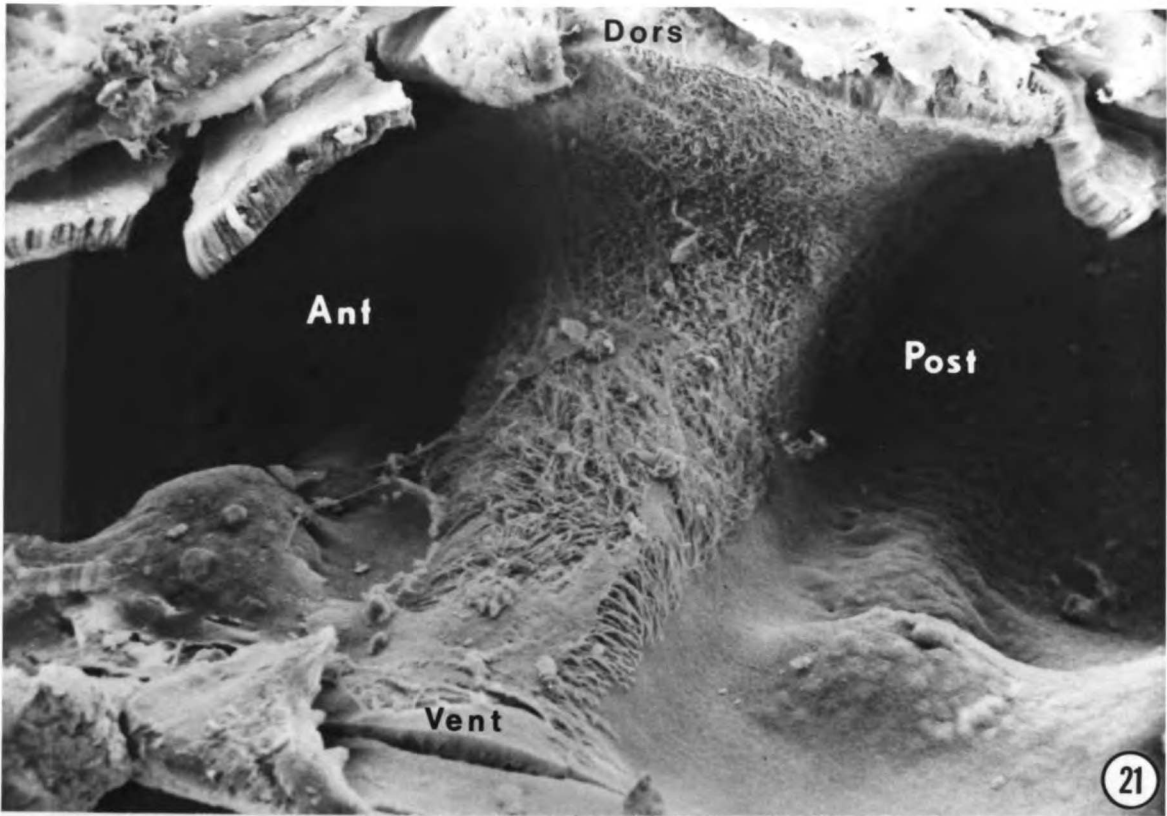
Figure 23. High power scanning micrograph showing hair cells on the cristal ridge of horizontal ampulla. White arrows point out rudimentary kinocilium of supporting cell. ~X20,000
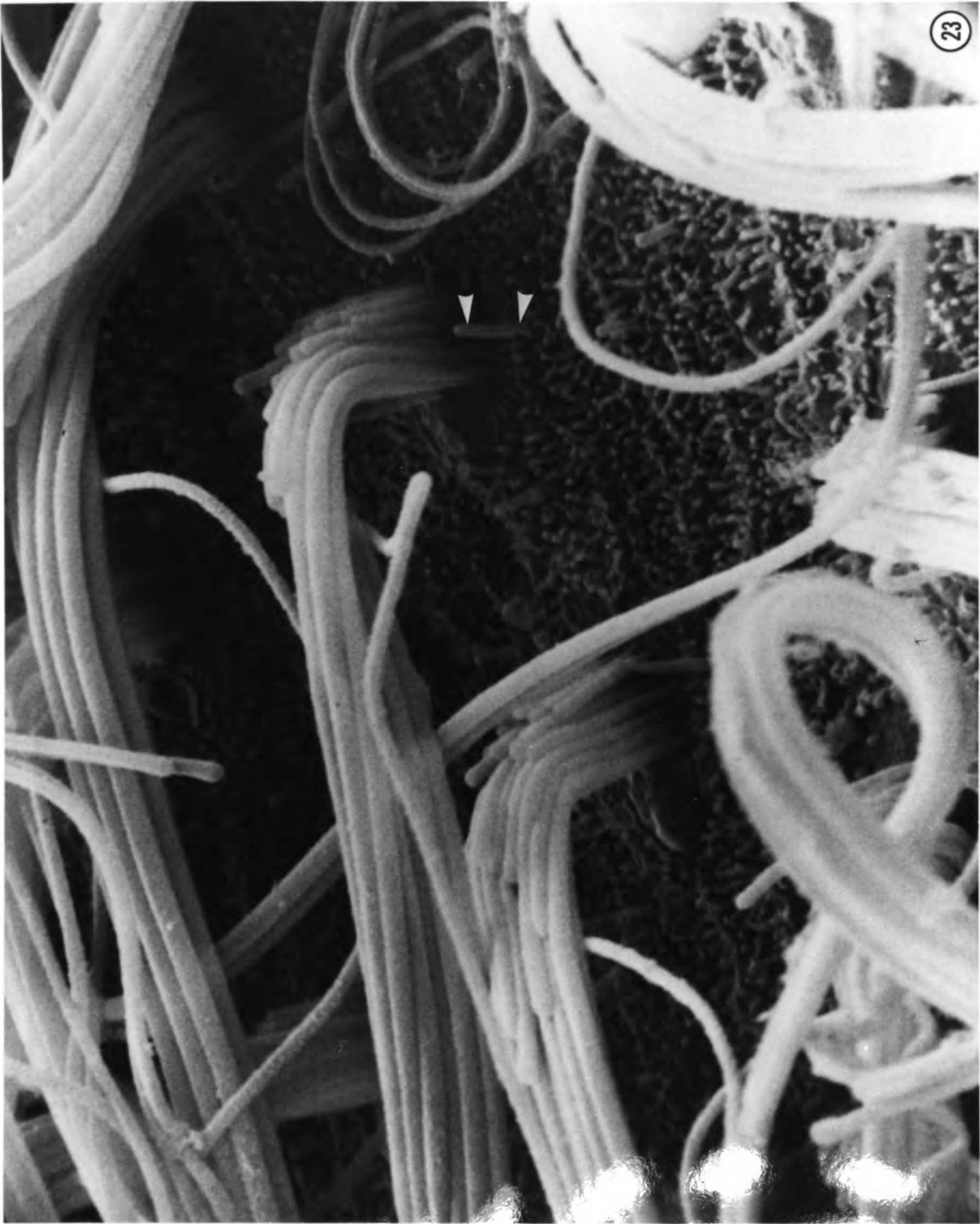
Figure 24. Montage of cristal hair cells along the right hand·margin
(i.e. the side of the crista related to the semicircular
canal) of the horizontal ampullary neuroepithelium
shown in Figure 21. ~X2,000

C

(24)
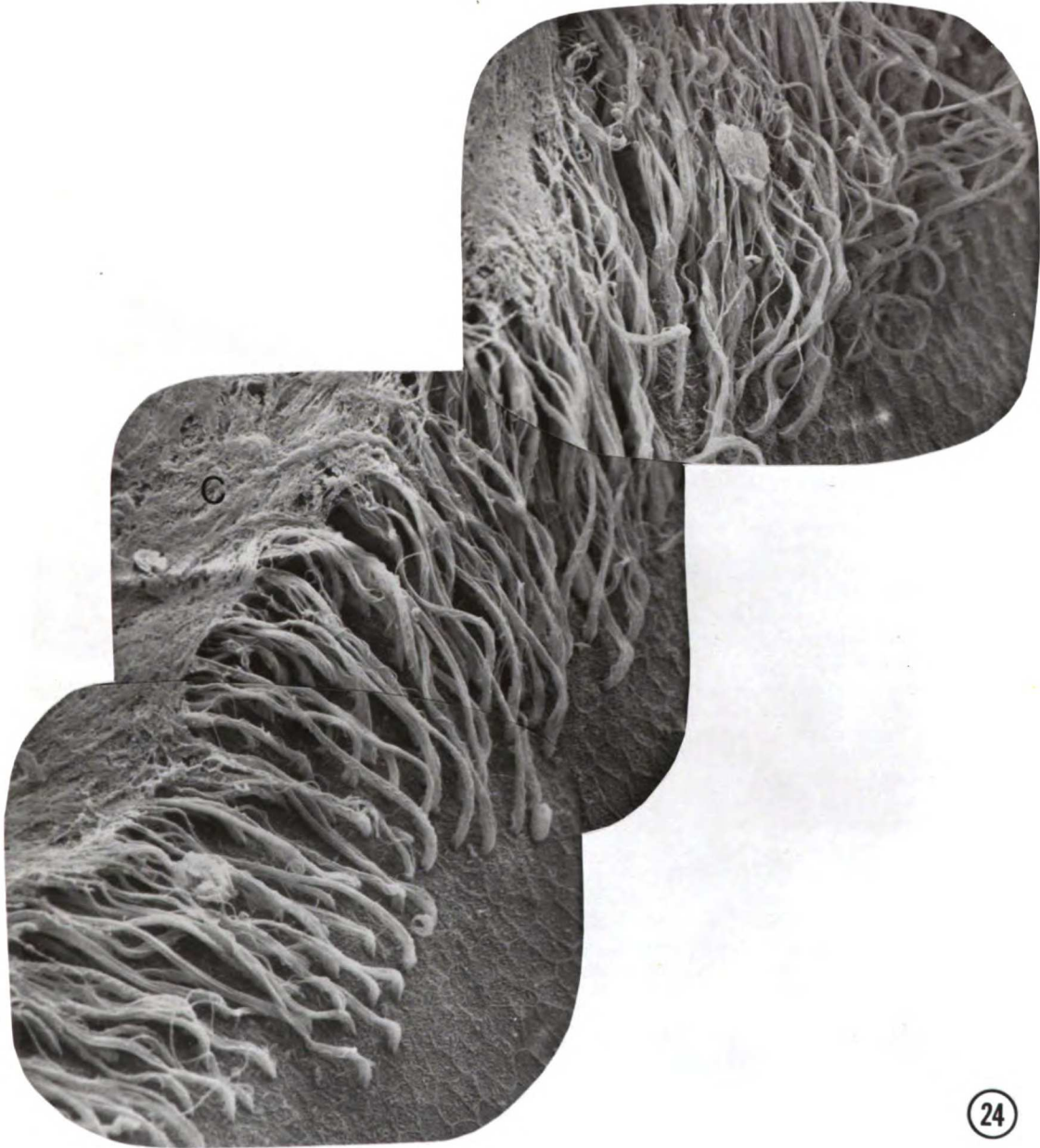
Figure 25. Right saccule showing curling of the membrane upon itself

which occurs during dehydration. ~X70

Figure 26. Ventral (inferior) limb of right saccule which has been

bissected through the opening of its U-shaped neuro-

epithelium. ~X250
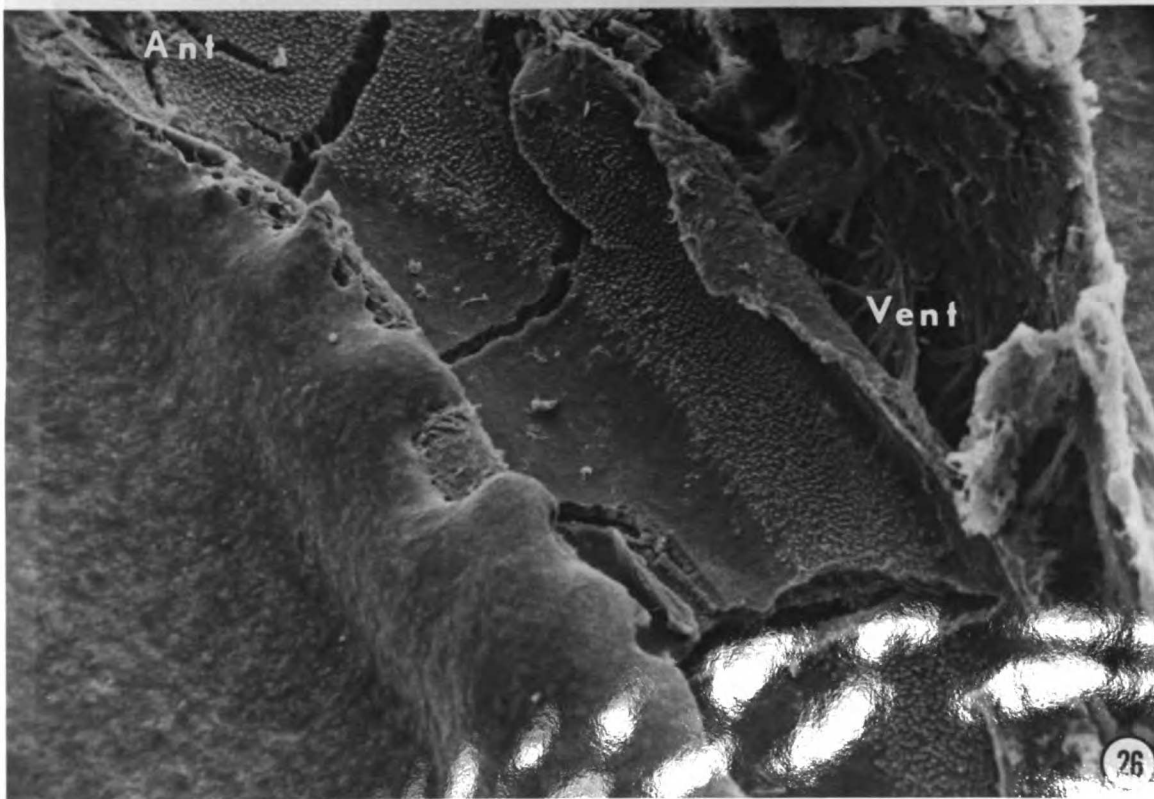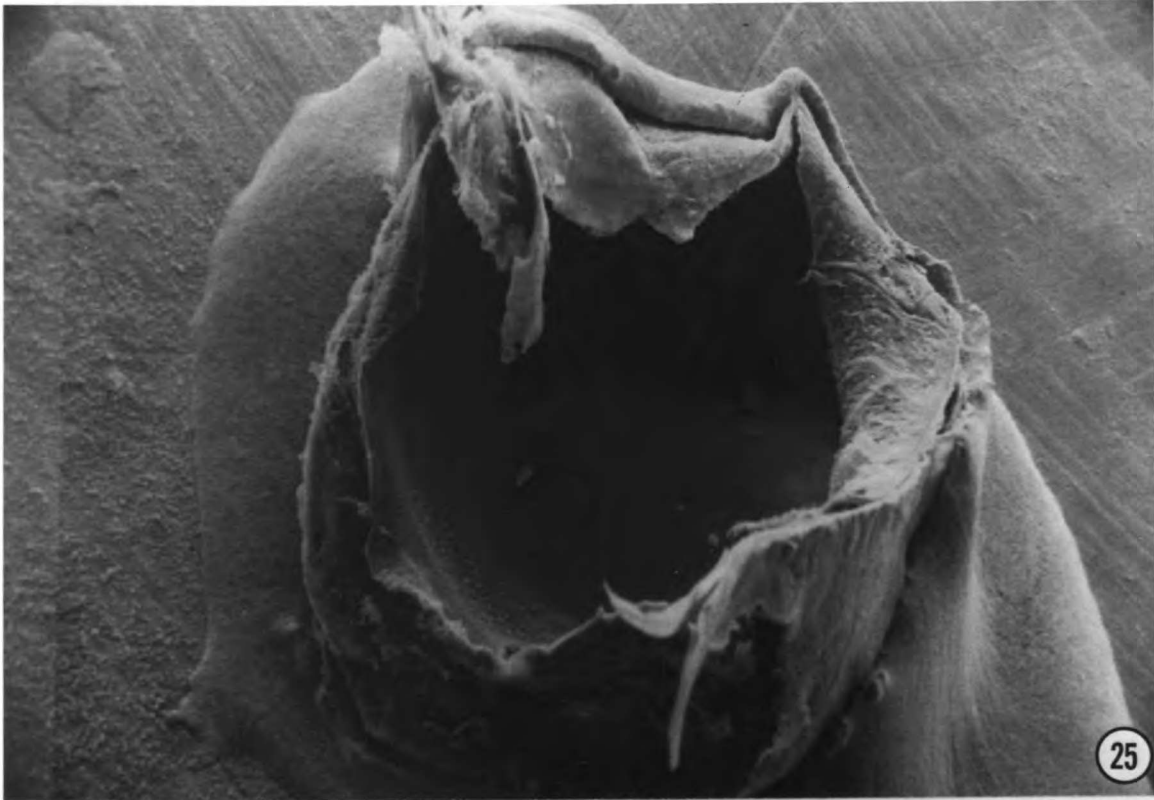
Figure 27. Higher magnification of anterior (upper) one-third of

ventral limb of saccular neuroepithelium shown in

Figure 26. Black line indicates position of line of

polarization reversal: sensory hair cells on both

sides of this line are oriented with their shortest

stereocilia toward and their kinocilium away from it.

~X380

Figure 28. Middle one-third of ventral limb of saccule in Figure 26,

showing position of line of polarization reversal (black

line). ~X700
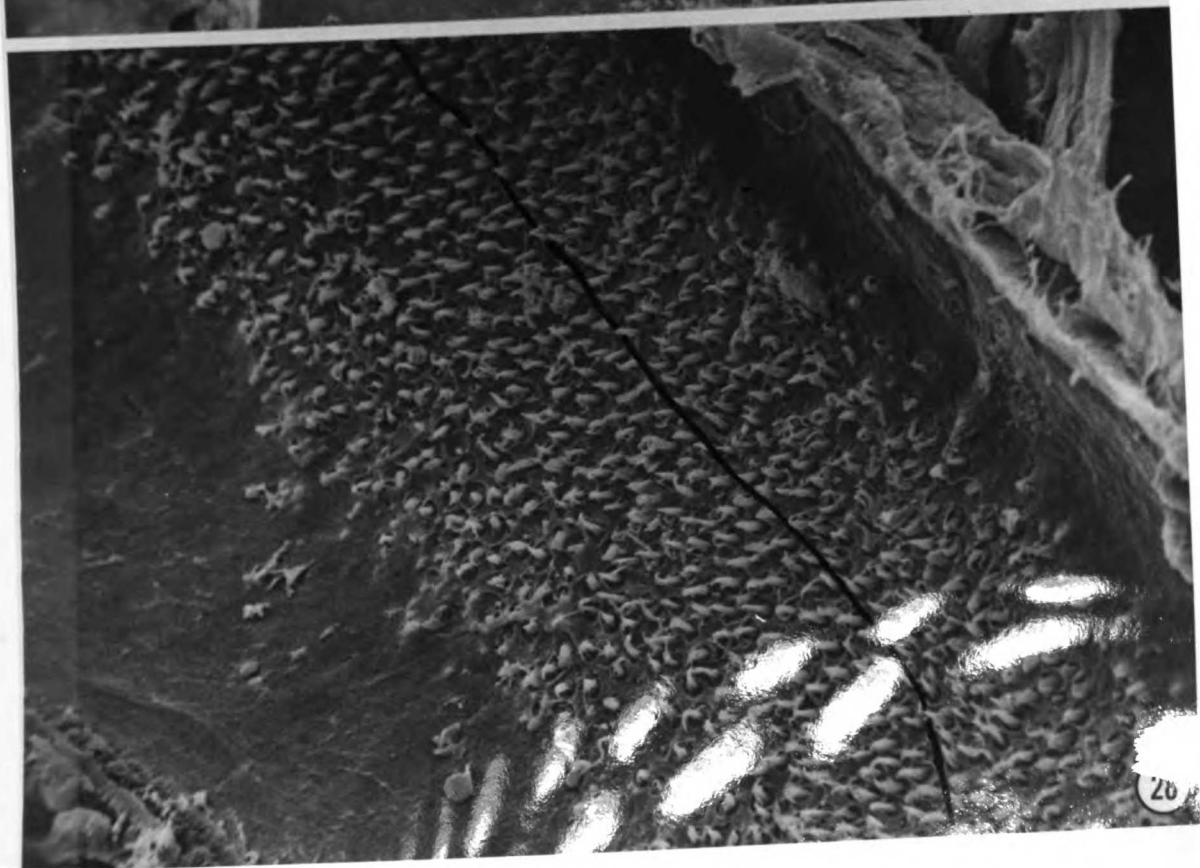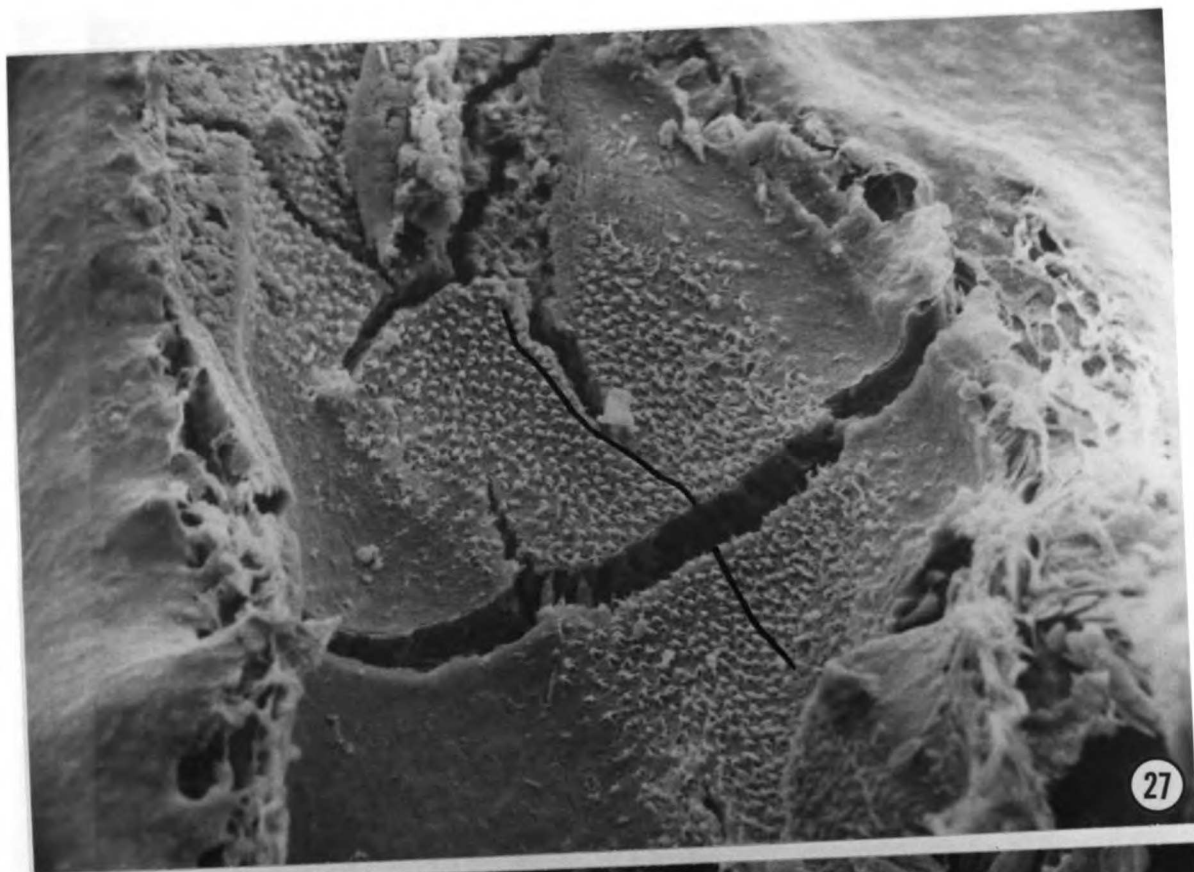
Figure 29. Posterior (lower) one-third of specimen in Figure 26,

showing the line of orientation reversal and the tapered

end of the inferior limb of the saccular hair cell strip.

Note the intact statolithic membrane in lower portion of

micrograph. ~X700

Figure 30. Higher magnification of saccular hair cells showing

opposite orientation along the line of reversal.

~X3,000

29
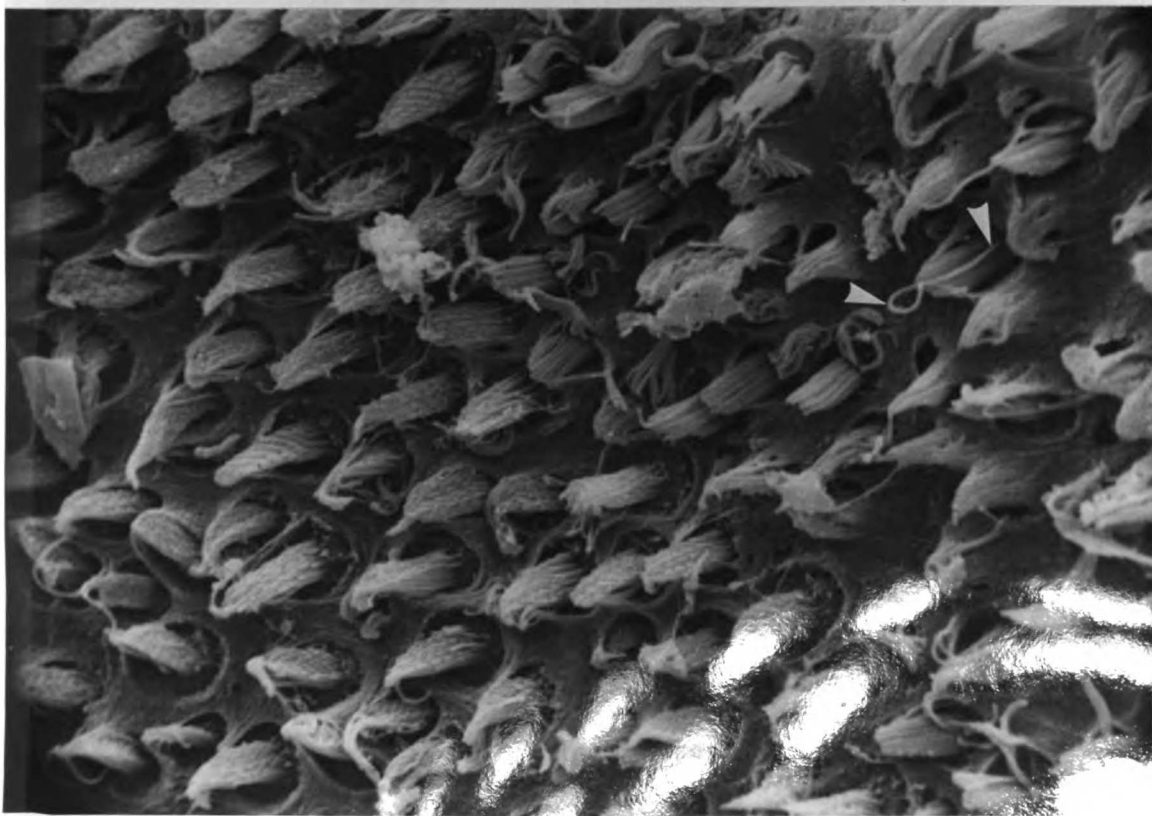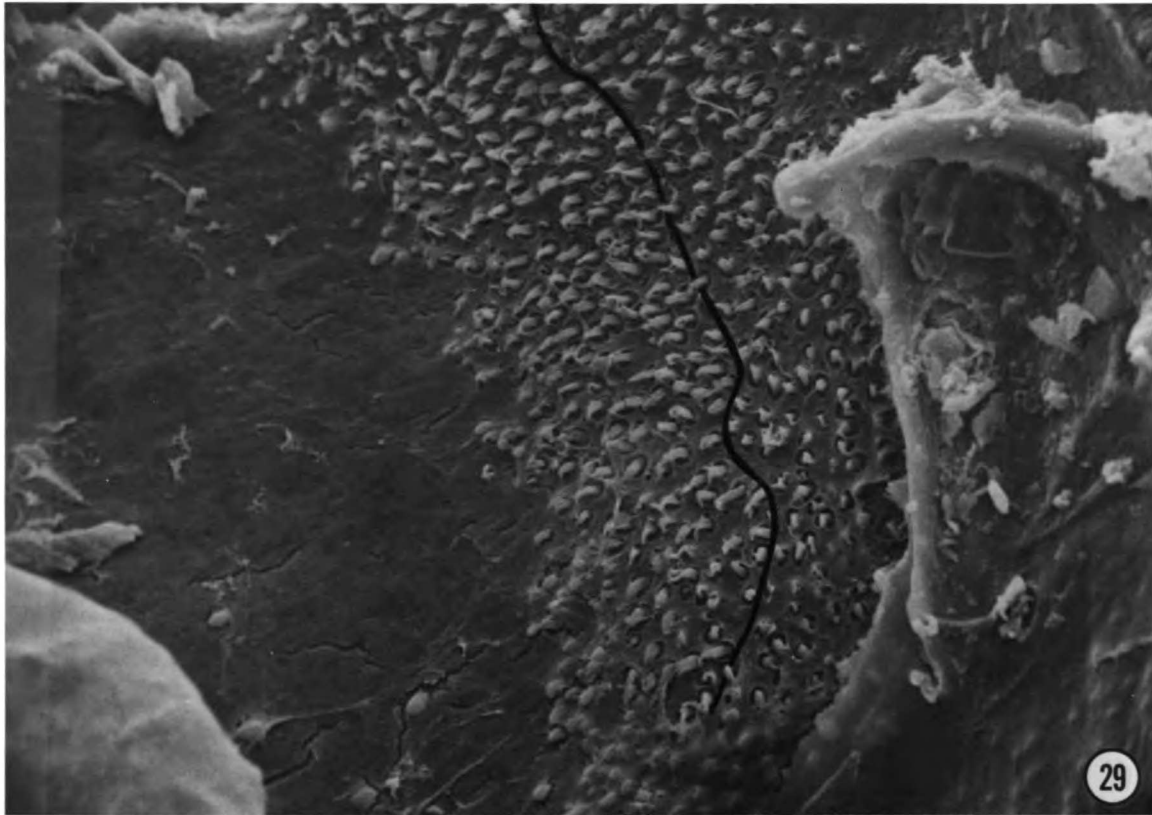
Figure 31. Saccular hair cells along the line of orientation

reversal. Note the fenestrated appearance of the

statolithic membrane in this region. ~X4,000

Figure 32. Tapered end of the interior limb of the saccular hair

cell strip showing the intact statolithic membrane

covering the sensory cells in this region. ~X3,000
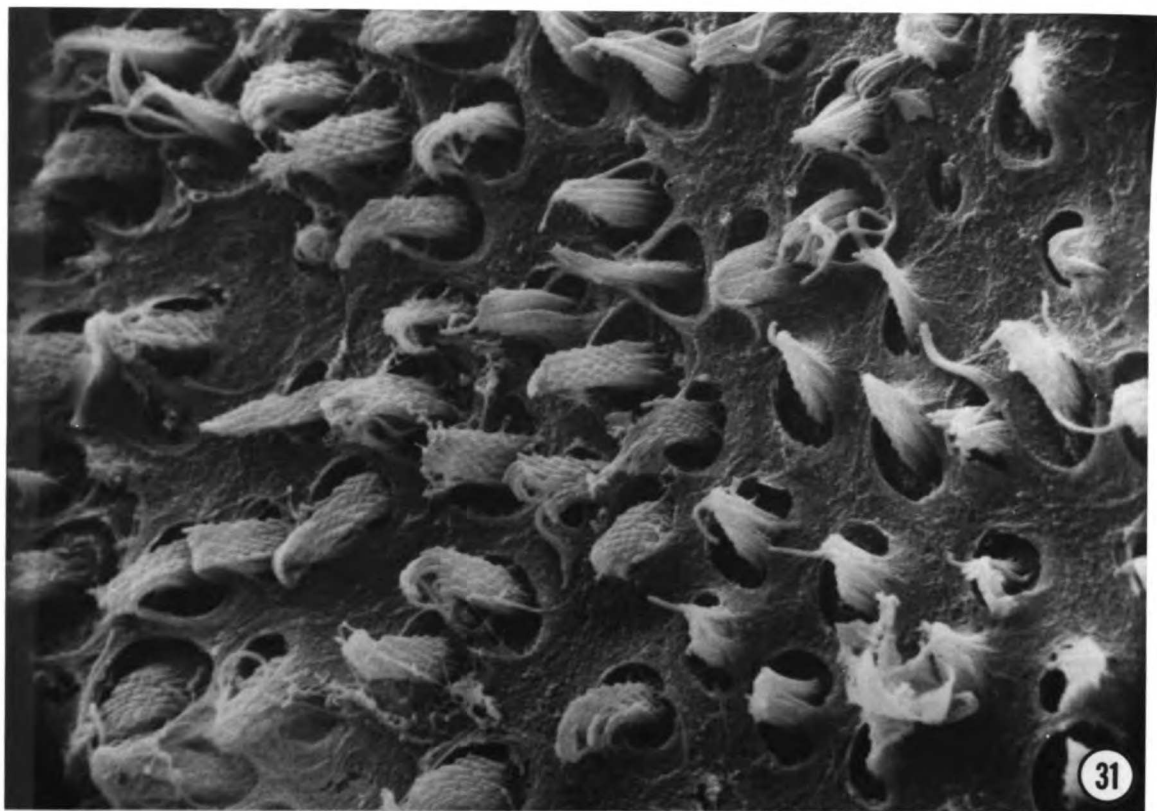
Figure 33. Otoconia of the saccular statolith. ~X1,800

Figure 34. Higher magnification of saccular otoconia. ~X8,000
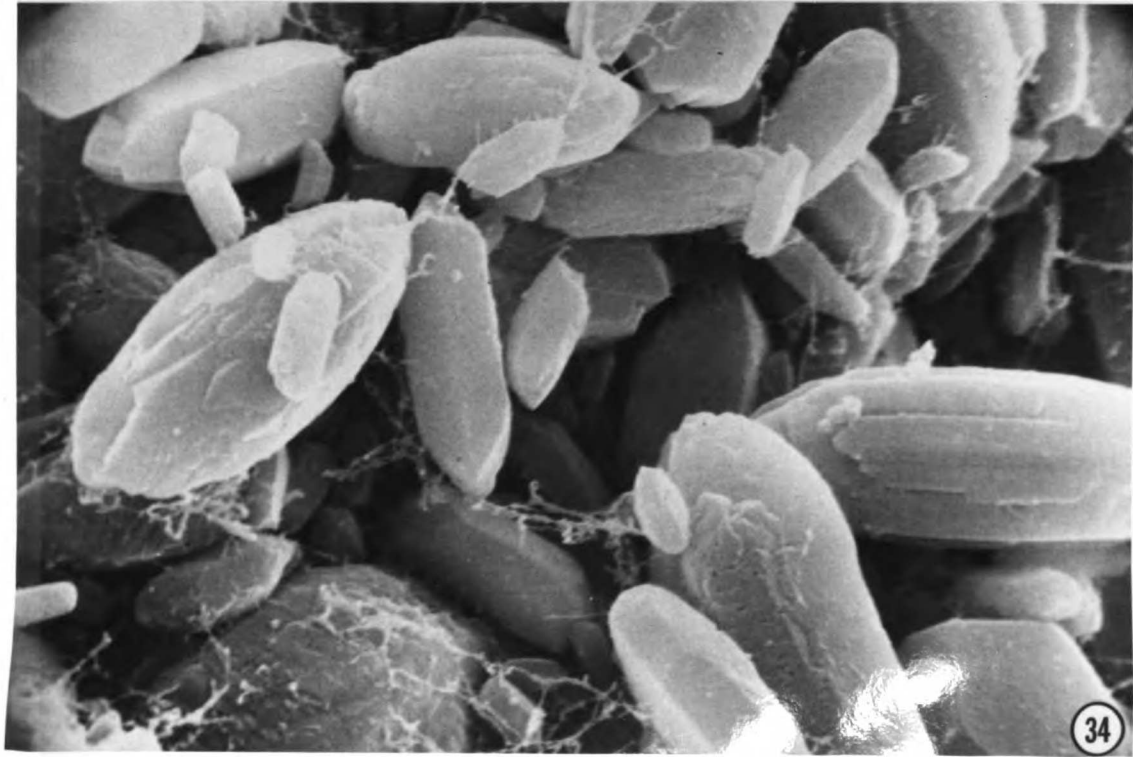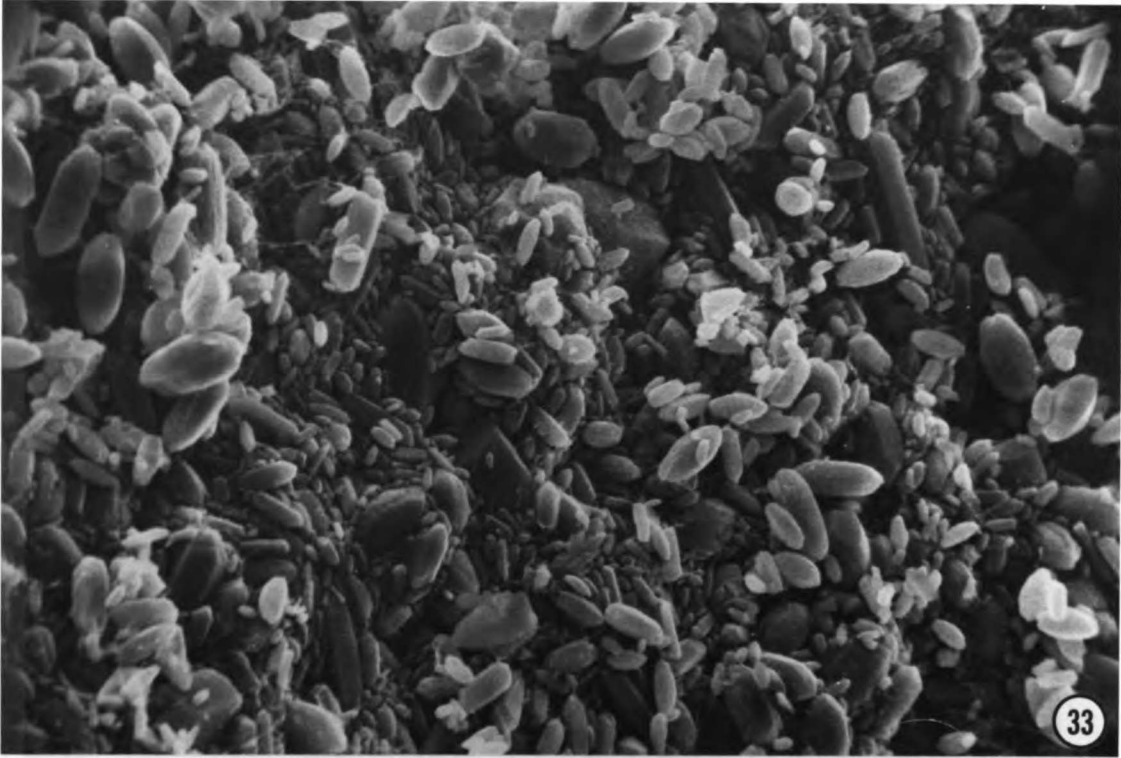
Figure 35. Left utricle. Note the relationship of the anterior (Ant) and horizontal (Lat) semicircular nerves to the anterior and lateral aspects of the utricle. ~X150

Figure 36. Utricular hair cells from the specimen shown in Figure 35. ~X2,500
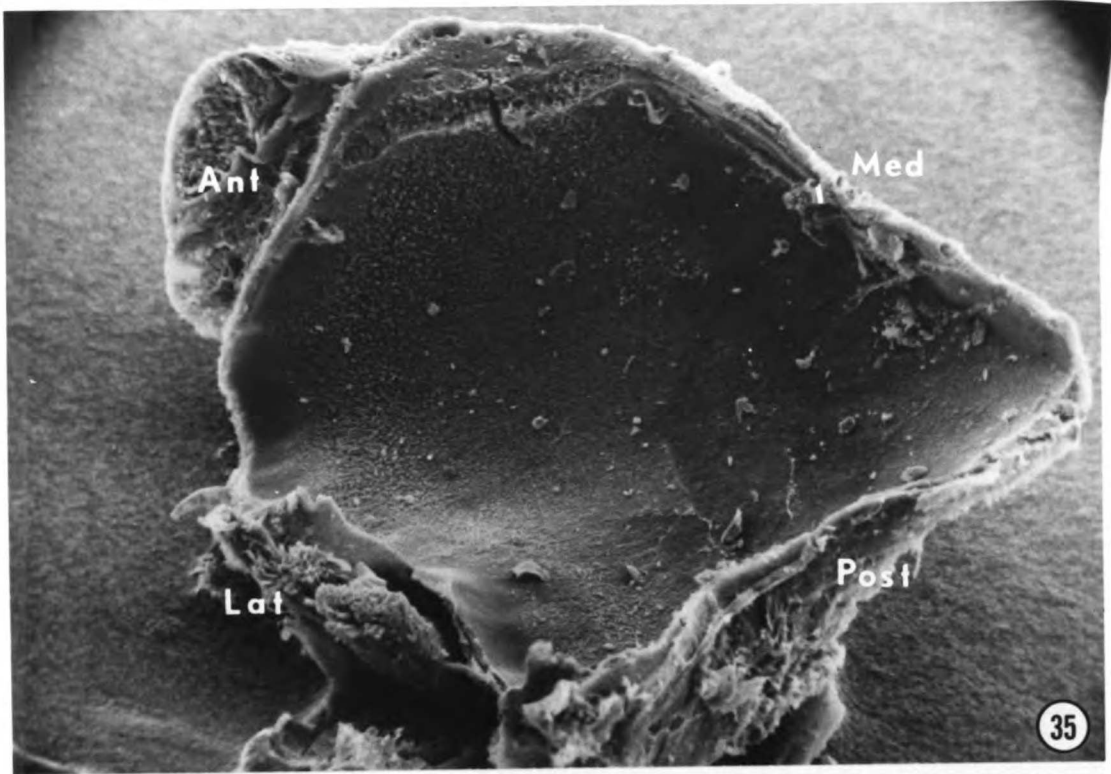
Figure 37. Higher magnification of utricular hair cells. Note that
two types of sensory cells are apparent: cells with
several long stereocilia and cells with only a single
long cilium, the kinocilium. ~X4,000

Figure 38. High magnification of one type of utricular sensory hair
cell, with relatively short stereocilia and a single
long cilium, the kinocilium. ~X20,000
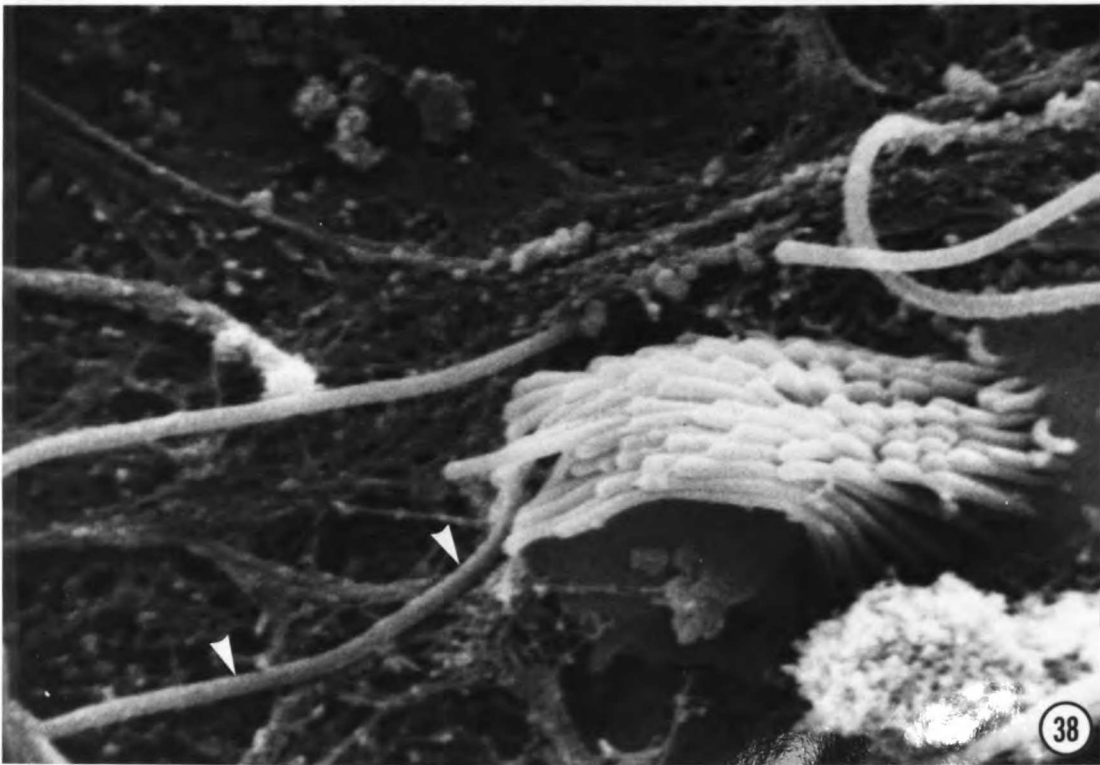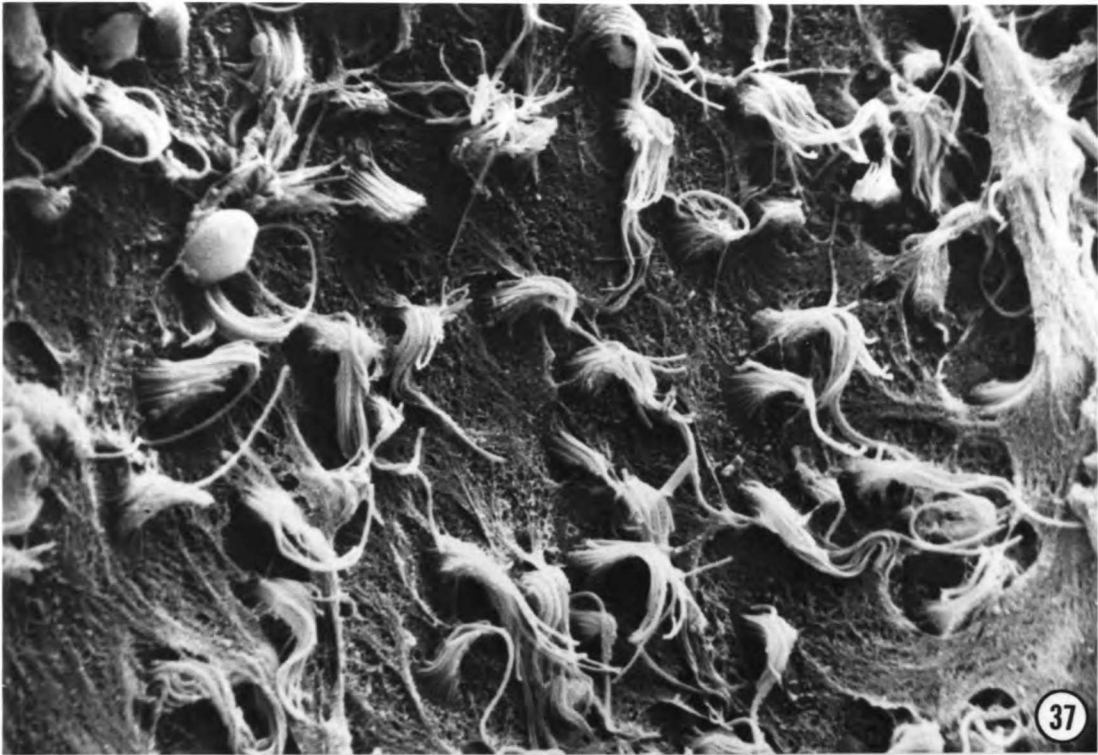
Figure 39. Region of the utricular neuroepithelium where the

statolithic membrane is intact and covers the hair cells.

Note that several otoconia are present in the field.

~X1,500
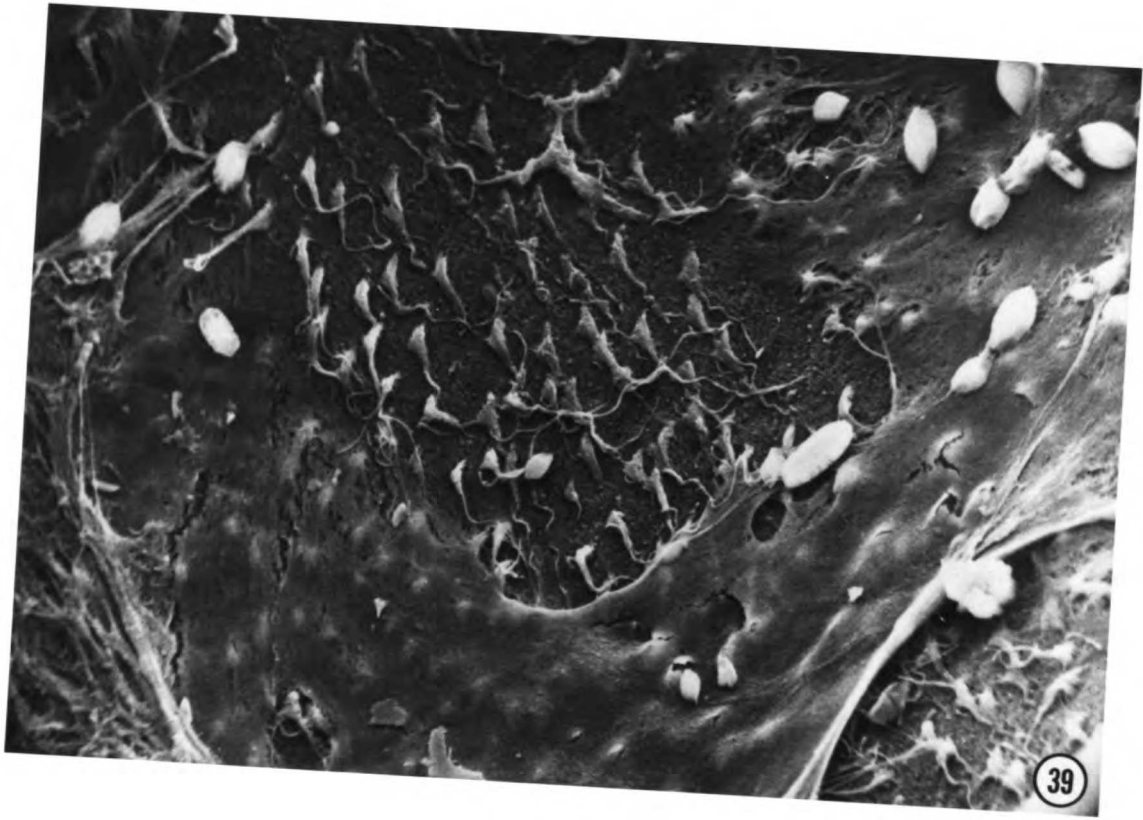
Figure 40. Schematic illustration of the right membranous labyrinth

of <u>Caiman</u> <u>crocodilus</u> (lateral aspect) showing the

relationships of nerves from the various sensory struc-

tures to the anterior and posterior ganglia of the eighth

nerve.

Abbreviations:

AC	anterior semicircular canal
A CR	crista ampullaris of the anterior canal
AG	ganglion cells of the anterior root of the VIIIth nerve
CC	common crus
HC	horizontal semicircular canal
H CR	crista ampullaris of the horizontal canal
ML	lagenar macula
N VII	facial nerve
PB	papilla basilaris
PC	posterior semicurcular canal
P CR	crista ampullaris of the posterior canal
PG	ganglion cells of the posterior root of the VIIIth nerve
PR	posterior root fibres proximal to ganglion
S	saccule
U	utricle

CC

AC

PC

HC

H CR

P CR

S

U

A CR

AG

N VII

PR

PG

PB

ML

40
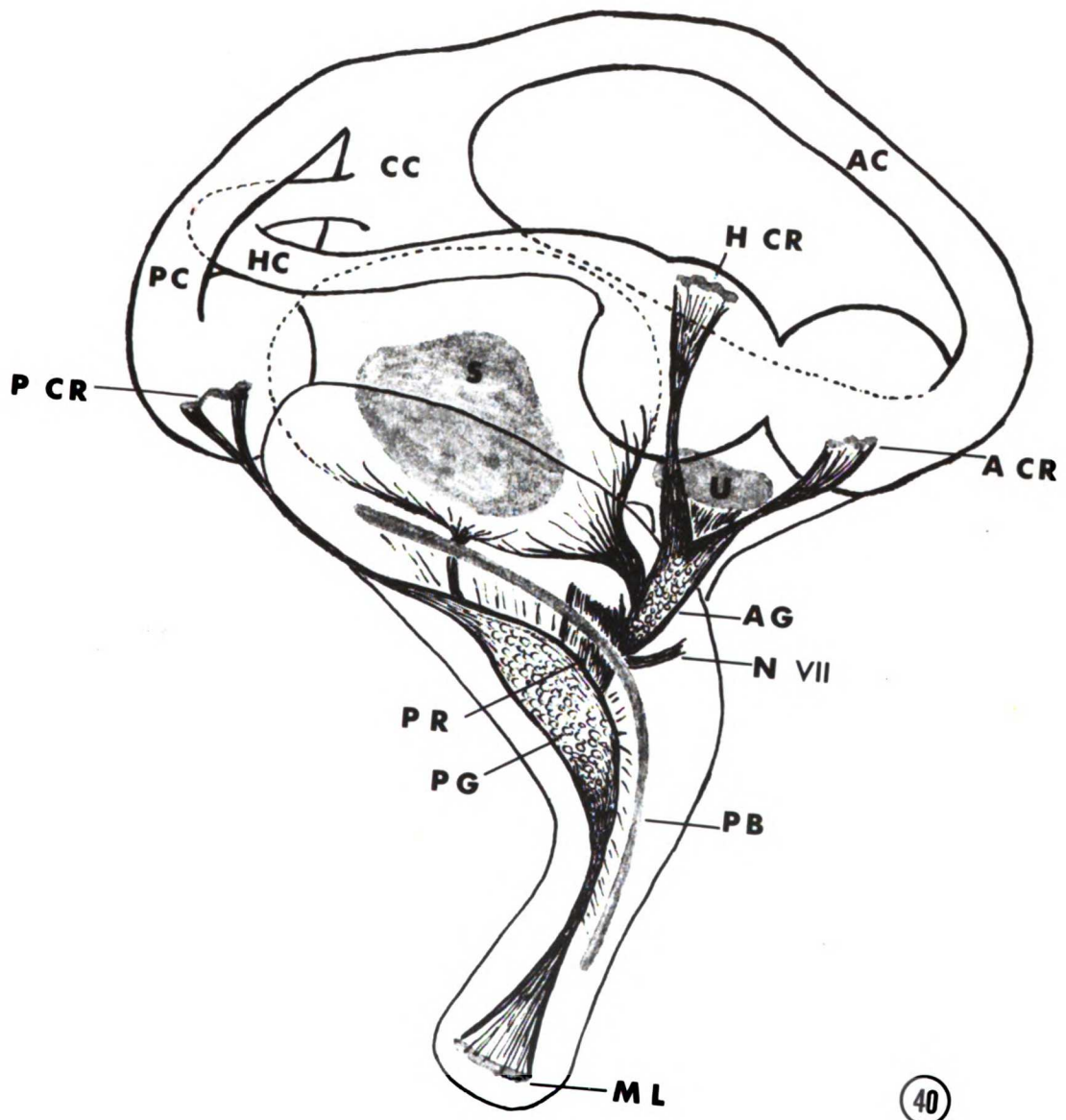
Figure 41. Series of transverse Nissl sections at progressively more

rostral levels through the acousticovestibular region.

Abbreviations:

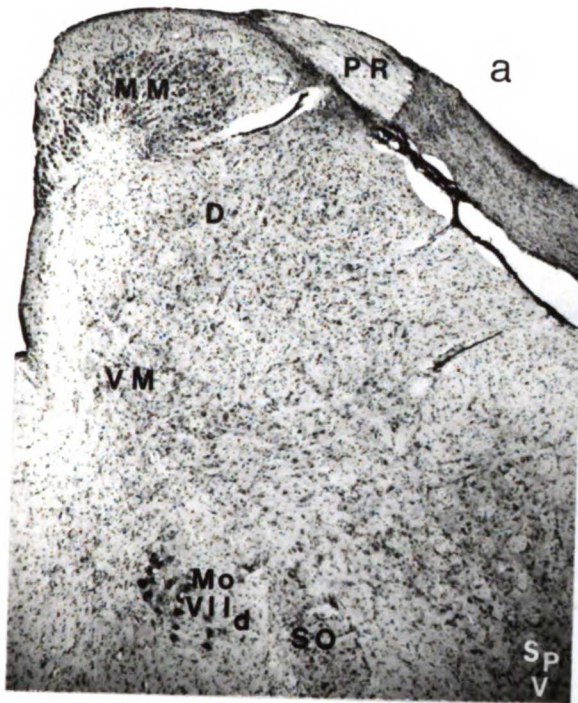|	
A	nucleus angularis
AR	anterior devision of the VIIIth nerve
AG	ganglion cells of the anterior root of the VIIIth nerve
D	descending vestibular nucleus
DL	dorsolateral vestibular nucleus
DM	dorsomedial vestibular nucleus
L	nucleus laminaris
L Cb	lateral cerebellar nucleus
M Cb	medial cerebellar nucleus
ML	lateral magnocellular nucleus
MM	medial magnocellular nucleus
Mo V	motor nucleus of the trigeminal nerve
Mo VII_d	dorsal division of the motor nucleus of the facial nerve
PR	posterior division of the VIIIth nerve
S	projection site of saccular fibers
SO	superior olive
Sp V	spinal tract and nucleus of the trigeminal nerve
T	tangential vestibular nucleus
VL	ventrolateral vestibular nucleus
VM	ventromedial vestibular nucleus
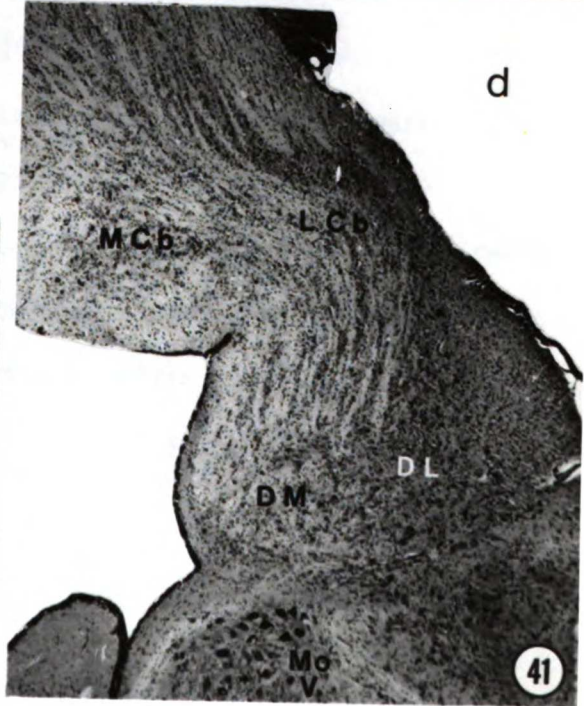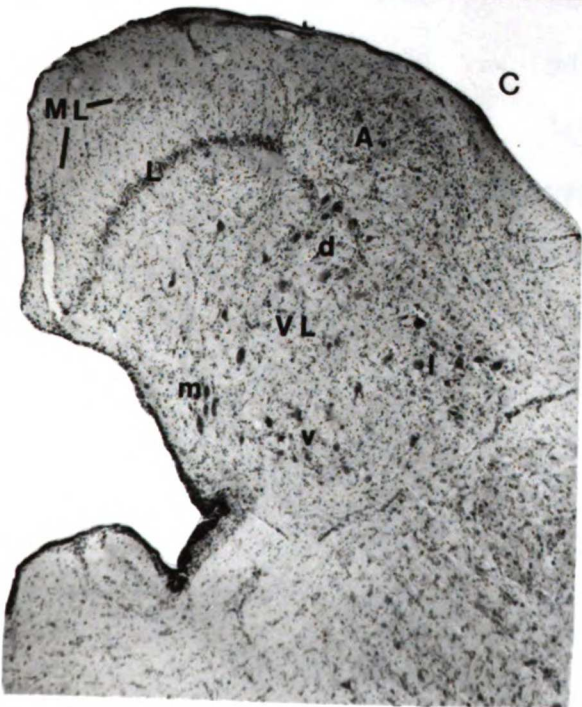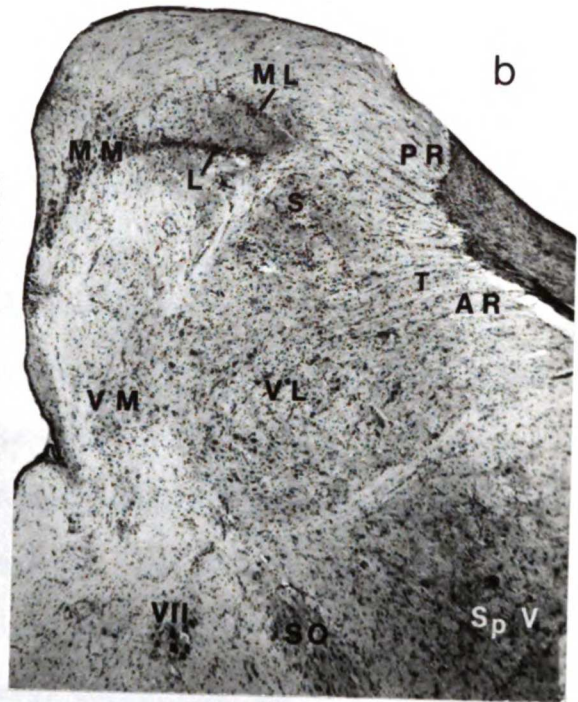
Figure 42.   Schematic illustration depicting locations and sizes of

experimental lesions (cross-hatched areas) in "E" series

of <u>Caiman</u> cases selected for analysis in this study.

(a is the most caudal section; d, the most rostral)

Abbreviations:

A	nucleus angularis
AR	anterior division of the VIIIth nerve
D	descending vestibular nucleus
DL	dorsolateral vestibular nucleus
DM	dorsomedial vestibular nucleus
L	nucleus laminaris
L Cb	lateral cerebellar nucleus
M Cb	medial cerebellar nucleus
ML	lateral magnocellular nucleus
MM	medial magnocellular nucleus
Mo V	motor nucleus of the trigeminal nerve
PR	posterior division of the VIIIth nerve
SO	superior olivary complex
Sp V	spinal tract and nucleus of the trigeminal nerve
VI	abducens nucleus
VII_d	dorsal division of the motor nucleus of the facial nerve
VII_v	ventral division of the motor nucleus of the facial nerve
VL	ventrolateral vestibular nucleus
VM	ventromedial vestibular nucleus

d

8

L Cb
M Cb
25   18   A   16
7   DM   DL
              Mo
              V

c

ML
7   A
25   VL
18   16
10   17
15
24   Sp V

VII v

SO

MM   PR
13   17   VL
8   10
15   VM
VI   VII d   Sp V
SO

b

5
13
14
20   D
             VM
             VII   Sp V
SO

a

42
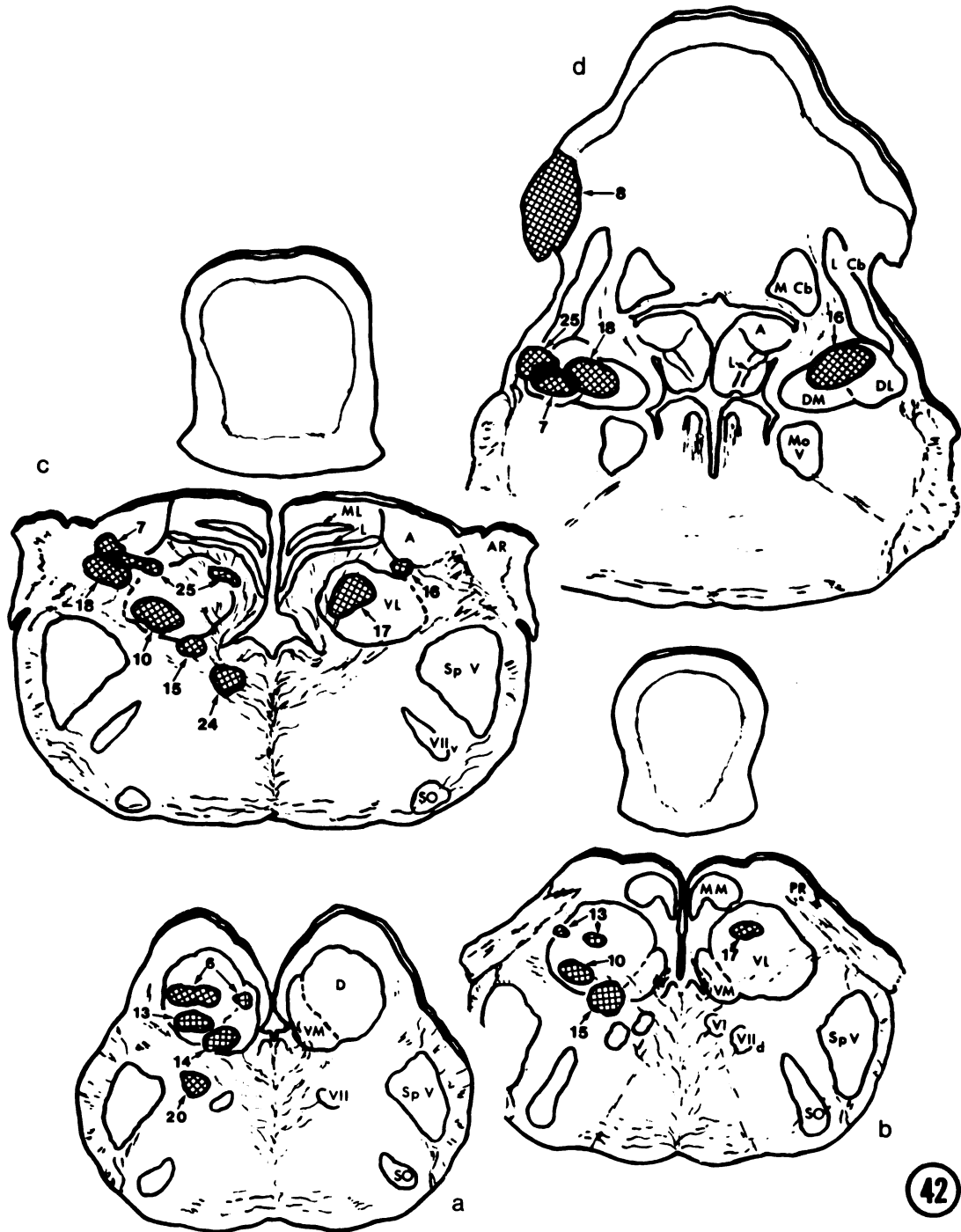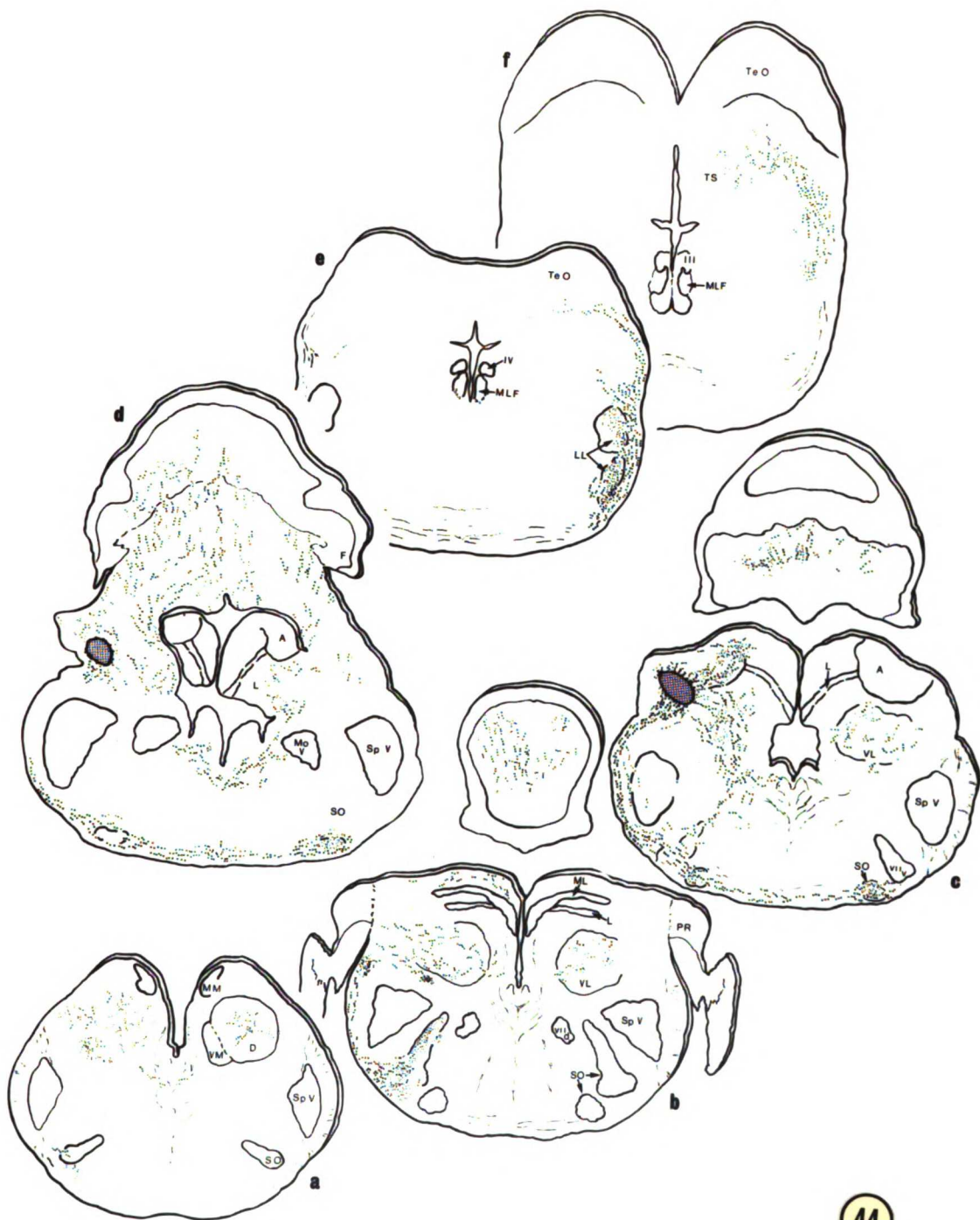
Figure 43. Schematic illustration depicting pattern of degeneration in
experimental case V10. Cross-hatched area shows extent of
lesion. Large dots represent degenerated axonal fragments;
fine stipple indicates preterminal degeneration. (a is the
most caudal section; f, the most rostral).

Abbreviations:

A	nucleus angularis	MM	medial magnocellular nucleus
AR	anterior division of the VIIIth nerve	Mo_v	motor nucleus of the trigeminal nerve
D	descending vestibular nucleus	PR	posterior division of the VIIIth nerve
III	oculomotor nucleus		
IV	trochlear nucleus	SO	superior olivary complex
F	flocculus	Sp V	spinal tract and nucleus of the trigeminal nerve
L	nucleus laminaris	Te O	optic tectum
L Cb	lateral cerebellar nucleus	TS	torus semicircularis
LL	nucleus of the lateral lemniscus	VI	abducens nucleus
		VII_d	dorsal division of motor facial nucleus
M Cb	medial cerebellar nucleus	VII_v	ventral division of motor facial nucleus
ML	lateral magnocellular nucleus	VL	ventrolateral vestibular nucleus
MLF	medial longitudinal fasciculus	VM	ventromedial vestibular nucleus

f

TS

III

MLF

e

IV

SO

d

MM

AR

VL

Sp V

VII

MM

SPR

D

VM

Sp V

SO

D

VM

Sp V

VII d

b

a

43
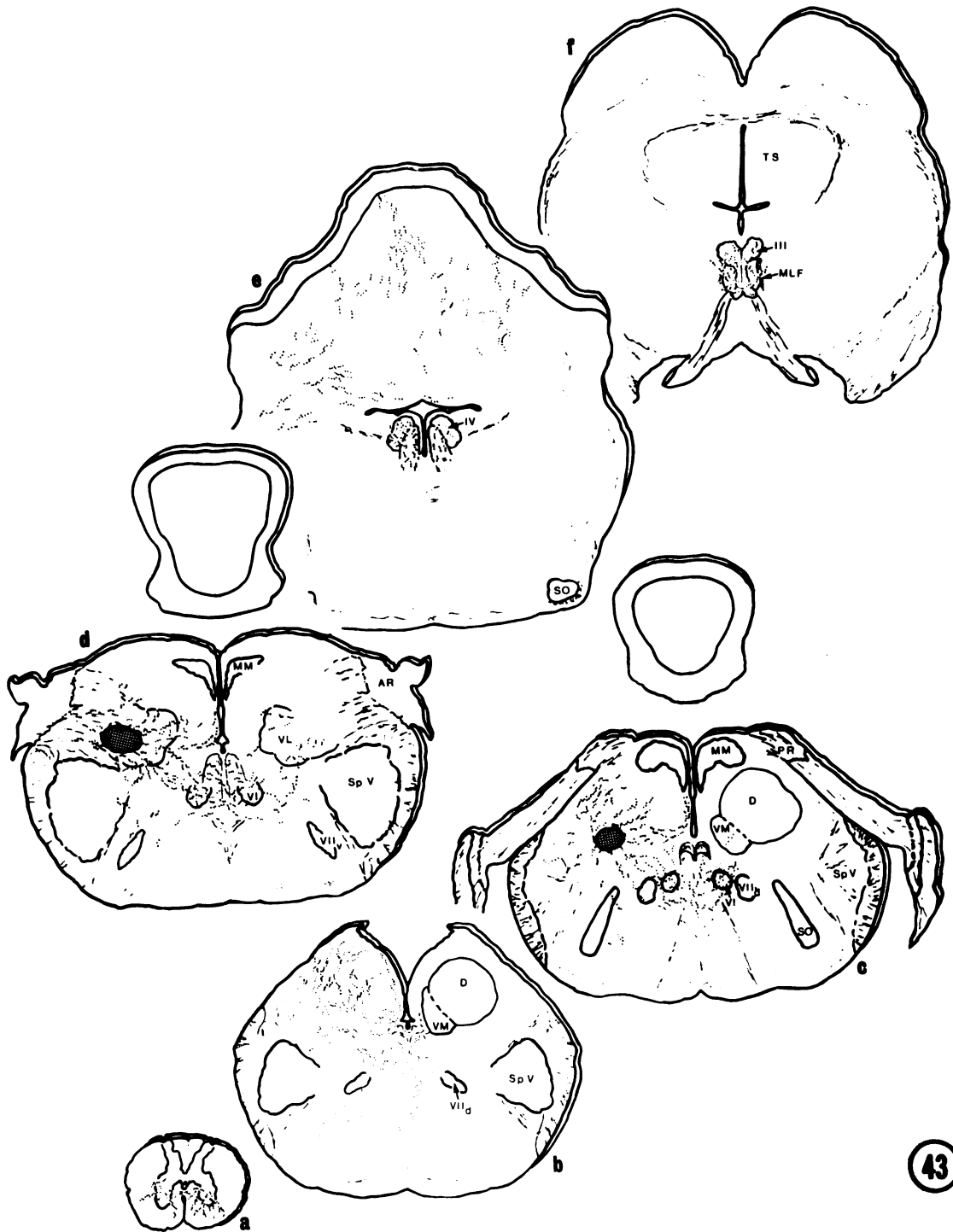
Figure 44.   Schematic illustration depicting pattern of degeneration

in experimental case V18 resulting from a lesion,

(cross-hatched area shows extend of lesion). Large dots

represent degenerated axonal fragments; fine stipple

indicates preterminal degeneration. (a is the most caudal;

f, the most rostral).

Abbreviations:

A	nucleus angularis	MM	medial magnocellular nucleus
D	descending vestibular nucleus	Mo V	motor nucleus of the trigeminal nerve
III	oculomotor nucleus		
IV	trochlear nucleus	PR	posterior division of the VIIIth nerve
F	flocculus	SO	superior olivary complex
L	nucleus laminaris	Sp V	spinal tract and nucleus of the trigeminal nerve
L Cb	lateral cerebellar nucleus	Te O	optic tectum
LL	nucleus of the lateral lemniscus	TS	torus semicircularis
M Cb	medial cerebellar nucleus	VI	abducens nucleus
		VII_d	dorsal division of motor fascial nucleus
ML	lateral magnocellular nucleus	VII_v	ventral division of motor facial nucleus
MLF	medial longitudinal fasciculus	VL	ventrolateral vestibular nucleus
		VM	ventromedial vestibular nucleus

Te O

TS

III
MLF

e

Te O

IV

MLF

d

F

A

L

Mo
V

Sp V

SO

A

VL

Sp V

SO   VII

c

ML

L

PR

MM

VL

Sp V

VM   D

VII

Sp V

SO

SO

a

b

44

Figure 45.   Light photomicrograph of transverse Nissl section through

the mesencephalon in the region of the oculomotor nuclei.

The medial longitudinal fasciculus (MLF) and oculomotor

nucleus (III) are outlined and labelled on the left side.

A ventromedial portion of the central nucleus of the torus

semicircularis can be seen in upper portion of photo-

graph, above sulcus limitans. ~X50

Figure 46.   Transverse Nissl section through the medulla in the region

of the abducens nucleus (VI) and the dorsal division of

the motor facial nucleus (VII) on the left side of the

brainstem. The right hand margin of the photograph is

aligned along the midline raphé. MLF, medial longitudinal

fasciculus. ~X75

Figure 47.   Transverse Nissl section through the mesencephalon in the

region of the trochlear nuclei. The medial longitudinal

fasciculus (MLF) and trochlear nucleus (IV) are outlined

and labelled on the left side. ~X75
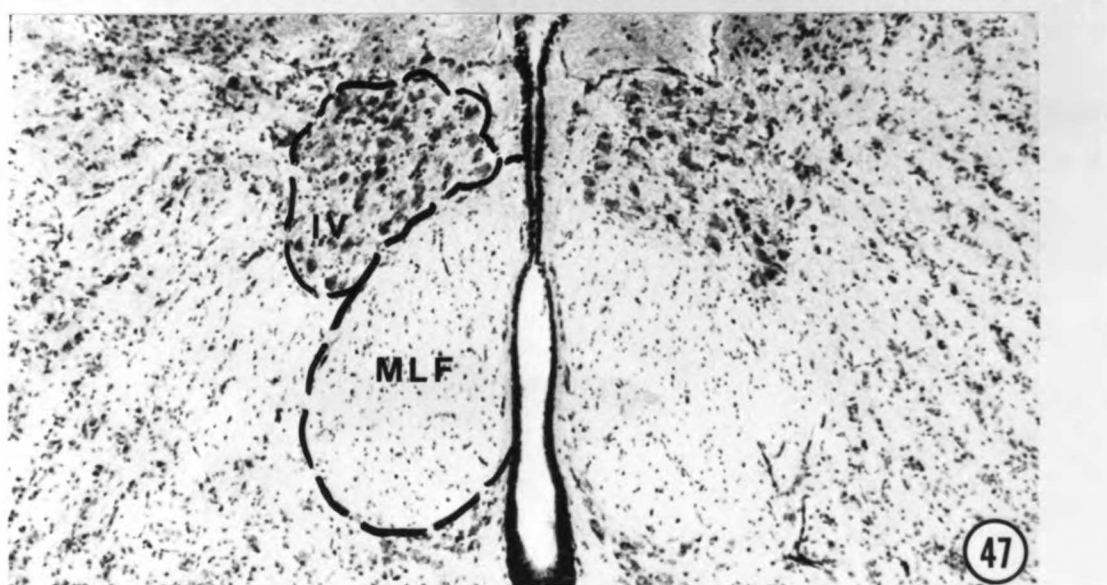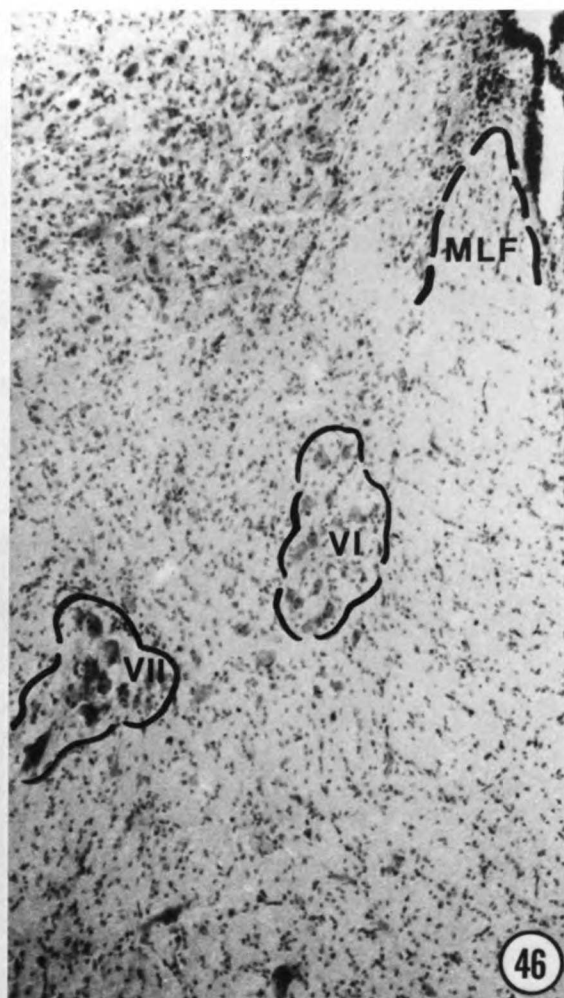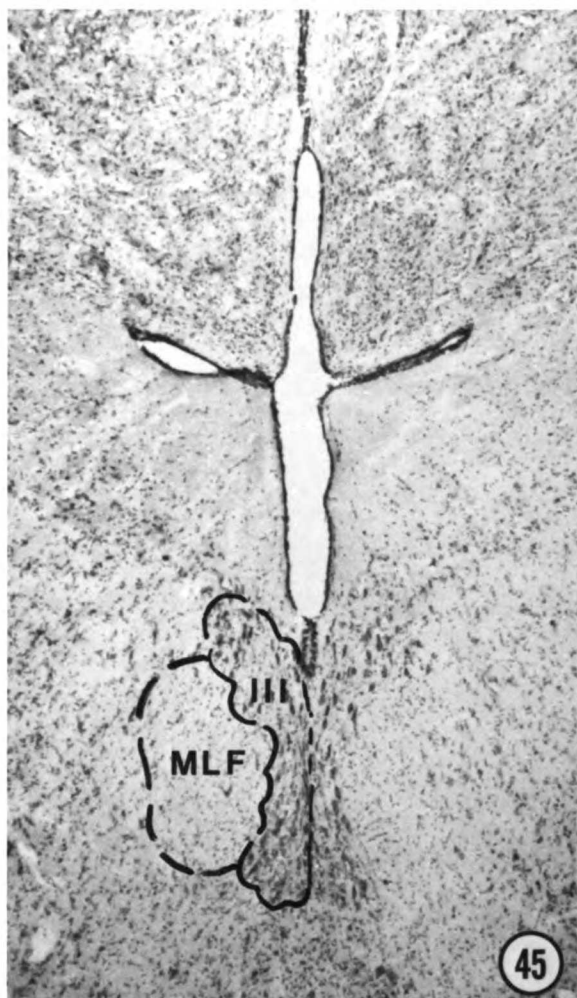
Figure 48a.   Schematic illustration of transverse section through the

brainstem at the level of the caudal portion of the

superior olivary complex.

        Abbreviations:

                MM   medial magnocellular nucleus

                SO   superior olive

                Sp V   spinal tract and nucleus of the trigeminal
                                  nerve

                VI   abducens nucleus

                VII   dorsal division of the motor facial
                                  nucleus

Figure 48b.   Light photomicrograph of transverse Nissl section showing

region outlined in 48a.   ~X50

MM

VI VII

Sp V

SO

a

b
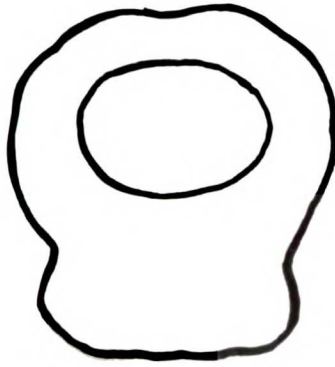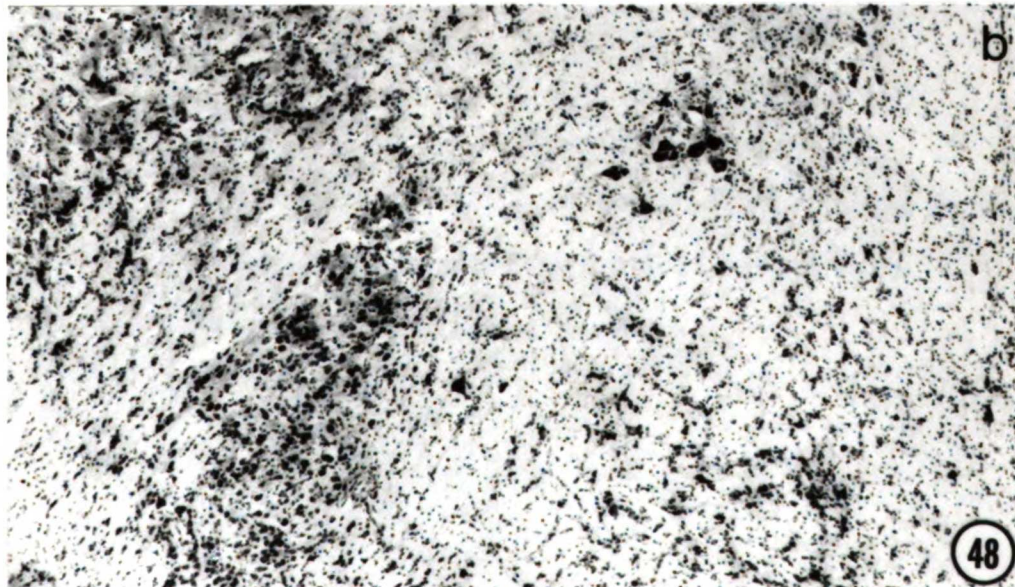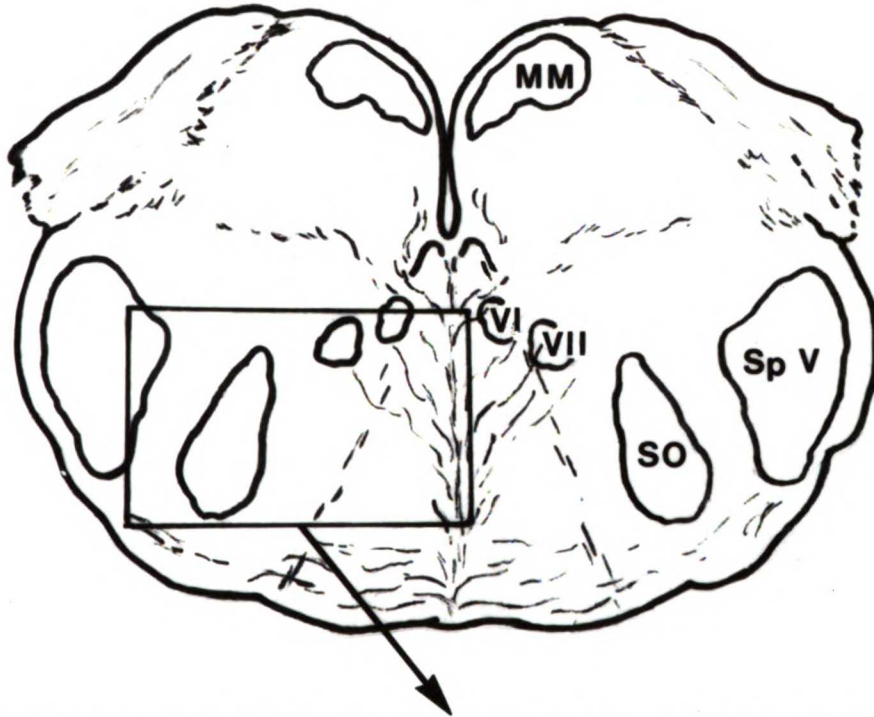
48

Figure 49. Nissl section at the level of the lesion in case V10.

The medial magnocellular nucleus in the upper left hand

corner and the posterior division of the VIIIth nerve in

the right hand corner of the photograph serve as land-

marks. Note that the image in this photomicrograph is

reversed and the lesion appears to be located on the

right side of the medulla; the microprojector tracings

in Figure 43 depict the actual position of the V10 lesion

on the left side. ~X50

Figure 50. Appearance of degenerated fibers emerging from lesion

(arrows) in case V18. Fink-Heimer technique. Note rever-

sal of image from Figure 44. ~X60

Figure 51. High magnification of degenerated fibers in the descending

vestibular impregnated with silver according to
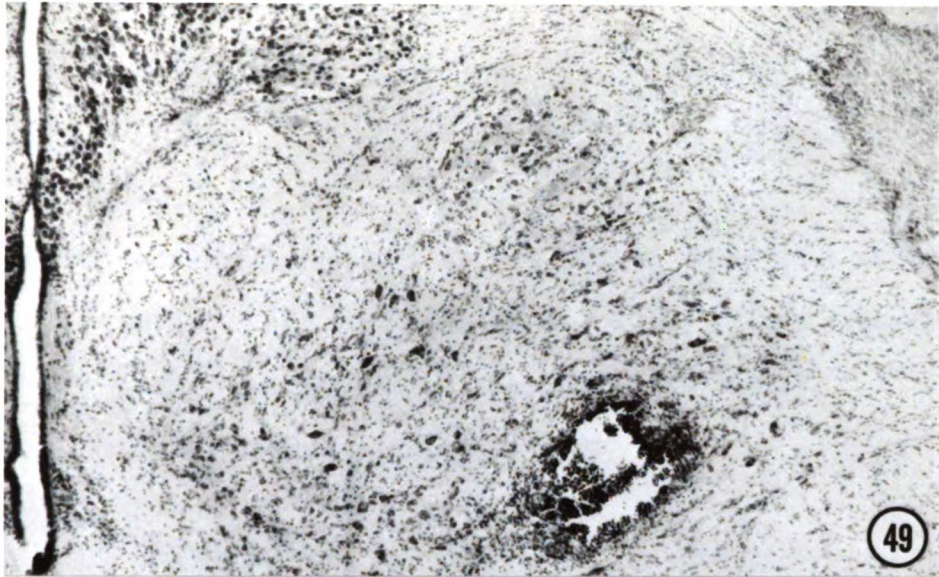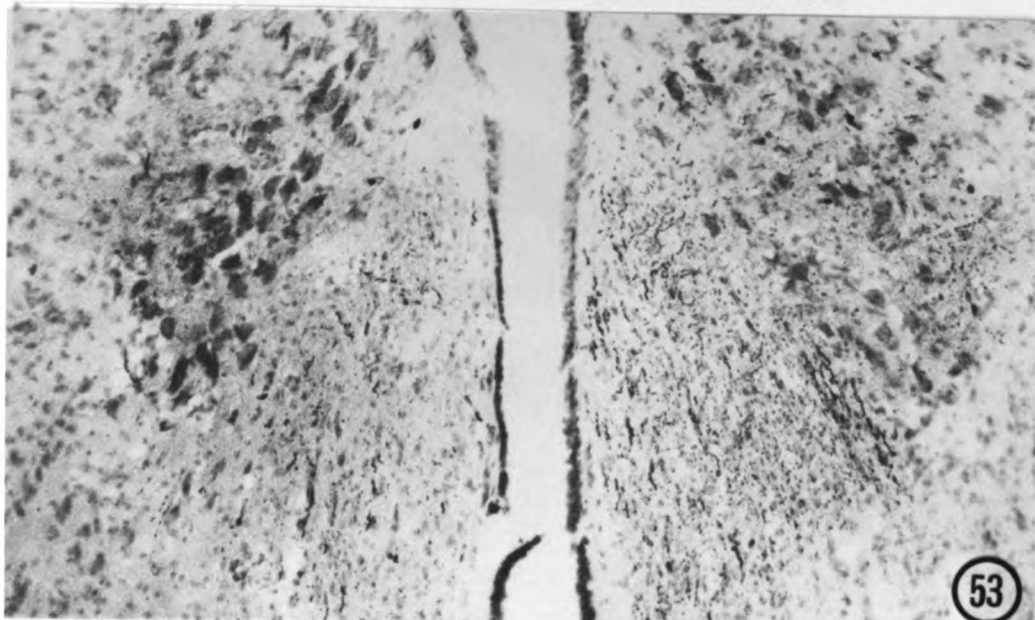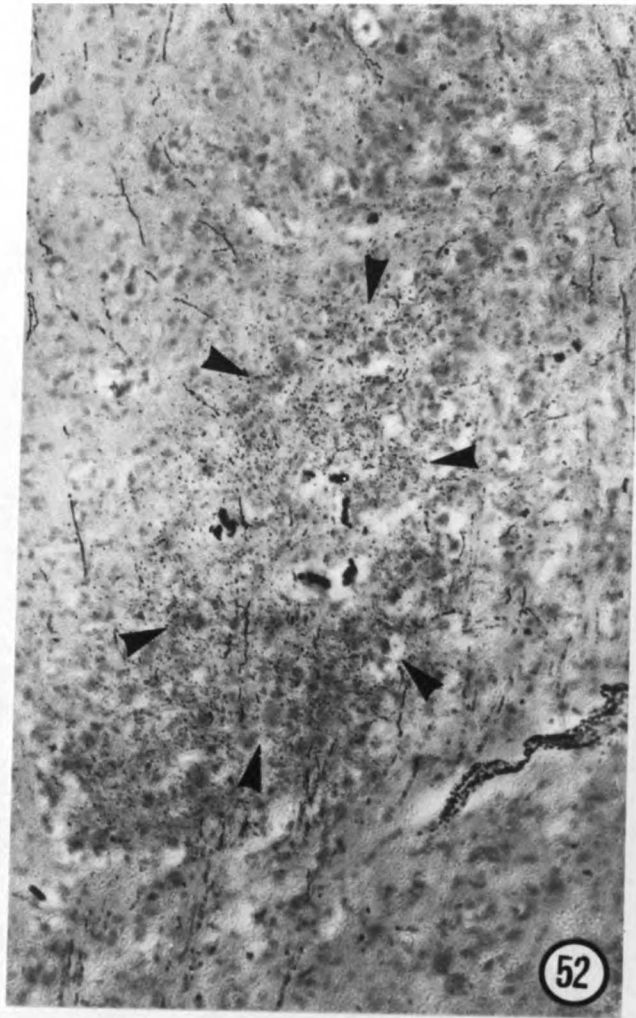
Fink-Heimer technique. ~X200
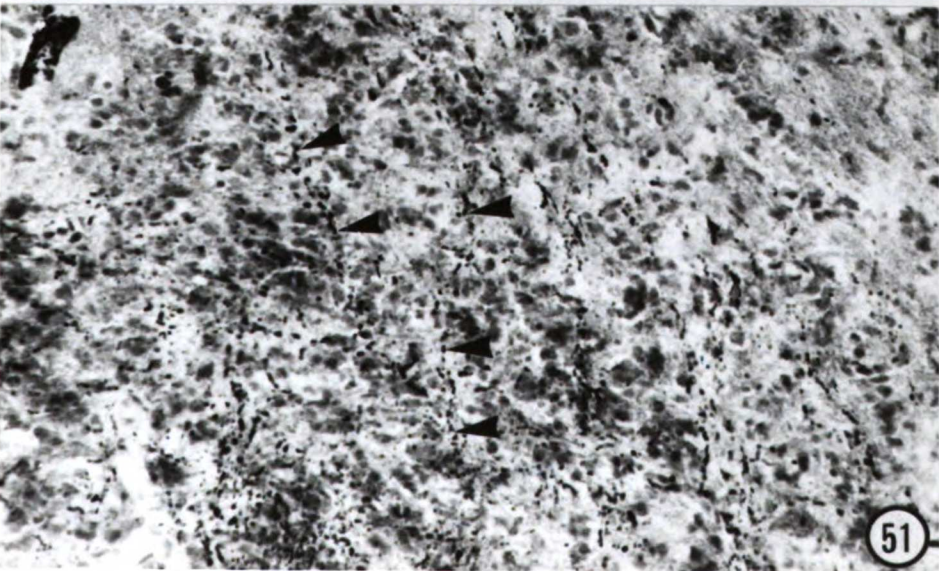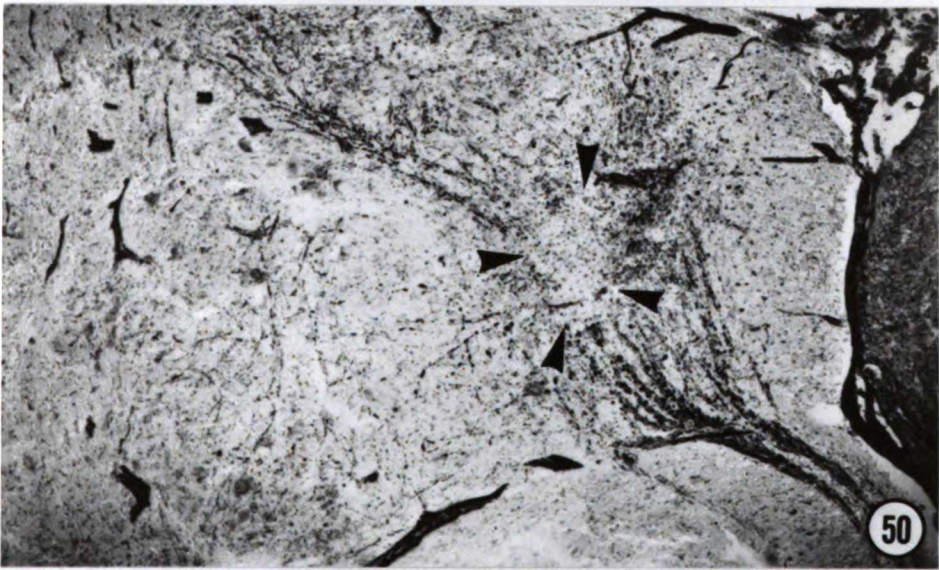
Figure 52. Degenerated fibers of the lateral leminiscus and fine

preterminal degeneration in nucleus of the lateral

lemniscus (arrows), as seen in case V17.

Fink-Heimer technique. ~X120

Figure 53. Degenerated fibers in the MLF and trochlear nuclei.

(see Figure 47 for orientation) Fink-Heimer technique,

counterstained with cresylecht violet. ~X120